UNIVERSITY OF CALIFORNIA

Santa Barbara

California riparian woodland responsive to groundwater availability in shallow aquifer

(Assessing Riparian Woodland Response to Shallow Groundwater Availability)

A Group Project submitted in partial satisfaction of the requirements for the degree of Master of Environmental Science and Management
for the
Bren School of Environmental Science & Management

by

Hector Leal Ibarra

Leah Makler

Vivian Phan

Leslie Serafin

Hannah Vaughn-Hulbert

Committee in charge:

Scott Jasechko

Name	Date of Signature
Hector Leal Ibarra	
Leah Makler	
Vivian Phan	
Leslie Serafin	
Hannah Vaughn-Hulbert	
Dr. Scott Jasechko	

Abstract

Groundwater dependent ecosystems are ecological communities that depend on groundwater occurring at or near the surface, many of which are vulnerable to drought and groundwater extraction. California's Sustainable Groundwater Management Act requires agencies to consider impacts to local groundwater dependent ecosystems, yet specific guidelines are not provided. Many groundwater dependent ecosystems are biodiversity hotspots and provide refuge for threatened species. Shallow groundwater is often accessible near the surface in these systems, allowing phreatophytes to thrive even during times of drought. In this study, we analyzed the impacts of groundwater flow and storage on ecosystem health in a riparian woodland—deemed a "likely groundwater dependent ecosystem." We assessed the influence of lithology and precipitation on shallow groundwater levels and the subsequent impacts of changing depth-to-groundwater on riparian vegetation health. We found a correlation between shallow groundwater levels and ecosystem health, which was even more evident during the summer months. These results are consistent with previous assumptions that this ecosystem relies on shallow subsurface flows, especially during dry periods. Remote sensing proved to be a valuable tool for assessing ecosystem health in groundwater dependent ecosystems. Our results and methodological framework can aid managers in determining the minimum groundwater level thresholds needed for these sensitive ecosystems to thrive. As interest in the management and protection of groundwater dependent ecosystems increases, the continued monitoring of these systems will be crucial to ensure the protection of these sensitive habitats from groundwater extraction and future droughts.

1. Introduction

1.1 Project Significance

Groundwater resources play a critical role in fulfilling the needs of both human and ecological water demands (Howard et al. 2023; Rohde et al. 2021a). In California, roughly four million acres of irrigated agriculture rely on groundwater supplies (Congressional Research Service 2015) and over two million acres of wetlands and riparian woodlands depend on groundwater to fulfill their ecological needs (Howard et al. 2023). During an average year, groundwater accounts for 40 percent of the state's total water supplies for human use and 60 percent or more during drought or dry years (California Department of Water Resources 2024). However, recurring droughts over the past four decades have intensified the strain on California's aquifers to fulfill agricultural and urban water requirements (Diffenbaugh et al. 2015; Gleick et al. 2014; Kibler et al. 2021). This demand management strategy, while crucial for sustaining human activities during dry periods, has often overlooked or underestimated the requirements of ecological

communities that also rely on groundwater (Howard et al. 2023; Nelson, R., Szeptycki, L. 2014; Rohde et al. 2021b).

Across California, groundwater dependent wetlands and riparian woodlands serve as crucial refuges for a diverse array of ecological communities. These ecosystems are commonly referred to as groundwater dependent ecosystems, defined as "ecological communities or species that depend on groundwater emerging from aquifers or on groundwater occurring near the ground surface" (Cal. Code Regs. Tit. 23, § 351; California Department of Water Resources 2018). Ecological communities within these ecosystems can include phreatophytic trees and species reliant on groundwater upwelling in interconnected surface water zones (Mattia Saccò et al. 2023; Stromberg 2013). Interconnected surface waters are defined by the California Code of Regulations as "surface water that is hydrologically connected at any point by a continuous saturated zone to the underlying aquifer and the overlying surface water is not completely depleted (Cal. Code Regs. Tit. 23, § 351)."

Phreatophytic trees can adjust their rooting depth according to local aquifer conditions and uptake groundwater in the capillary fringe above the water table (Stromberg 2013). While phreatophytes exhibit a level of plasticity, they are sensitive to rapid or prolonged declines in groundwater levels in shallow alluvial aquifers (Fan et al. 2017; Kibler et al. 2021; Rohde et al. 2021b; Scott et al. 1999; Stromberg 2013; Wang et al. 2021). The surface expression of groundwater (i.e., groundwater upwelling) in interconnected surface waters can also support critical habitat needs for aquatic communities in groundwater dependent ecosystems (Rohde et al. 2019). However, declining groundwater levels can reduce inflows to streams and rivers, making aquatic communities vulnerable to depletions of interconnected surface waters (California Department of Water Resources February 2024).

Climatic and hydrologic disturbances have been documented to impact groundwater dependent ecosystem health (Kibler et al. 2021; Rohde et al. 2021a; Rohde et al. 2021b). Declining shallow groundwater levels are found to be more prevalent during prolonged dry periods in California and can contribute to riparian woodland die-off and declines in vegetative greenness, especially in semi-arid regions (Kibler et al. 2021; Rohde 2021a). Given historical trends of increased groundwater pumping during dry and drought periods in California, research has suggested that groundwater extractions can also contribute to groundwater levels declining past the critical rooting depth of riparian phreatophytes, resulting in declining vegetative health (Cooper et al. 2003; Dong et al. 2019; Rohde at al. 2021a; Scott et al. 1999). Additionally, groundwater extractions can reduce or eliminate baseflows in locations where surface waters are hydrologically connected to the underlying aquifer (California Department of Water Resources February 2024). Implementing practical management tools is crucial for balancing human and ecological groundwater demands in future cyclical dry periods and prolonged droughts.

Until the enactment of the California Sustainable Groundwater Management Act (SGMA) in 2014, groundwater pumping in the state was largely unregulated. This groundwater regulation provides a management framework for Groundwater Sustainability Agencies to bring the state's groundwater subbasins to a sustainable balance by 2040 while preventing negative hydrologic impacts such as groundwater overdraft and depletion of interconnected surface waters (Department of Water Resources 2014; Miro & Famiglietti 2019). Given the substantial declines of California riparian wetlands and woodlands due to hydrologic alterations (California Natural Resource Agency 2010; Rohde et al. 2021a; Vaghti & Greco 2007), SGMA presents an opportunity to integrate protective measures for riparian vegetation, especially within groundwater dependent ecosystems. Nonetheless, existing regulatory constraints under SGMA must be addressed to ensure adequate assessment and management of groundwater dependent ecosystems for long-term sustainability.

1.2 Knowledge Gaps

Protecting groundwater dependent ecosystems is not a specific requirement of SGMA. Instead, Groundwater Sustainability Agencies must "consider impacts on groundwater dependent ecosystems" (Sustainable Groundwater Management Act 2014). The California Department of Water Resources has not adopted standardized protocols to inform the effective assessment, monitoring, or conservation of these ecosystems. There are 260 Groundwater Sustainability Agencies in California, many of which are responsible for protecting multiple groundwater dependent ecosystems (California Department of Water Resources 2024). The absence of specific requirements has left these agencies to navigate these issues independently. As a result, many Groundwater Sustainability Agencies have failed to comprehensively assess the impact of groundwater extraction and other activities on local groundwater dependent ecosystems. Evaluating the connection between hydrology and ecology is essential in managing groundwater dependent ecosystems, but there are no standard methods to measure these relationships (Tomlinson 2011). The challenge in establishing standardized methods stems from the spatial and temporal diversity of groundwater dependent ecosystems.

Groundwater dependent ecosystems can occur in different habitats and landscapes—from wetlands to springs and from beaches to mountains—and can support a variety of ecological communities (Rohde et al. 2020; Kibler et al. 2021). Furthermore, diverse ecosystems require varying amounts of groundwater, and may access groundwater using different methods (Kibler et al. 2021). Since groundwater dependent ecosystems are impacted differently by groundwater extraction, managers must assess the health and functioning of groundwater dependent ecosystems on a local scale. There is a pressing need to establish a standard framework for evaluating and monitoring the hydrology and ecology of these complex systems.

Due to the designation of groundwater dependent ecosystems as "beneficial users" under the Sustainable Groundwater Management Act (SGMA), agencies must grasp the impacts of

groundwater extraction on these sensitive communities (Sustainable Groundwater Management Act 2014). As such, Groundwater Sustainability Agencies should assess how groundwater extraction affects local ecosystems. By implementing a clear framework for assessment and management, these agencies can ensure the protection of groundwater dependent ecosystems for the foreseeable future.

1.3 Study Objectives

The primary objective of this study is to quantify the impact of local lithology, depth-to-groundwater, and climatic influences on riparian ecosystem health in a specific groundwater dependent ecosystem in California.

Our primary objective is split up into four sub-objectives: (a) characterize lithologies to determine vertical and lateral heterogeneity, (b) quantify direction and magnitude of vertical hydraulic gradient, (c) assess responses of shallow groundwater levels to precipitation events, and (d) analyze impacts of groundwater-level changes on plant water content in riparian ecosystems. Our study will consist of four distinct methodologies to assess the interactions between the geology, hydrology, and ecology within our study area (Figure 1).

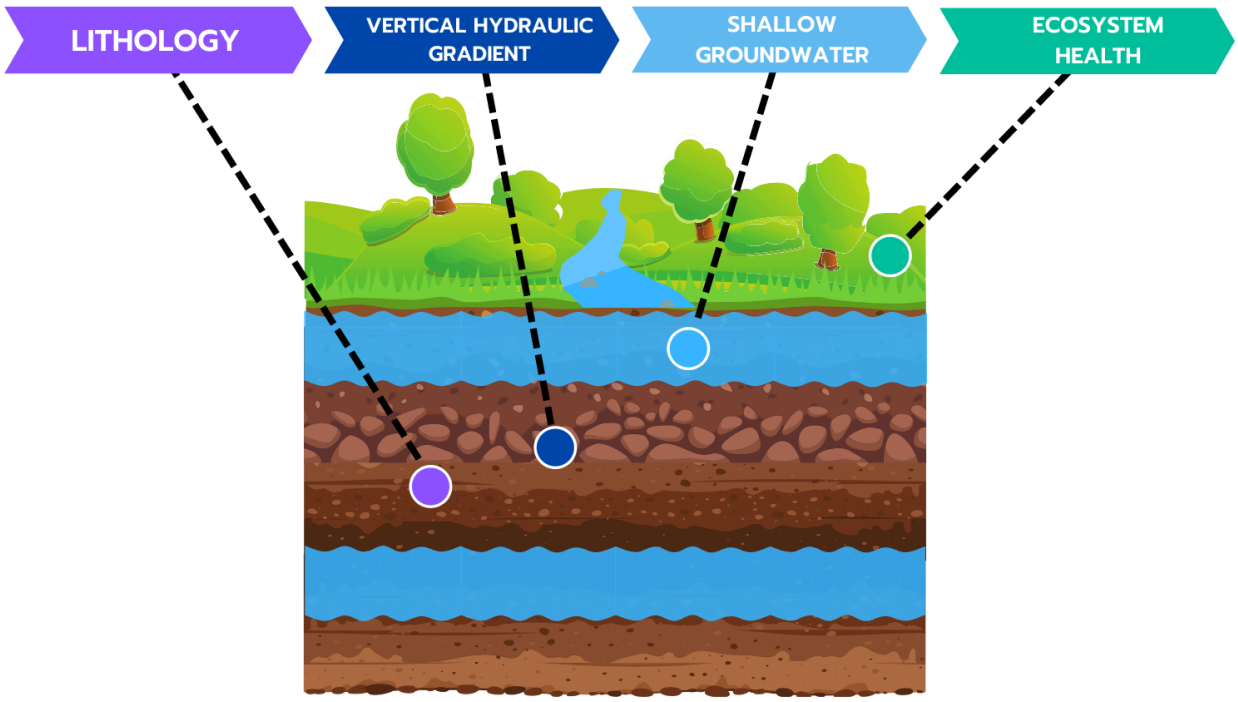

Figure 1. Schematic of the four components of this study's methodologies to complete the objectives above in Section 1.3: lithology, vertical hydraulic gradient, shallow groundwater, and ecosystem health. Lithology of the Fillmore Subbasin was analyzed to determine the impact of soil permeability on groundwater flow. Vertical hydraulic gradient was calculated to verify the

existence of rising groundwater in the system. Changes in shallow groundwater hydrology were assessed and compared to climatic conditions over the study period. This assessment was then used to determine the impact of shallow groundwater levels on ecosystem health in East Grove.

2. Study Area

The Santa Clara River, located in Ventura and Los Angeles Counties, is considered one of the last natural rivers in Southern California, as its primary channel remains relatively unobstructed by artificial barriers (United States Fish and Wildlife Service 2019). The river's watershed stretches from the San Gabriel Mountains in Los Angeles County to the Pacific Ocean in Ventura County. The watershed encompasses five groundwater subbasins—Santa Clara River Valley East, Piru, Fillmore, Santa Paula, and Mound Basin. Sections of the river can run dry during the summer months due to a lack of precipitation (Stillwater Sciences 2021; Western Regional Climate Center 2013). The local geology impacts subsurface and surface flows (Stillwater Sciences 2021). Shallow groundwater can saturate soil above the water table and has the potential to rise into the floodplain (Stillwater Sciences 2021). The hydrogeological connection between the shallow aquifer and the riverbed can be described as “interconnected surface waters,” where groundwater can rise up through geologic seeps and contribute to surface flows during dry periods (Cal. Code Regs. Tit. 23, § 351; Stillwater Sciences 2021). This connectivity between surface and subsurface flows has the potential to sustain groundwater dependent ecosystems.

The Santa Clara River Watershed supports several groundwater dependent ecosystems (Kibler et al. 2021; Stillwater Sciences 2021). These ecosystems are inhabited by native plants and several species listed under the Endangered Species Act, which depend on both shallow groundwater and the surface expression of groundwater (Beller et al. 2016; Downs et al. 2013; Rohde et al. 2021a; Stillwater Sciences 2021). Some of the native riparian plants include cottonwoods (*Populus spp*.) and willows (*Salix spp.*) which provide critical habitat for the endangered least Bell’s vireo (*Vireo bellii pusillus*) and willow flycatcher (*Empidonax traillii*) (Rohde et al. 2021a). Some of the watershed has supported rearing and spawning grounds for the federally listed southern steelhead trout (*Oncorhynchus mykiss*) and the endemic Santa Ana sucker (*Catostomus santaanae*) (National Marine Fisheries Service 2016; Stillwater Sciences 2021; Stoecker & Kelley 2005). The aforementioned species make up the complex and sensitive ecosystems found in the Santa Clara River, which are at risk from several environmental and anthropogenic factors.

The many groundwater dependent ecosystems in the Santa Clara River Watershed are adversely affected by the spread of the deep-rooted giant reed (*Arundo donax*)—an invasive plant that outcompetes native plants for shallow groundwater (Stephens and Associates 2021). These ecosystems face additional risks, including extensive groundwater pumping for agricultural

production and precipitation deficits (Court et al. 2000; Kibler et al. 2021). Groundwater pumping can lower groundwater levels beyond the rooting depths of native riparian woodlands, leading to declines in riparian health and the potential loss of habitats (Court et al. 2000; Environmental Science Associates 2021). Prolonged precipitation deficits have been associated with decreased vegetation cover and riparian woodland die-off in recognized groundwater dependent Santa Clara River ecosystems (Kibler et al. 2021). More information on the Santa Clara River and its groundwater dependent ecosystems can be found in Supplemental Materials, Section 1.

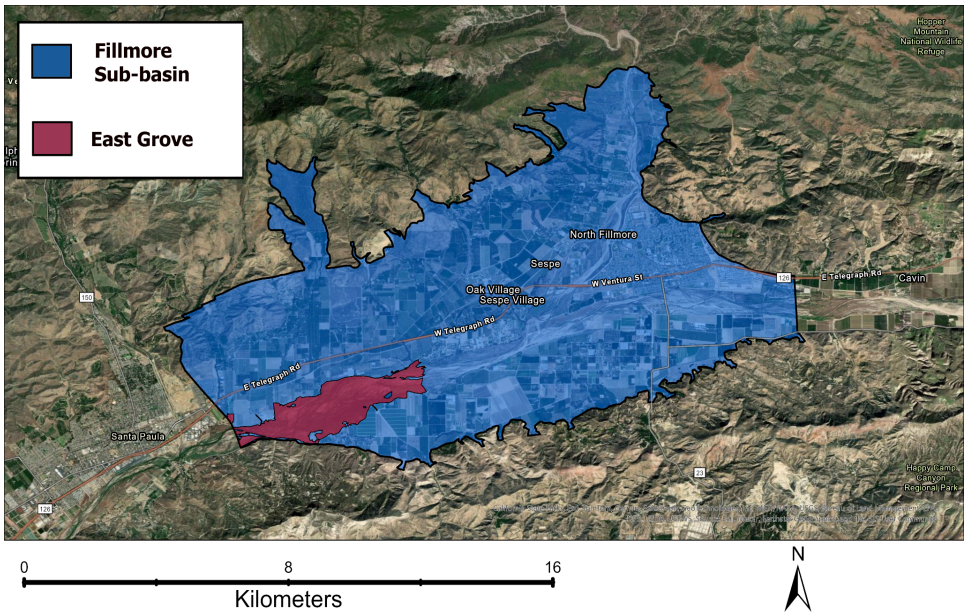

Figure 2. Location of East Grove within the Fillmore Subbasin of the lower Santa Clara River Watershed.

The Fillmore Subbasin (Figure 2) of the Santa Clara River Watershed was classified as a "high-priority basin" under California's Sustainable Groundwater Management Act (SGMA) (Moore 2018). Under SGMA, high-priority basins are required to form Groundwater Sustainability Agencies. These agencies are responsible for submitting Groundwater Sustainability Plans—long-term plans to ensure sustainable groundwater management—to the Department of Water Resources (Sustainable Groundwater Management Act 2014; California Department of Water Resources 2024). Fillmore's "high priority" status reflects the basin's risk of groundwater overdraft and local reliance on groundwater for agricultural and domestic water demands (Moore 2018; Stephens and Associates 2021). In 2023, pumping in the Fillmore Subbasin groundwater totaled 33,000 acre-feet. Agricultural use accounted for 94% of total groundwater extractions (Stephens and Associates 2021).

The Department of Water Resources recently ranked Fillmore Subbasin's 2018 Groundwater Sustainability Plan as "Incomplete" (California Department of Water Resources 2023).

According to the Department of Water Resources, the Groundwater Sustainability Plan failed to specify which of the Sustainable Groundwater Management Act's "undesirable results" were of most concern in the Fillmore Subbasin (Sustainable Groundwater Management Act 2014; California Department of Water Resources 2023). Furthermore, the Department of Water Resources found that the Plan had an inadequate assessment of "minimum thresholds" for groundwater levels in the basin and how these may impact beneficial use in the basin (California Department of Water Resources 2023). The Fillmore Basin Groundwater Sustainability Agency should consider the conservation of groundwater dependent ecosystems when determining minimum thresholds in the basin.

For the purposes of this study, we focused on a riparian woodland called East Grove, classified as a "likely groundwater dependent ecosystem" within the Fillmore Subbasin (Figure 2) (Stillwater Sciences 2021). East Grove presents specific indicators of groundwater dependent ecosystems, including the upward movement of groundwater (Stillwater Sciences 2021). East Grove is comprised of riparian habitat that houses multiple threatened and endangered species, and is thus considered to have "high ecological value" (Rohde et al. 2018; Stillwater Sciences 2021). Therefore, agencies must consider the protection and management of East Grove under SGMA and the California and federal Endangered Species Acts (Sustainable Groundwater Management Act 2014; Cal. Fish & G. Code § 2050-2118; 16 U.S.C. § 1531-1544).

3. Methods

3.1 Lithology

3.1.1 Data Acquisition & Sorting

To obtain information on the lithology of the Santa Clara River, we reviewed well-completion reports from the California Department of Water Resources. Well-completion reports are separated by the Public Land Survey System (PLSS), a method of subdividing land. Using the well-completion report map, we searched for 1-4 reports per available PLSS. Well drilling reports are imperfect, may be publicly unavailable, or have limited lithological information. We transcribed 63 well reports, extracting public land survey system numbers, well-completion numbers, geologic log descriptions per depth, street addresses, coordinates, total well depths, and distance to perforate intervals. We used Geocoder for wells lacking exact coordinates to obtain coordinates from reported street addresses. From transcribing the well completion reports, we ultimately ended up with 61 wells along the Santa Clara River, with only one in East Grove (Figure 3.1.1). We reclassified the numerous lithologic descriptions into 12 simplified lithological categories (Table 3.1.1). These new categories separate lithologies based on grain size, level of consolidation, and the relative abundance of material. Grain size refers to the

diameter of either individual sediment grains or particles in clastic rocks. Consolidation refers to the level of lithification; unconsolidated materials can be more easily drilled.

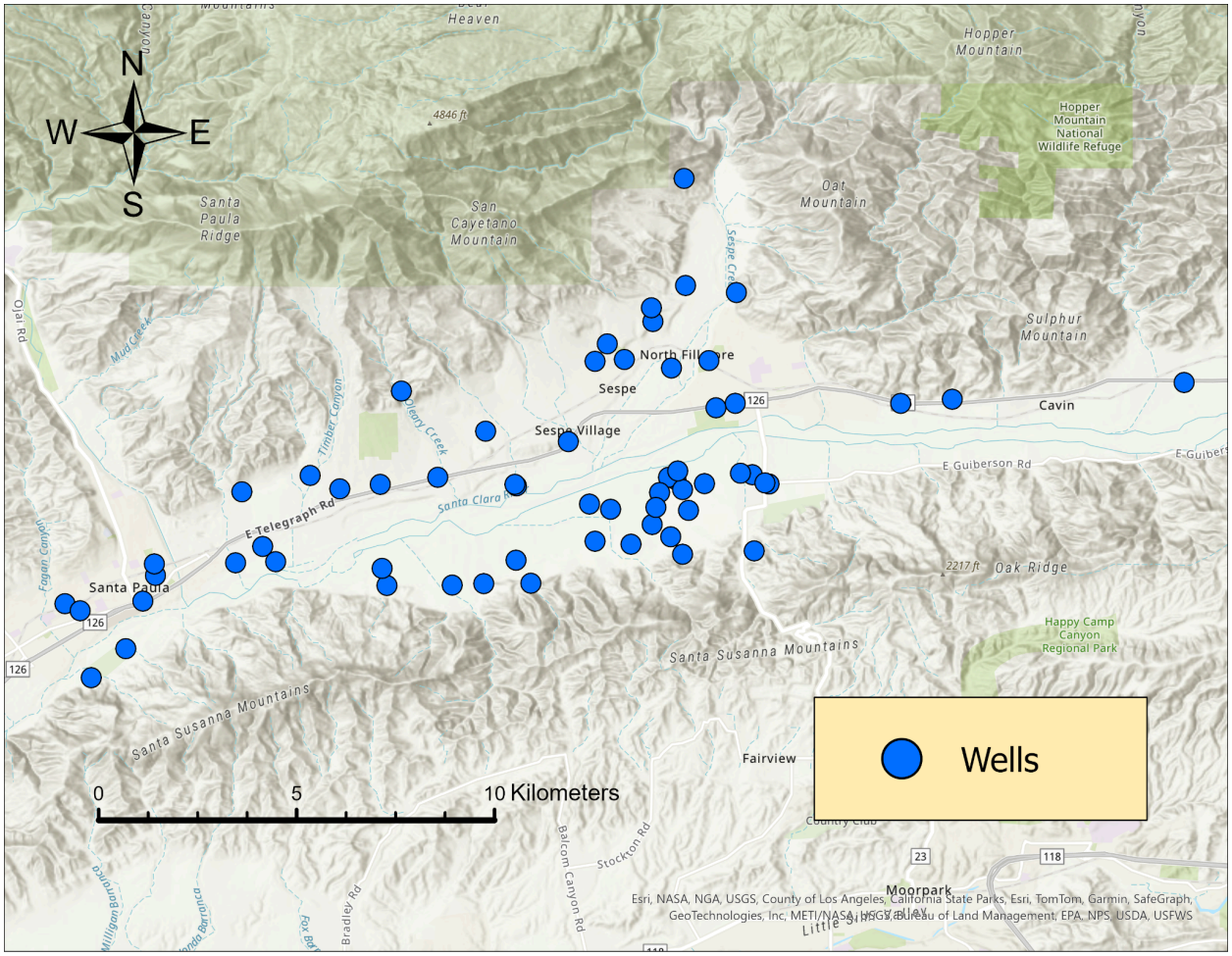

Figure 3.1.1
A map of the 61 wells across the Santa Clara River where well completion reports were obtained. Well-completion reports were gathered from the Department of Water Resources.

Table 3.1.1 Simplified lithological categories along with some example descriptions.

Number	Category	Examples
1	Coarse-grained material	Sand, gravel, cobbles, boulders
2	Mostly coarse-grained, some fine-grained material	Silty sand, silty gravel, sand with clay
3	Mixture of coarse and fine grained	Sand and clay, gravel and clay
4	Mostly fine-grained, some coarse-grained material	Sandy clay, clay with sand
5	Fine grained material	Clay, silt

Number	Category	Examples
6	Consolidated: Coarse-grained material	Sandstone, conglomerate
7	Consolidated: Mostly coarse-grained material with some unconsolidated material	Sandstone and or with unconsolidated material like; sand/cobbles/gravel/clay
8	Consolidated: Mixture of coarse and fine grained	Shale and sandstone
9	Consolidated: Mostly fine-grained material, some unconsolidated material	Shale and/with sand, shale and/with clay
10	Consolidated: Fine grained material	Shale, Siltstone
11	Bedrock	Bedrock, volcanics, rock
12	Unknown	“Hand augered to 4 feet”, “neat cement”

3.1.2 Cross-Sections

First, we plotted wells with their corresponding lithologies using “StratigrapheR”, an open-source integrated stratigraphy package for RStudio. This package allowed us to generate plots of the individual wells using the 12 simplified lithologic categories.

To plot each of the wells with the corresponding elevations, we used a digital elevation model of the Santa Clara River to obtain land surface elevation for each of the wells. We then filtered for wells with a total depth greater than 100 feet and at least 3 unique categories. We produced 3 cross-sectional diagrams using these filtered wells, the lengths of each cross-section ranged from 10 to 16 km (Figure 3.1.3, Table 3.1). Two of our chosen cross-sections run west to east along the valley near the East Grove site, crossing the Santa Clara River at least once. One cross-section has a north-eastern trend, terminating near the north of Fillmore (Figure 3.1.3). We aimed to adequately represent the varied lithologies of East Grove and the surrounding area. We used a lithostratigraphic correlation strategy to connect the observed lithologies across wells. In the cross-section diagram, full lines connect similar sections while dashed lines indicate inferred correlation.

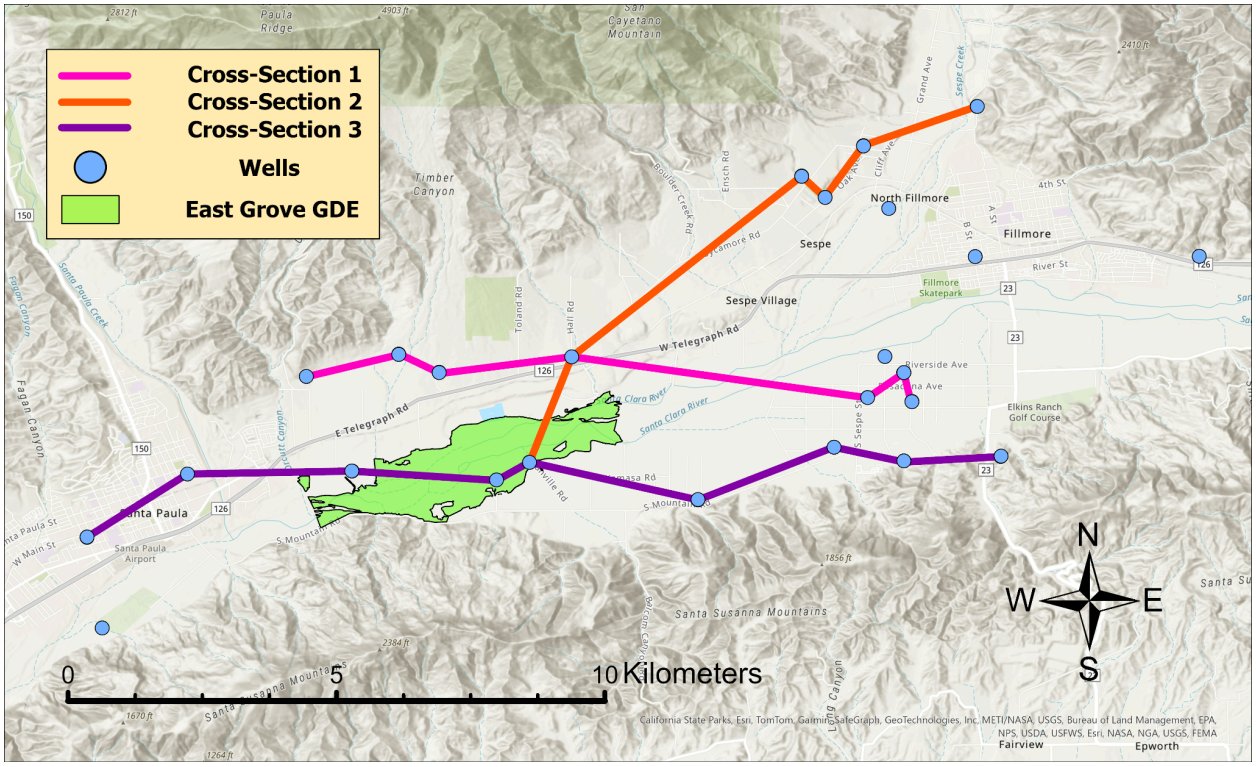

Figure 3.1.2 Lithological cross-section lines of the wells along the Santa Clara River used to create cross-section plots. The cross-section lines include wells gathered from the California Department of Water Resources and the data from a nested well (more information on the nested well is described in section 3.2) provided by the United Water Conservation District.

Table 3.1 Well ID and completion number of wells found in each of the lithological cross-sections.

Cross-section Line	Well ID	Well Completion Number
Cross-section Line 1	Well 12	WCR2010-010156
Cross-section Line 1	Well 13	WCR2004-015524
Cross-section Line 1	Well 14	WCR2010-010413
Cross-section Line 1	Well 22	WCR1998-010940
Cross-section Line 1	Well 42	WCR2006-011431
Cross-section Line 1	Well 44	WCR2016-005853
Cross-section Line 1	Well 41	WCR2007-012988

Cross-section Line 2	Well 17	WCR2016-008246
Cross-section Line 2	Well 1	WCR2004-015336
Cross-section Line 2	Well 6	WCR2008-011034
Cross-section Line 2	Well 8	WCR2018-009168
Cross-section Line 2	Nested Well	WCR2022-013828
Cross-section Line 2	Well 29	WCR2010-010444
Cross-section Line 2	Well 54	WCR2006-013424
Cross-section Line 2	Well 40	WCR1974-004128
Cross-section Line 2	Well 57	WCR0307632
Cross-section Line 3	Well 8	WCR2018-009168
Cross-section Line 3	Well 22	WCR1998-010940
Cross-section Line 3	Well 32	WCR2018-005473
Cross-section Line 3	Well 37	WCR2013-009374
Cross-section Line 3	Well 53	WCR2013-009055
Cross-section Line 3	Well 52	WCR1988-016945

3.2 Vertical Hydraulic Gradient

Previous studies have characterized East Grove as a gaining reach of the Santa Clara River (Beller at al. 2016; Stillwater Sciences 2021), wherein groundwater is observed to flow upwards, or upwell, into the riparian corridor. However, to our knowledge, empirical quantification of the magnitude of groundwater upwelling in East Grove has not been documented in existing literature before this study (Beller at al. 2016; Stillwater Sciences 2011; Stillwater Sciences 2021). To quantify the magnitude and existence of groundwater upwelling in East Grove, we calculated the vertical hydraulic gradient, which evaluates the vertical movement and magnitude of groundwater in an aquifer. We completed nine different vertical hydraulic gradient calculations using depth-to-groundwater measurements and well bottom elevations of a deep and shallow well within a nested monitoring well. The nested monitoring well is located within the East Grove boundary (Figure 3.2.1) and was installed in November of 2022. The East Grove nested monitoring well contains four wells that are screened at different intervals—all of which

are embedded in the same borehole at the same ground surface elevation (see Section 2.2 in the Supplemental Materials for specifications on all wells).

3.2.1 Data Acquisition

Unpublished data from the United Water Conservation District was used to evaluate the magnitude of vertical hydraulic gradients. The dataset included nine depth-to-groundwater measurements that were recorded throughout 2023 (see Supplemental Materials, Section 2.2).

The Ventura County Watershed Protection District provided lithology data of the nested monitoring well in the form of a well completion report. Using this report, we applied identical lithologic categorization methods, as described in Section 3.1 above, to delineate the various geologic materials surrounding the well. This allowed us to assess the lithologic influence on groundwater upwelling in East Grove. We used Adobe Illustrator to represent the surrounding geologic materials at the nested monitoring well site (Figure 4.2a).

Figure 3.2.1. Map of the nested monitoring well located on the south-central border of East Grove. East Grove is represented by the green-shaded polygon.

3.2.2 Data Analysis

To assess the vertical hydraulic gradient, we used the 2023 static water level measurements from the deepest well and the shallow-most well (see Supplemental Materials, Section 2.2 for all water level measurements). A depth-to-groundwater time-series plot for these two wells is shown below (Figure 3.2.2a.).

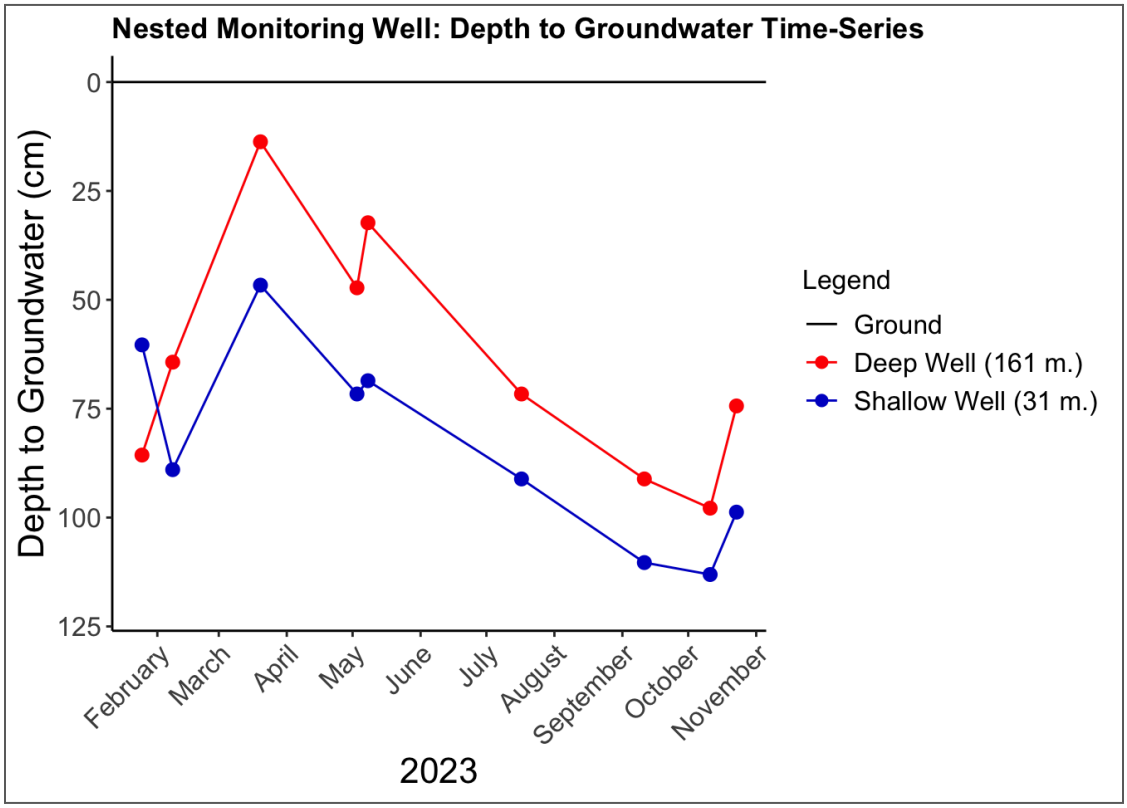

Figure 3.2.2a. Time-series graph of depth-to-groundwater levels of a deep well (in red) and a shallow well (in blue). The total well depth of the deep well is 161 meters below ground surface (~530 feet). The total well depth for the shallow well is 31 meters below ground surface (~100 feet). Depth-to-groundwater levels are represented on the y-axis as centimeters below the ground surface, with the ground surface at 0 centimeters. The date of the recorded depth-to-groundwater measurement is represented as monthly values on the x-axis. Water level measurements at the deeper well are consistently shallower, or closer to the land surface, than the shallow well's water level measurements from 2/8/2023 to 10/23/2023. This trend implies the existence of an upward-oriented vertical hydraulic gradient, indicating the presence of groundwater upwelling (Jasechko & Perrone 2020). The water level measurements on 1/25/2023 deviated from the observed trends between 2/8/2023 and 10/23/2023. This discrepancy may be attributed to significant rainfall in late December 2022 and early January 2023, following a period of reduced precipitation throughout the 2022 calendar year.

We calculated nine vertical hydraulic gradients (Δh/Δz) using total well depths and depth-to-groundwater measurements from the shallow and deep wells. In these calculations, we evaluated the change in water level from the shallow well to that of the deep well divided by the change in vertical distance of these two wells. Below is the formula used to calculate the nine vertical hydraulic gradient magnitudes.

$$\boldsymbol{\Delta} h/\boldsymbol{\Delta} z \;=\; (h_1 - h_2)/(z_1 - z_2)$$

The change in hydraulic heads is denoted as **Δ**h and the change in vertical distance is denoted as **Δ**z. h_1 represents one depth-to-groundwater measurement taken at the shallow well at a certain date and h_2 represents one depth-to-groundwater measurement taken at the deep well on the same date. z_1 is the total well depth of the shallow well and z_2 is the total well depth of the deep well.

3.3 Groundwater Fluctuations

To further assess groundwater flow and storage in the Fillmore Subbasin, we analyzed changes in groundwater levels using production and monitoring wells both in and outside the East Grove boundary. We obtained records of depth-to-groundwater measurements from 43 wells between 2010 and 2023 to understand fluxes in deep and shallow aquifers in this system. Furthermore, we assessed the impact of differing precipitation regimes on groundwater storage in East Grove and the encompassing Fillmore Subbasin.

3.3.1 Groundwater Data Acquisition

East Grove Shallow Groundwater Monitoring Wells

In late 2015, a UCSB research team installed 21 shallow groundwater monitoring wells within East Grove (Figure 3.3.1a). These shallow wells range from 2 to 3.6 meters in total well depth. From late 2015 to early 2023, monthly water level measurements were taken manually at these 21 wells. These recorded depth-to-groundwater measurements were used in time-series plots and subsequent regression analyses.

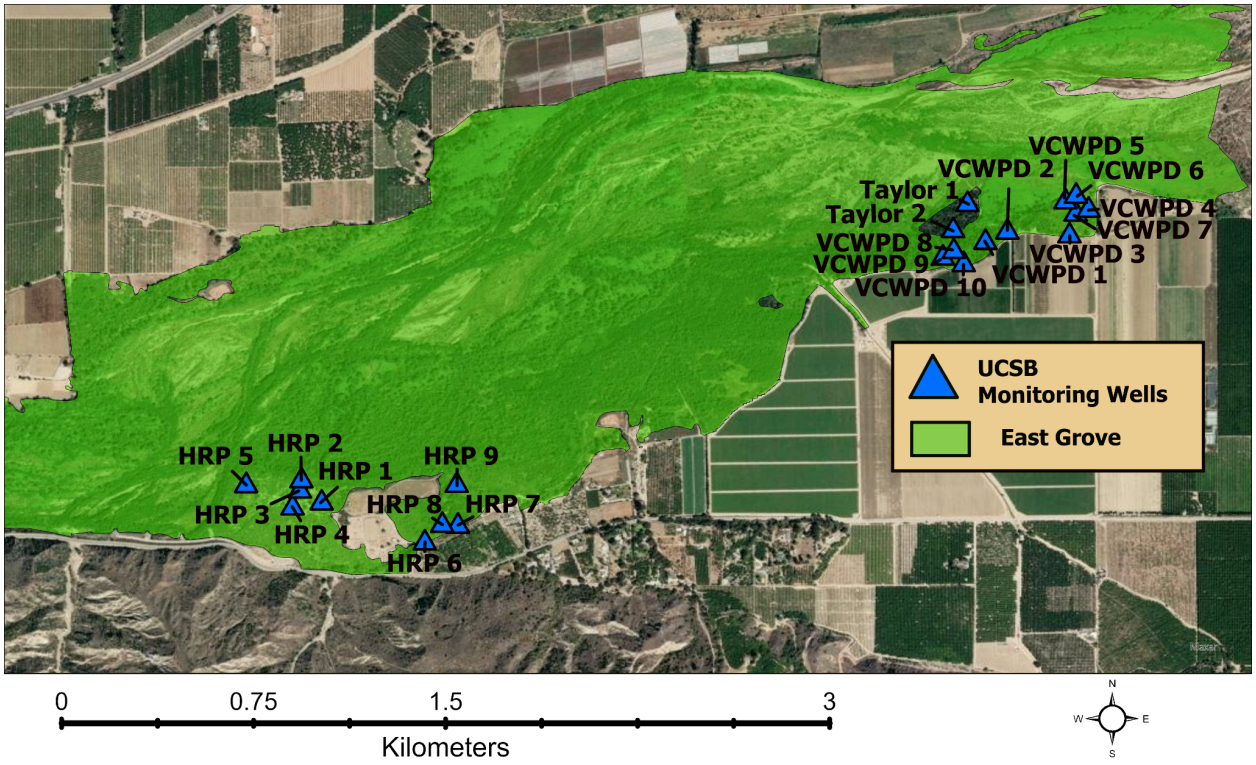

Figure 3.3.1a. UCSB shallow groundwater monitoring well locations within East Grove. See Supplemental Materials, Section 2.3.1 for well naming conventions.

Fillmore Subbasin Wells

Groundwater level data for wells with various well depths were retrieved from the Department of Water Resources' SGMA Data Viewer web tool. We used data cleaning and filtering protocols to evaluate wells suitable for the study's groundwater fluctuation analysis (see 2.3.1 in Supplemental Materials for a description of the data and protocols). Using these protocols, we identified 22 wells in the Fillmore Subbasin and categorized them according to the reliability and completeness of their data spanning from 2010 to 2023 (Figure 3.3.1b). Data from these 22 wells were used for time-series and recharge analysis.

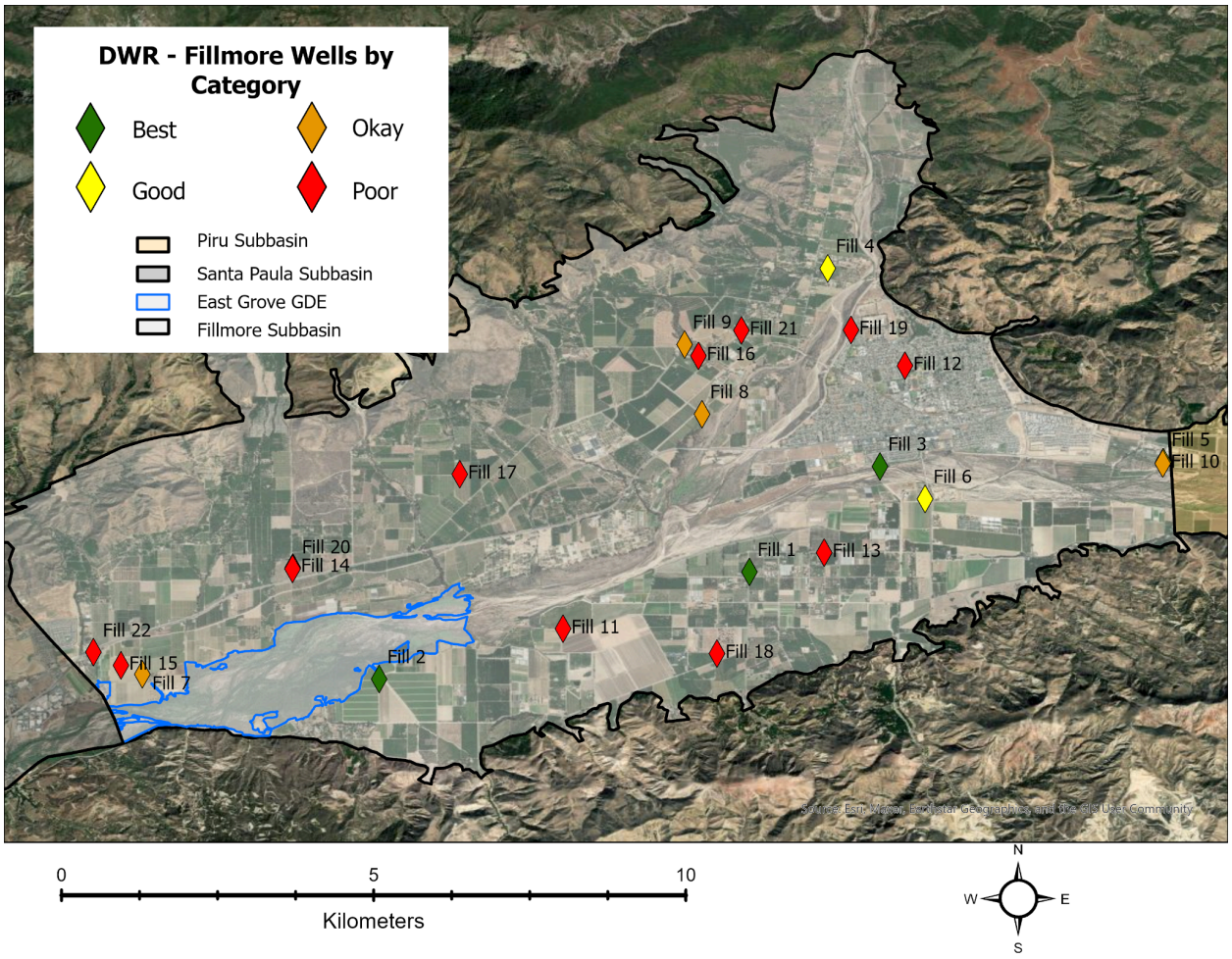

Figure 3.3.1b. Map of the 22 Fillmore Subbasin wells used to evaluate groundwater level conditions surrounding East Grove. Wells are categorized based on data relevance (Best, Good, Okay, Poor). See Section 2.3 in Supplemental Materials for the categorization protocols.

3.3.2 Depth-to-Groundwater and Precipitation Time-Series

Using the "ggplot" package in R, we created time-series graphs for the 21 shallow monitoring wells in East Grove and the 22 wells in the surrounding Fillmore Subbasin (see Supplemental Materials, Section 3.2.1 for all plotted time-series). Each time-series includes depth-to-groundwater measurements and precipitation data. The depth-to-groundwater measurements reflect the vertical distance between the ground surface and the groundwater level.

We could not obtain consistent precipitation data from the closest CIMIS weather station—an automated weather station paid for by the Department of Water Resources, located in Santa Paula (California Department of Water Resources 2023). Therefore, we needed to use model data to estimate the daily precipitation during the study period. We selected PRISM Climate Data

precipitation estimates for Fillmore (PRISM Climate Group 2023). To verify the accuracy of the PRISM model for this region, we completed a Pearson correlation analysis between the PRISM and limited CIMIS data from the Santa Paula station to verify that the modeled PRISM results were a valid replacement (see Supplemental Materials, Section 2.3.1). We found that the PRISM and CIMIS precipitation measurements were highly correlated, with a Pearson correlation of 0.928 (Figure 3.3.2). Thus, using the precipitation data modeled by PRISM as a replacement for actual precipitation measurements was appropriate. The precipitation data was used throughout our time-series and water-level rise analyses (see Section 2.3.1 and 3.2 in Supplemental Materials).

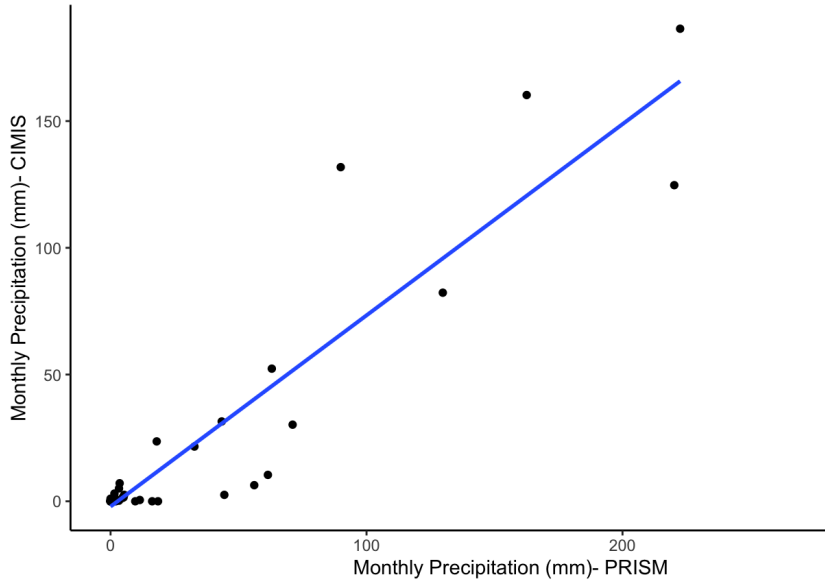

Figure 3.3.2. PRISM modeled daily precipitation and CIMIS station measurements between 2015 to 2023. All common months were paired, so months in which CIMIS did not have measurements were not included. PRISM modeled data and CIMIS precipitation measurements were highly positively correlated (Pearson's r=0.928). The blue line represents the linear relationship between PRISM-modeled precipitation and CIMIS measurements.

3.3.3 Water-Level Rise

Water-Level Rise Analysis

The filtered groundwater level data was used to assess water-level rise within East Grove and the Fillmore Subbasin. Water-level rise events were calculated by first identifying the local maximums (or "valleys") and local minimums (or "peaks") in the fluctuations of groundwater levels at each well site. The difference between the valley and the peak that followed was then calculated to represent a water-level rise event (Figure 3.3.3). Using our time-series data, we applied for-loops in R to return all peaks (local minimums) and valleys (local maximums) for each well. A data frame was generated with data points for each water-level rise event and its

respective date. These values were used to calculate the total time interval (t) and water-level rise (delta-H) for each event of water-level rise for each well.

This provided us with a data frame with all water-level rise events containing information on the timing, water-level rise (delta-H), and total precipitation for all wells' water-level rise events. See Supplemental Materials, Section 2.3.3 for details on water-level rise calculations and calculations for the ratios between water-level rise and precipitation.

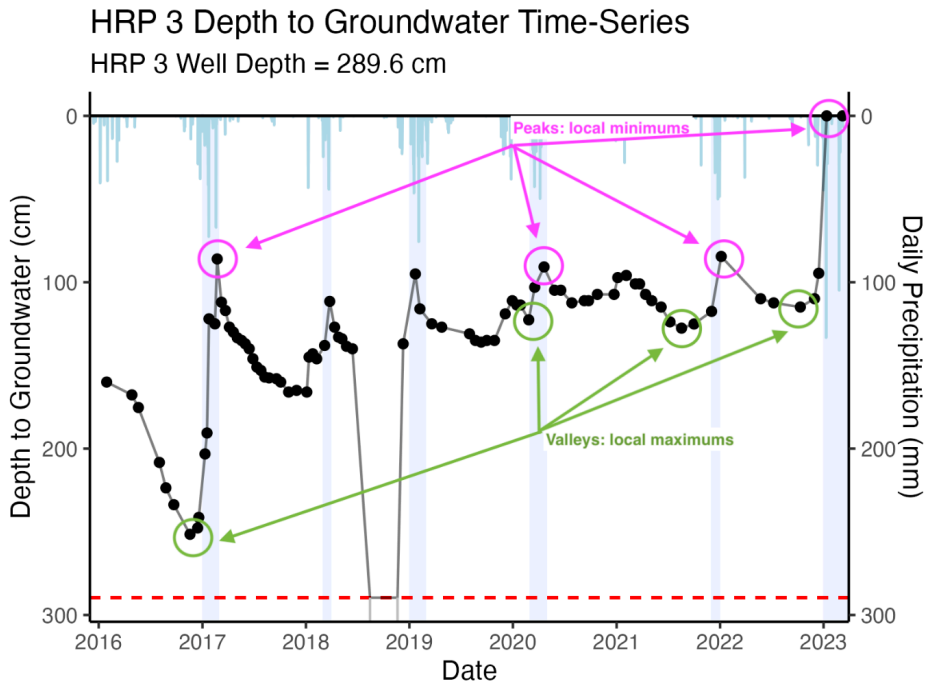

Figure 3.3.3. Visual representation of depth-to-groundwater peaks (pink) and valleys (green) on time-series of Hedrick Ranch Preserve (HRP) 3. These peaks and valleys were used to calculate water-level rise (delta-H) and time intervals of water-level rise events. The water-level rise (delta-H) is the vertical change between a valley and a peak in centimeters, and the total precipitation is the summed precipitation during the same time interval. Not all water-level rise events are represented in this image.

Theil-Sen Linear Regression

Theil-Sen regression is a statistical tool that resists the impact of outliers (Goldstein-Greenwood 2023). The output data frames were used to create Theil-Sen models on the relationship between precipitation and recharge for each well. The Theil-Sen models estimated ratios of water-level rise to precipitation to assess the influence of surface processes on groundwater fluctuations. The models resulted in estimates of slopes and y-intercepts for each well's water-level rise events, with corresponding p-values. Using R's ggplot package, we used the Theil-Sen models to add regression lines to scatter plots for each well (see Supplemental Materials, Section 3.2.2). The

regression lines allowed us to visualize the impact of precipitation on water-level rise. See Supplemental Methods, Section 2.3.3 for detailed Theil-Sen regression methods.

3.4 Remote Sensing

3.4.1 NDVI

The normalized difference vegetation index (NDVI) is a metric used to quantify greenness in vegetation as a proxy for vegetative health (Pettorelli et al. 2005). In this study, we calculated NDVI using high-resolution, top-of-atmosphere, satellite-derived imagery from the Copernicus Sentinel-2 program. Using 10 meter by 10 meter resolution spectral data, NDVI was calculated from the near-infrared to red reflectance ratio:

$$NDVI = \frac{NIR - RED}{NIR + RED}$$

NIR represents the near-infrared wavelength reflectance, and RED represents the red wavelength reflectance. Healthy vegetation reflects more near-infrared radiation and absorbs more energy from the red wavelength because chlorophyll absorbs red light while the mesophyll structure of a plant scatters near-infrared radiation, indicating photosynthetic activity (Rhew et al. 2011; Pettorelli et al. 2005). NDVI values range from -1 to +1. Negative values indicate the absence of vegetation, and values closer to +1 correspond to higher vegetation greenness (Pettorelli et al. 2005).

We calculated NDVI using Google Earth Engine. We also used Google Earth Engine to acquire monthly satellite imagery from the Copernicus Sentinel-2 program for the years 2016-2023 (Gorelick et al. 2017; Copernicus Sentinel-2 2021). We loaded the Harmonized Sentinel-2 MSI: MultiSpectral Instrument, Level-1C image collection into Google Earth Engine and filtered it to the bounds of our study area (East Grove) and dates of interest (01-01-2016 to 12-31-2023). The NDVI function was added, where the band B8 represented the NIR wavelength reflectance and B4 represented the RED wavelength reflectance. The resulting NDVI was clipped to our region of interest, where the median NDVI value per month was calculated. An image collection of monthly composites was created, listing the months of January to December as 1 to 12, respectively.

3.4.2 NDMI

The normalized difference moisture index (NDMI) is a metric used to quantify water stress levels in plants and is commonly used to monitor changes in vegetation water content and drought stress (Gao 1996; Strashok et al. 2022). We used 20 meter by 20 meter resolution

spectral data derived from the Copernicus Sentinel-2 program to calculate NDMI, using the short-wave infrared to near-infrared reflectance ratio:

$$NDMI = \frac{NIR - SWIR}{NIR + SWIR}$$

NIR represents the near-infrared wavelength reflectance, and SWIR represents the short-wave infrared wavelength reflectance. (Kim et al. 2015; Strashok et al. 2022). Changes in plant water content and the spongy mesophyll structure of plants influence SWIR. While water is absorbed strongly in SWIR, the leaf's internal structure scatters NIR (Kim et al. 2015; Strashok et al. 2022). NDMI values range from -1 to +1. Negative values indicate water stress and positive values closer to +1 correspond to abundant water content (Strashok et al. 2022).

To calculate NDMI, Google Earth Engine was used to acquire monthly satellite imagery from the Copernicus Sentinel-2 program for the years 2016-2023 (Gorelick et al. 2017; Copernicus Sentinel-2 2021). The Harmonized Sentinel-2 MSI: MultiSpectral Instrument, Level-1C image collection was loaded into Google Earth Engine and filtered to the bounds of our study area (East Grove) and dates of interest (01-01-2016 to 12-31-2023). The NDMI function was added, where the band B8A represented the NIR wavelength reflectance and B11 represented the SWIR wavelength reflectance. We clipped the resulting NDMI to our region of interest, where the median monthly NDMI value was calculated. An image collection of monthly composites was created, listing the months of January to December as 1 to 12, respectively.

3.4.3 Zonal Statistics

Radius buffers of 50 meters and 100 meters were created around each shallow groundwater monitoring well. The median NDVI and NDMI values previously calculated were clipped to these radius buffers in Google Earth Engine. Zonal statistics of these clipped NDVI and NDMI values were subsequently calculated for the 10^{th} through 90^{th} percentiles.

3.4.4 Ecohydrological Analysis

Data Cleaning and Assessment

The previous zonal statistics resulted in a dataset of monthly median values of NDVI and NDMI for each well from January 2016 to September 2023. We then created a dataset that combined the remote sensing data with the depth-to-groundwater data from the shallow groundwater monitoring analyses from the corresponding months. We removed remote sensing medians for months without depth-to-groundwater data, which excluded months following March 2023. Furthermore, in months when there were multiple groundwater measurements, we averaged depth-to-groundwater measurements to a singular value. We used R to construct time-series plots that compared trends in depth-to-groundwater, NDVI, and NDMI over the study period.

Rank Regression Analyses

We used the R package "Rfit" to perform rank-based estimation analyses on the association between mean depth-to-groundwater and monthly median NDVI and NDMI values (Torgo 2012). Rank-based regressions are used as a substitute for least-squares regression to protect against the influence of outliers in results. Rfit calculates the regression estimator using Jaeckel's dispersion function instead of minimizing Euclidean distance (Torgo 2012; Jaeckel 1972).

We used the "rfit" function to calculate regression coefficients and p-values of the relationship between depth-to-groundwater and remote sensing indicators (NDVI and NDMI) over the study period. We completed these analyses for all wells and individual wells over the entire study period and overlaid the rank regression functions onto scatter plots.

We separated the data into seasonal categories by month as shown in Table 3.4.4. We isolated the summer values and performed the same analyses as in the complete data set. In the study region, riparian ecosystems are highly productive in summer, and there is little to no precipitation (Garsen et al. 2014; Western Regional Climate Center n.d.). We created the same scatter plots with rank regression slopes for the summer as for the full dataset.

Table 3.4.4. Season groups by month as used in this analysis, with month numbers included. Month groupings were selected based on the start date of each season (equinoxes and solstices; winter: December 21, spring: March 20, summer: June 21, fall: September 20).

Month Grouping	**Month #**	**Season**
December, January, February	12, 1, 2	Winter
March, April, May	3, 4, 5	Spring
June, July, August	6, 7, 8	Summer
September, October, November	9, 10, 11	Fall

Spearman Correlation

Spearman's rank-order correlation is a non-parametric alternative to Pearson correlation and results in a single value (ρ, rho) that indicates the magnitude and direction of the relationship between two ranked variables (Laerd Statistics 2018). Spearman's rho is calculated by assessing monotonic association, rather than a linear relationship, appropriate when analyzing non-parametric data. We used R to calculate Spearman's rank-order correlation values on depth-to-groundwater and remote sensing indicators (NDVI and NDMI) and depth-to-groundwater in all wells and for each individual well. We also determined Spearman correlations for the summer-isolated data.

4. Results

4.1 Lithology

Of the final 61 wells, 29.5% of them had depths of around 61 meters and 14.8% of around 91 meters. For individual wells' plots, see Section 3.1 in the Supplemental Materials. Our resulting cross-sections show lithology can vary greatly with depth even within a single valley. However, after visual inspection some trends become apparent. Cross-sections exhibit an abundance of unconsolidated, coarse-grained layers at shallower depths. In 74% of wells (greater than 61 meters), the uppermost 60 meters of the subsurface was composed of either coarse (Number 1, Table 3.1.1) or mostly coarse material (Number 2, Table 3.1.1). About 8.5% of wells were comprised of fine (Number 4, Table 3.1.1) to mostly fine (Number 5, Table 3.1.1) material in the uppermost 60 meters. There is a relative lack of both consolidated and unconsolidated fine-grained material with few exceptions. Cross-section 1 features the least amount of lithological variability with only one layer of coarse, laterally noncontinuous, consolidated material appearing in Well 12. Cross-sections 2 and 3 exhibit a more significant variability of observed lithologies, notably the presence of more consolidated material and bedrock around 80 to 120 meters depth (Figure 4.1b, Figure 4.1c). The presence of mixed coarse and fine material (Number 3, Table 3.1.1) is difficult to characterize visually. It can appear at both depth and near the surface, however, cross-section 3 has the least amount of mixed material (Figure 4.1c.). Cross-section 3 has the most consolidated material, however, these are not laterally continuous, they appear once or twice and don't seem to connect in adjacent wells. Possible explanations include a lateral thinning of layers near Well 52 and 53.

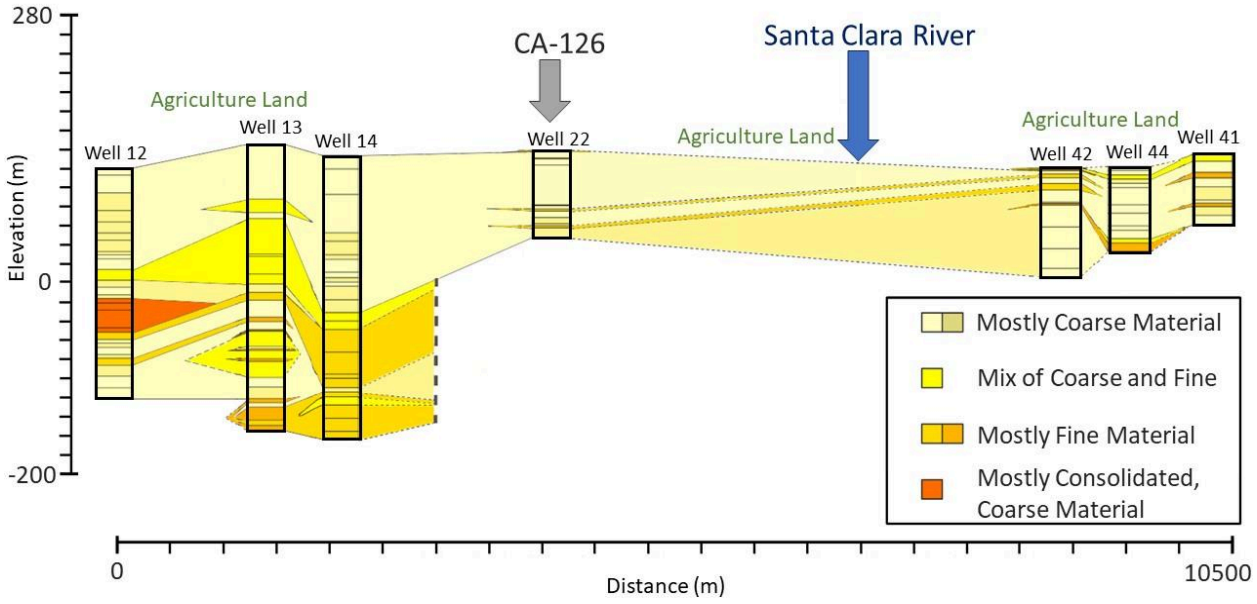

Figure 4.1a. The lithological cross-section of line 1, which travels about 10,500 m from west to east of East Grove. The cross-section consists of the following wells: Well 12 (WCR2010-010156), Well 13 (WCR2004-015524), Well 14 (WCR2010-010413), Well 22 (WCR1998-010940), Well 42 (WCR2006-011431), Well 44 (WCR2016-005853), Well 41 (WCR2007-012988). There are generally few consolidated materials and more abundance of coarse-grained materials above 0 meters in elevation.

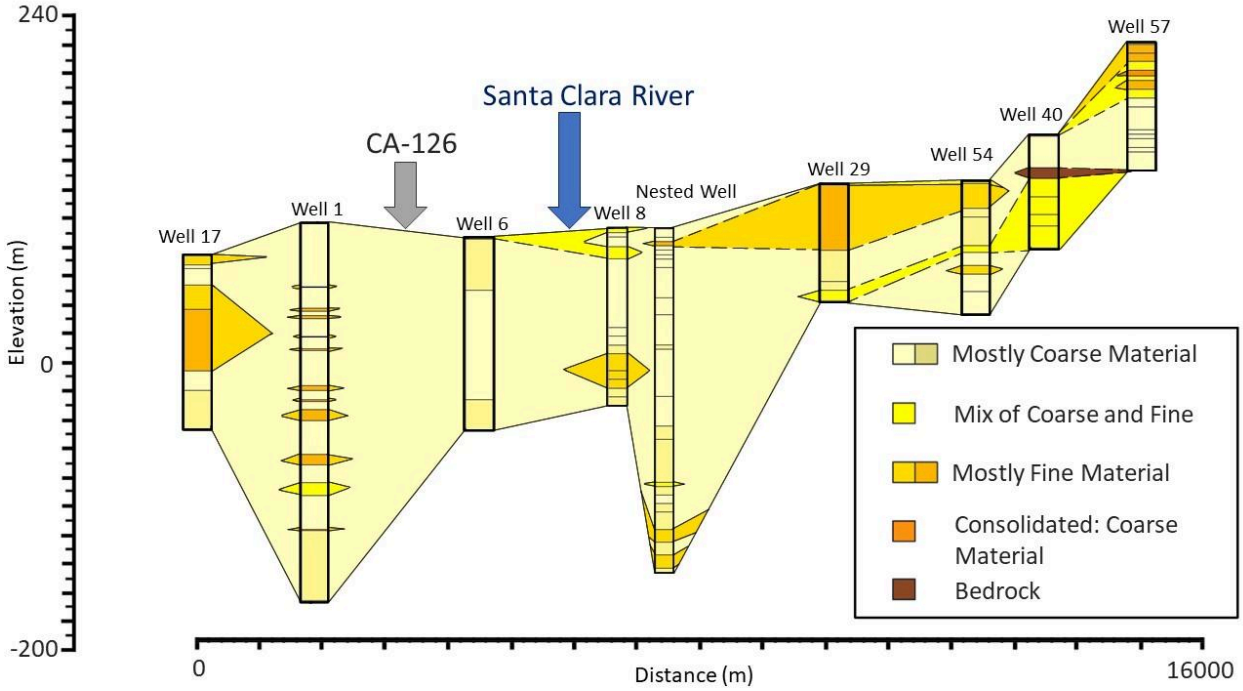

Figure 4.1b.

The lithological cross-section of line 2, that travels about 16,000 m from west to east of East Grove. The cross-section consists of the following wells: Well 17 (WCR2016-008246), Well 1 (WCR2004-015336), Well 6 (WCR2008-011034), Well 8 (WCR2018-009168), Nested Well, Well 29 (WCR2010-010444), Well 54 (WCR2006-013424), Well 40 (WCR1974-004128), Well 57 (WCR0307632). There is a relatively even distribution of wells along the cross-section. Some fine material can be found near the land surface as shown by wells 29, 54, and 57.

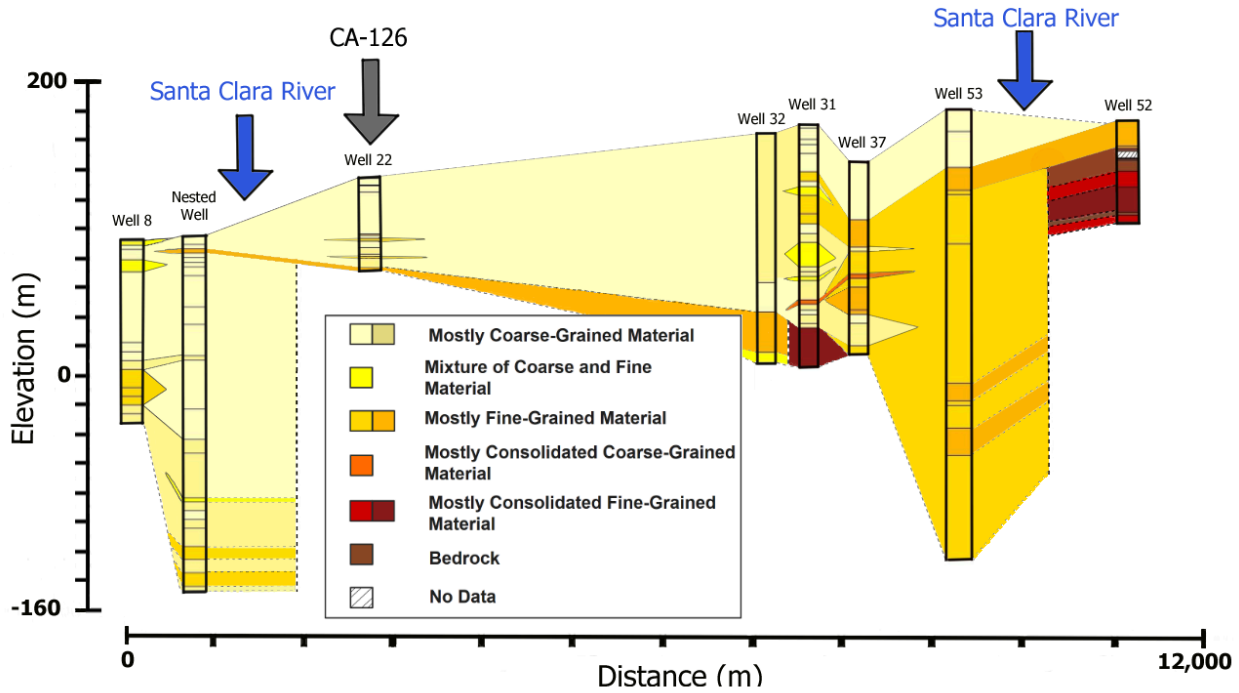

Figure 4.1c.
The lithological cross-section of line 3, that travels about 12,000 m from southwest to northeast of East Grove. The cross-section consists of the following wells: Well 8 (WCR2018-009168), Well 22 (WCR1998-010940), Well 32 (WCR2018-005473), Well 37 (WCR2013-009374), Well 53 (WCR2013-009055), Well 52 (WCR1988-016945). Lithological cross-section line 3 increases approximately 81 meters in elevation from beginning to end. There is a close grouping of wells starting around 7,000 meters. Relatively more consolidated material is present along with some discontinuous strata. However, coarse-grained material remains prevalent.

4.2 Vertical Hydraulic Gradient

A 2-D cross-section was created where one of the deep and shallow wells of the nested well were plotted with their 2023 median water levels (Figure 4.2a). The cross-section schematic is a visual representation of the upward-oriented vertical hydraulic gradient trends experienced between the deep and shallow well at the East Grove nested monitoring site, where the deeper well has a median water level (h_2) that is closer to the land surface than that of the shallow well (h_1).

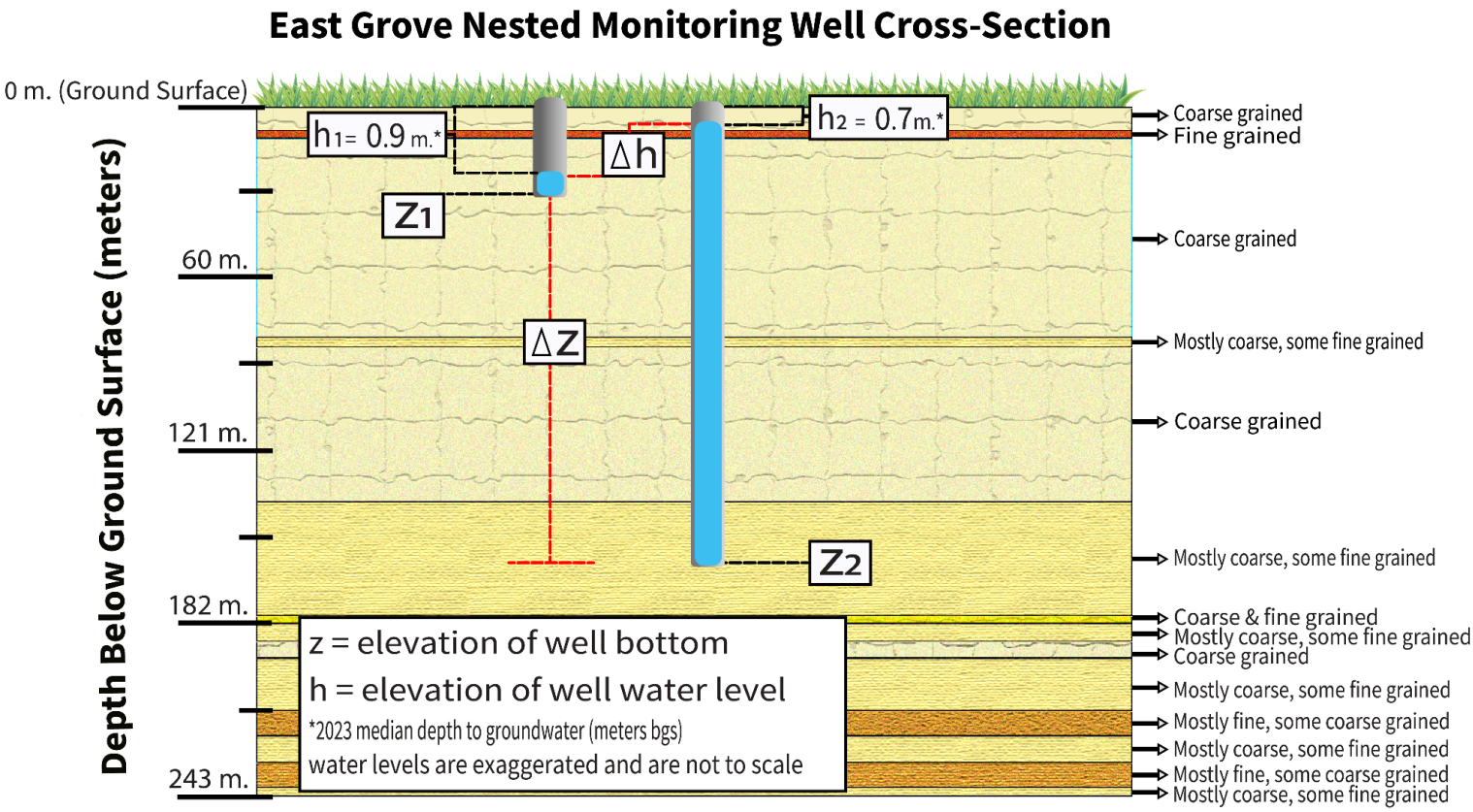

Figure 4.2a. A 2-D schematic of the upward-oriented vertical hydraulic gradient trends experienced between the deep and shallow well at the East Grove nested monitoring well site (located at 34.362 °N, -118.996 °W). h_1 and h_2 represent the 2023 median water level in meters below ground surface for the shallow and deep well respectively. The change in head, or the difference between h_1 and h_2, is represented as Δh. The change in vertical distance between the two wells, or the difference between z_1 and z_2, is represented as Δz. z_1 is referencing the total well depth of the shallow well at 31 meters below ground surface (100 feet) and z_2 is the total well depth of the deep well at 161 meters below ground surface (530 feet). The surrounding lithology consists of coarse to mostly coarse-grained material, with fine to mostly fine-grained material appearing below 200 meters.

Out of the nine calculated vertical hydraulic gradients, eight of the calculations were negative (Figure 4.2b). A negative $\Delta h/\Delta z$ represents an inverse correlation between the change in head (Δh) and the change in vertical distance (Δz). This would imply that a lower elevation head results in a higher hydraulic head. This relationship is consistent with the hydrologic behavior of a gaining river reach, or an area experiencing groundwater upwelling. Gaining streams are areas in a drainage basin where groundwater can naturally flow upwards towards the surface. This upward-flow dynamic is also called groundwater discharge or "baseflow" (Batelaan et al. 2003). In these gaining reaches, groundwater levels tend to naturally reside at shallower depths, closer to the land surface.

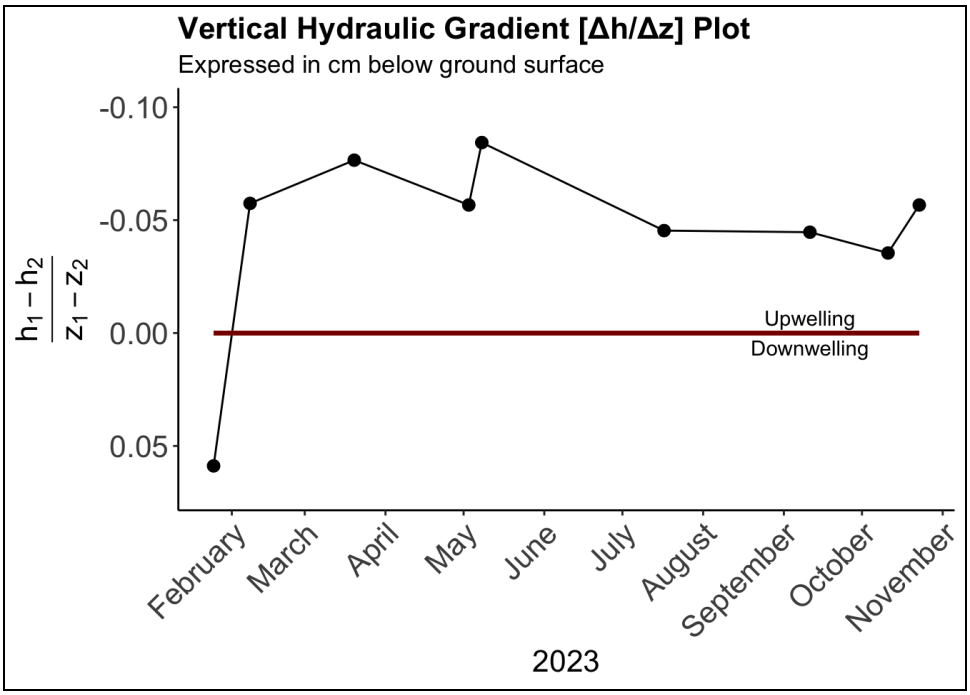

Figure 4.2b Graphical representation of the 2023 vertical hydraulic gradients (Δh/Δz) at the East Grove nested monitoring well site. The change in hydraulic heads is denoted as **Δ**h and the change in vertical distance is denoted as **Δ**z. The variable h_1 corresponds to a depth-to-groundwater measurement taken at the shallow well on a specific date, while h_2 represents a measurement taken at the deep well on the same date. Similarly, z_1 and z_2 correspond to the total well depths of the shallow and deep well, respectively. Each data point on the graph reflects the calculated magnitude of the vertical hydraulic gradient on a particular date. Negative vertical hydraulic gradients are plotted above the red horizontal line, which serves as the threshold. The threshold distinguishes between magnitudes indicating events of "downwelling" (a downward-oriented vertical hydraulic gradient) and "upwelling" (an upward-oriented vertical hydraulic gradient).

4.3 Groundwater Trends

4.3.1 Time-Series Analysis

UCSB Shallow Monitoring Wells

Figure 4.3.1a is a histogram of depth-to-groundwater measurements for all wells over the study period. It is skewed to the right, and values between 50 and 120 centimeters are the most common. Values between -5 and 5 centimeters were the second-most common depth measurement.

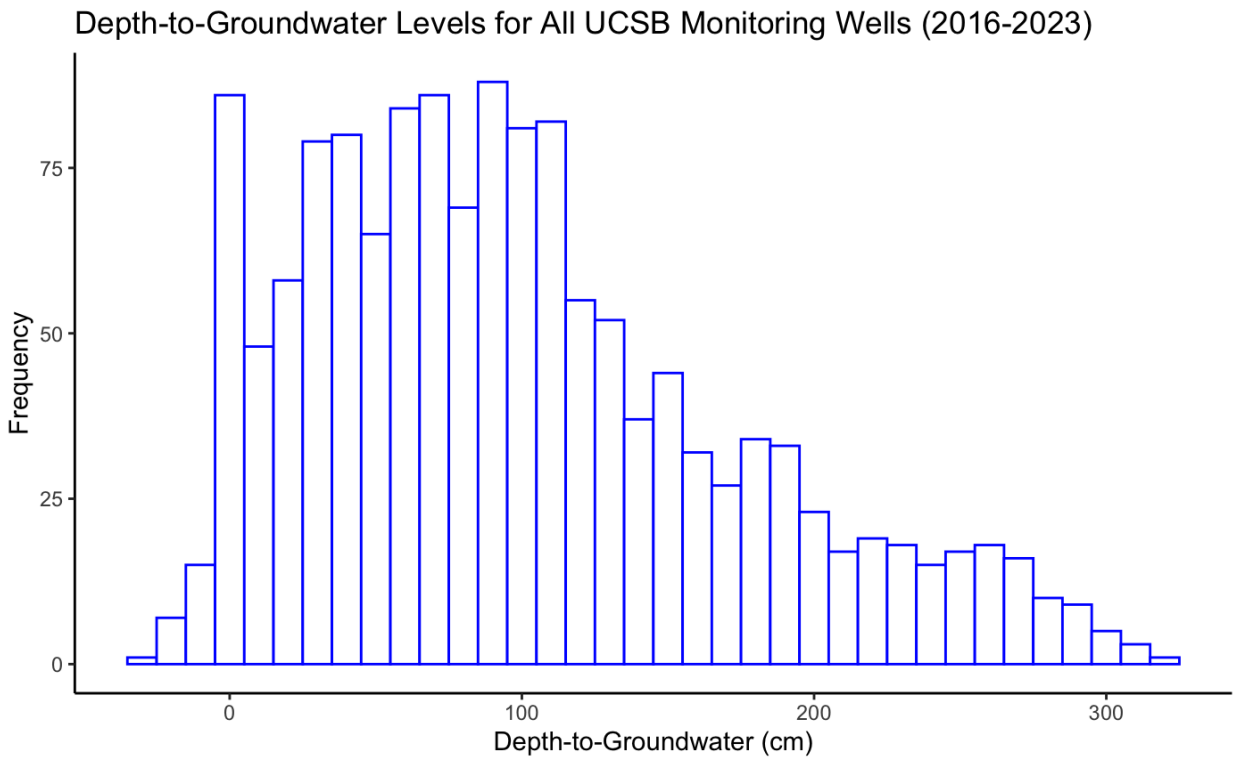

Figure 4.3.1a. Histogram of 1,414 depth-to-groundwater measurements in all UCSB wells December 2015 to March 2023, with a bin-width of 10. The median depth-to-groundwater measurement was 89 centimeters and mean of 100 centimeters. The maximum depth and minimum depth were 320 centimeters and -30 centimeters, respectively. 50% of the values fell between 41 and 143 centimeters.

depth-to-groundwater measurements in each of the 21 UCSB monitoring wells varied greatly over the study period (Figure 4.3.1b). Measurements were often taken on the same day at different wells, leading to overlap between points (Figure 4.3.1b). The deepest depth-to-groundwater measurement was 320 centimeters, measured on January 10, 2017, at Hedrick Ranch Preserve Well #4. The greatest height of standing water above ground level was -30 centimeters, measured on April 20, 2020 in Ventura County Watershed Protection District's Well #8. The mean depth-to-groundwater measurement was 100 centimeters, and the median measurement was 89 centimeters.

Periods of high precipitation were found to have a qualitative association with water-level rise (Figure 4.3.1c). Each high precipitation interval is followed by a drop in depth-to-groundwater; this is prominent when looking at individual well plots such as Well HRP 1 (Figure 4.3.1d).

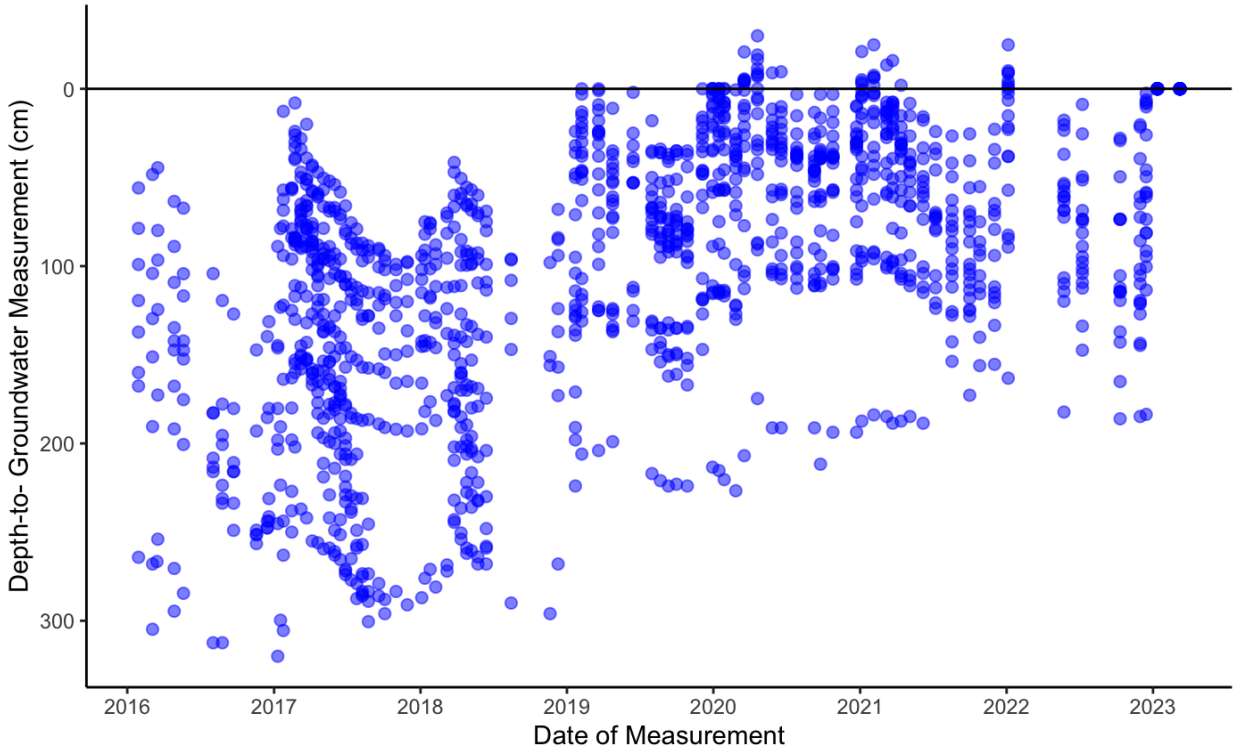

Figure 4.3.1b. All depth-to-groundwater measurements (1,414 total measurements) taken by the UCSB team in the East Grove shallow groundwater monitoring wells from December 2015 to March 2023. Values are often clustered, reflecting patterns of groundwater levels in the shallow aquifer. The extreme drought in California between 2013 and 2017 is reflected in the plot, where groundwater levels are deeper on average in 2016 and 2017 than in periods following heavy rains (2019-2023).

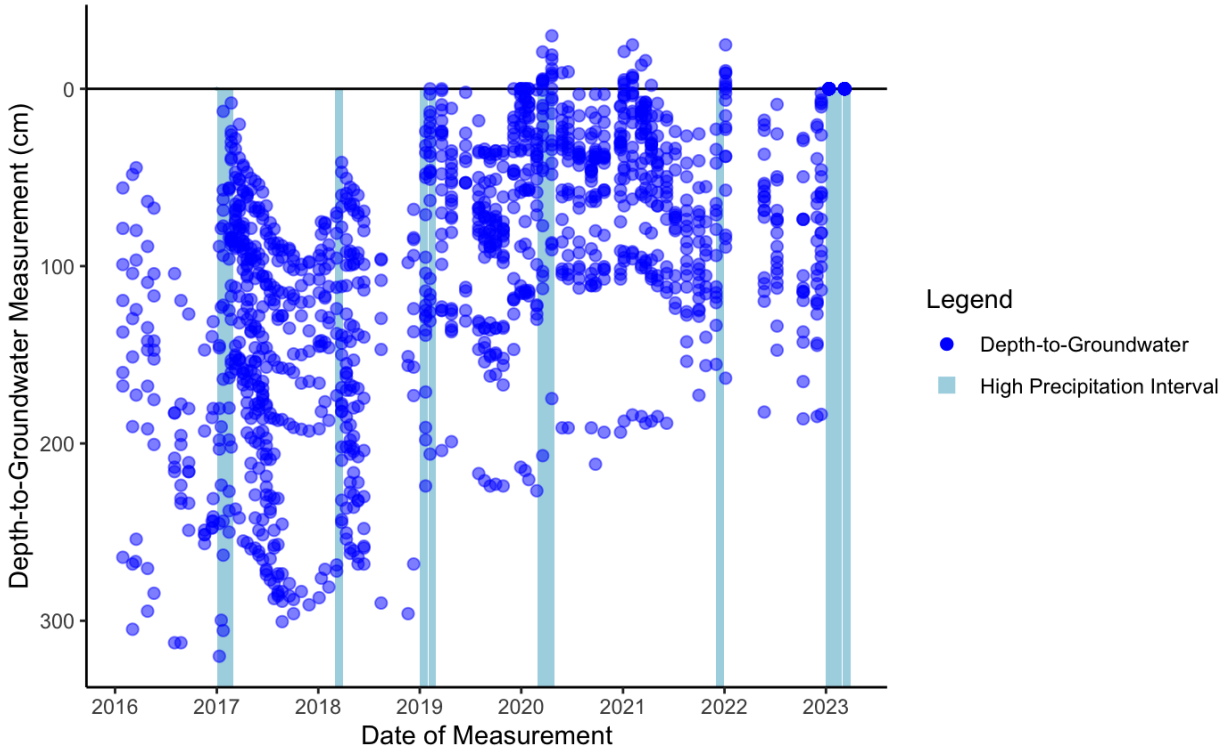

Figure 4.3.1c. All depth-to-groundwater measurements for all UCSB wells during the study period December 2015 to March 2023. High precipitation intervals are months with total precipitation greater than one standard deviation above the mean. This plot displays a pattern, where groundwater levels are shallower during and after high precipitation intervals. This suggests a relationship between precipitation and groundwater storage.

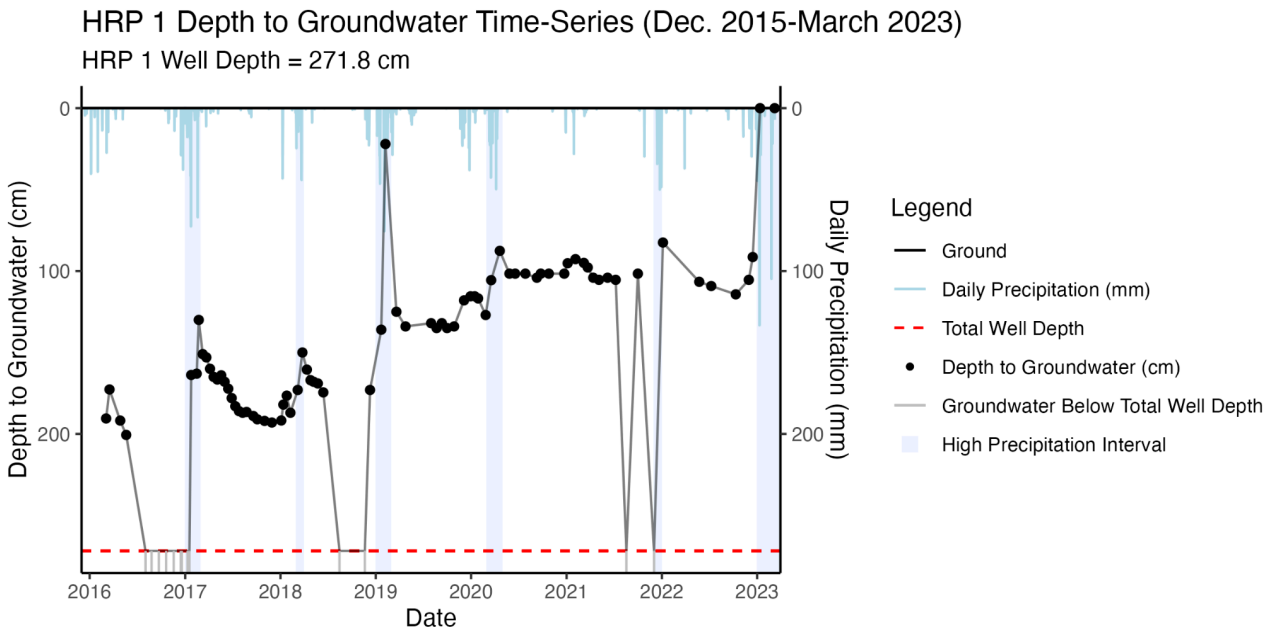

Figure 4.3.1d. Depth-to-groundwater time-series plot for Hedrick Ranch Preserve Well #1, including total well depth, daily precipitation, and high precipitation intervals—months with total precipitation greater than one standard deviation above the mean. Gray bars below the red dashed line represent dates when researchers recorded "no water" at the well, meaning that depth-to-groundwater was below the total well depth and was thus unknown. See Supplemental Materials, Section 3.2.1 for all time-series graphs for the East Grove monitoring wells.

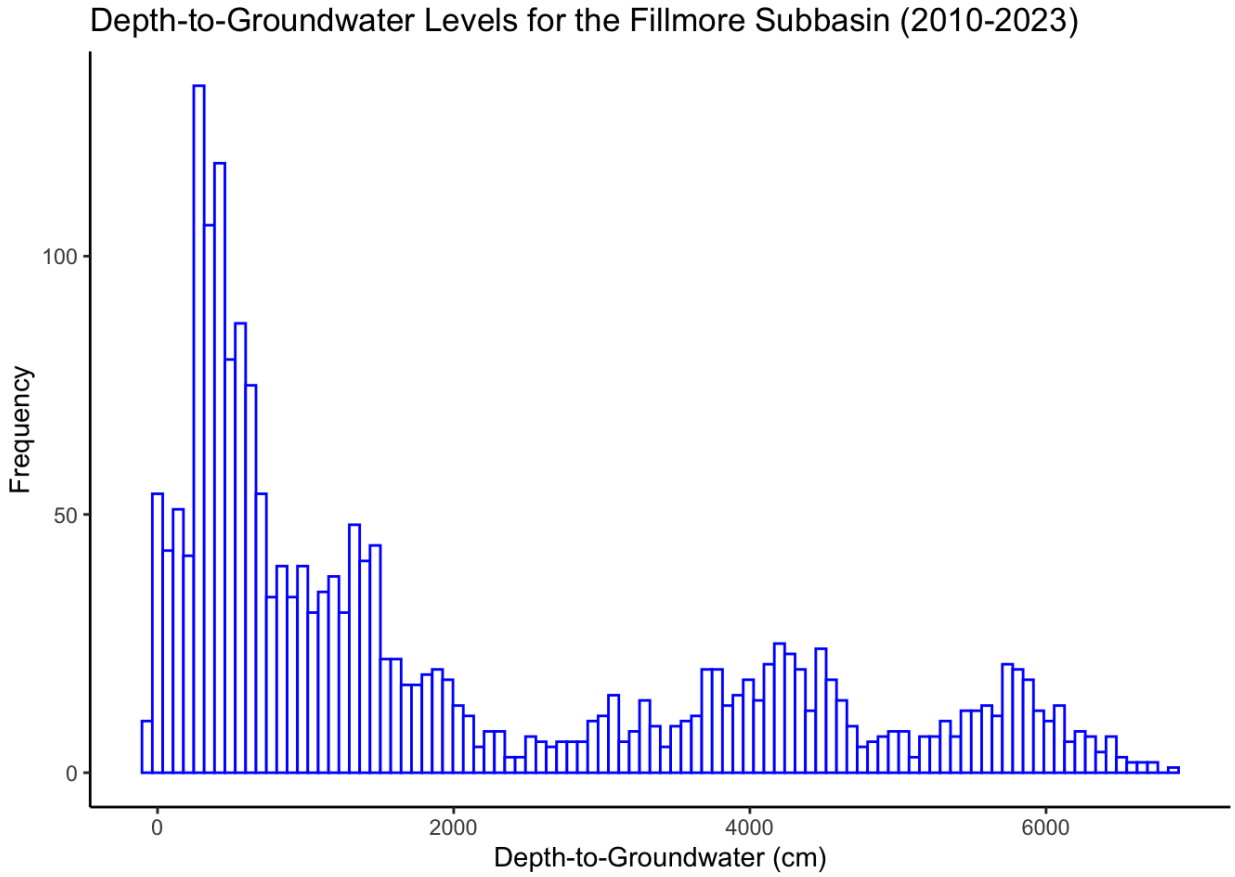

Figure 4.3.1e. Histogram of 2,118 depth-to-groundwater measurements in all 22 Fillmore Subbasin wells from 2010 to 2023. (Bin-width = 70). The maximum and minimum depths were 6,848 centimeters and -71 centimeters, respectively. 50% of the values fell between 436 centimeters and 3601 centimeters. The median depth-to-groundwater is 1143 centimeters.

All recorded depth-to-groundwater for the Fillmore wells were plotted (Figure 4.3.1f). Depth-to-groundwater measurements in each of the 22 Fillmore wells varied over the 2010 to 2023 study period, with larger values (indicating lower/deeper groundwater levels) during the 2016 to 2019 drought and early drought recovery period.

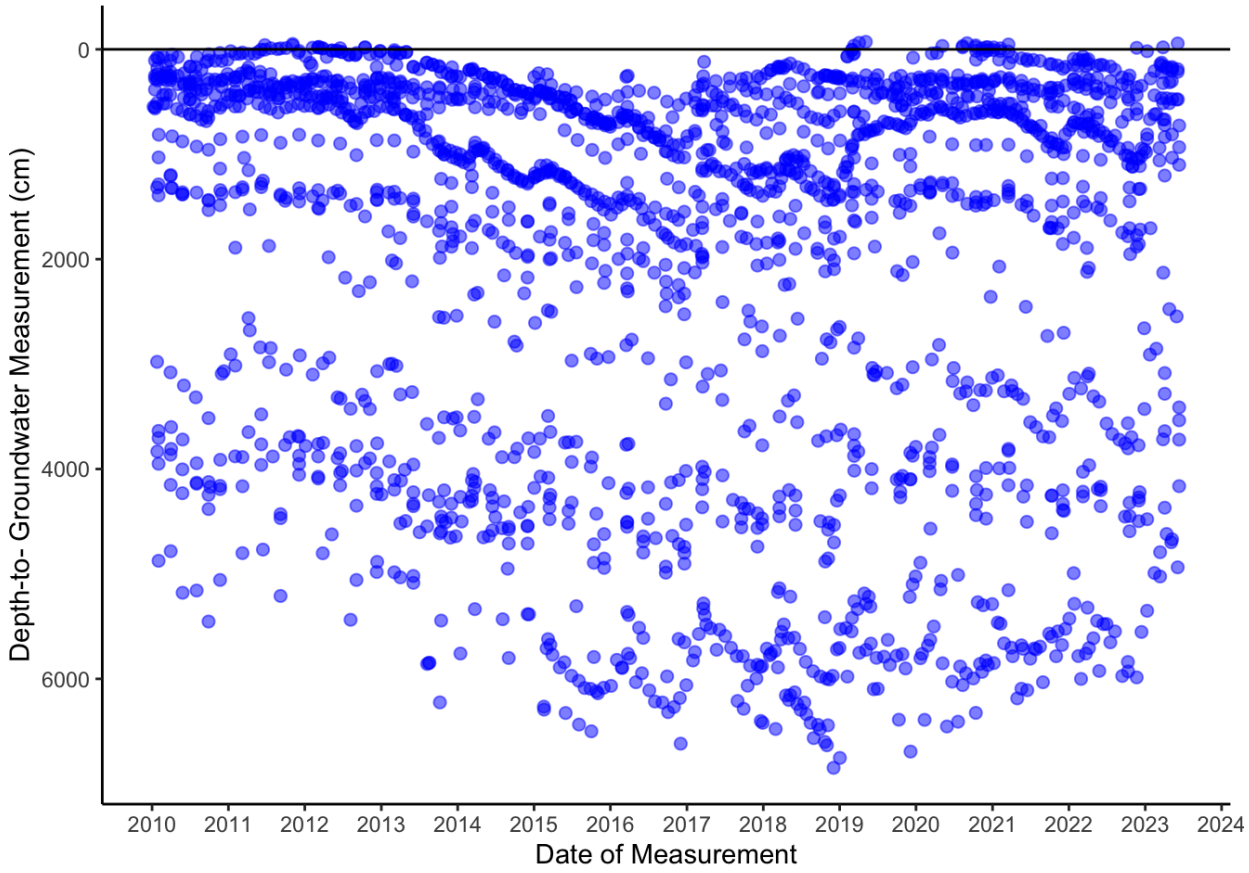

Figure 4.3.1f. All depth-to-groundwater measurements for the Fillmore Subbasin wells from January 2010 to March 2023, accessed via the SGMA data viewer. The deepest depth-to-groundwater measurement was 6,848 centimeters (224.68 feet), measured on December 3, 2018, at the Fillmore 9 well. The greatest height of standing water in the well casing (above ground level) was -71 centimeters (-2.34 feet), measured on May 6, 2019, at the Fillmore 5 well. The mean depth-to-groundwater measurement was 1,951 centimeters (64 feet) and the median measurement was 1143 centimeters (37.5 feet).

Time-series graphs were plotted for each of the 22 Fillmore Wells (see Supplemental Materials, Section 3.2 for all time-series graphs). The subtitles of these graphs include additional information about each well, including the well type (Irrigation, Residential, Observation, or an Unknown well), the reported total well depth, and the site code of each well (a unique identifier provided by the Department of Water Resources). The graph is reversed so that ground level is shown at the top in black, and total well depth near the bottom of the graph is represented by a red dashed line (see Figure 4.3.1g below as an example). For wells with unknown total well depths, a dashed blue line was utilized to represent the maximum recorded depth-to-groundwater measurements during the specified time period (refer to Figure 4.3.1h for a visual example). Additionally, the legend series includes the "Max Recorded DTG" to denote the maximum

recorded depth-to-groundwater in meters (Figure 4.3.1h). As a reference for each well's location, please refer to Figure 3.3.1b.

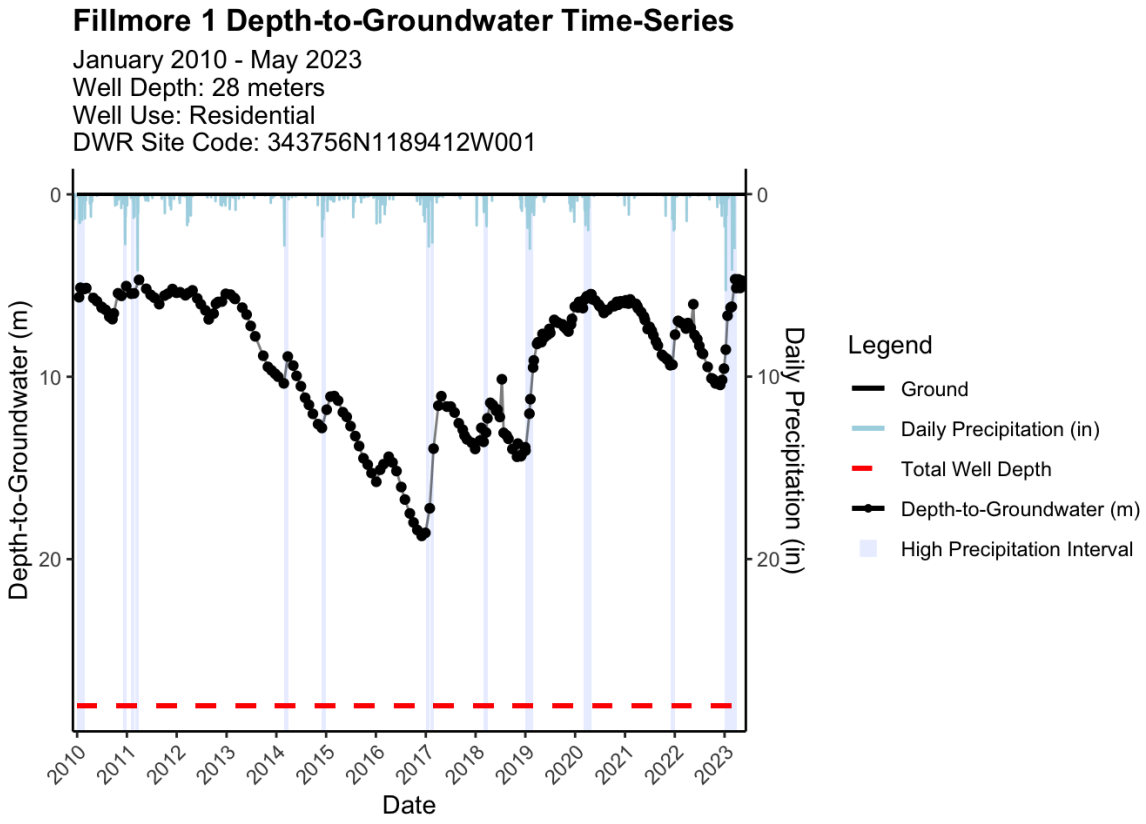

Figure 4.3.1g. Depth-to-groundwater time-series plot for Fillmore Well 1 located including the total well depth, daily precipitation, and high precipitation intervals—months with total precipitation greater than one standard deviation above the mean. Daily precipitation values in inches are shown as light blue lines coming from the top of the graph, corresponding to dates on the x-axis and estimates of precipitation in inches on the right y-axis. The known total well depth of this residential supply well is 28 meters below the ground surface.

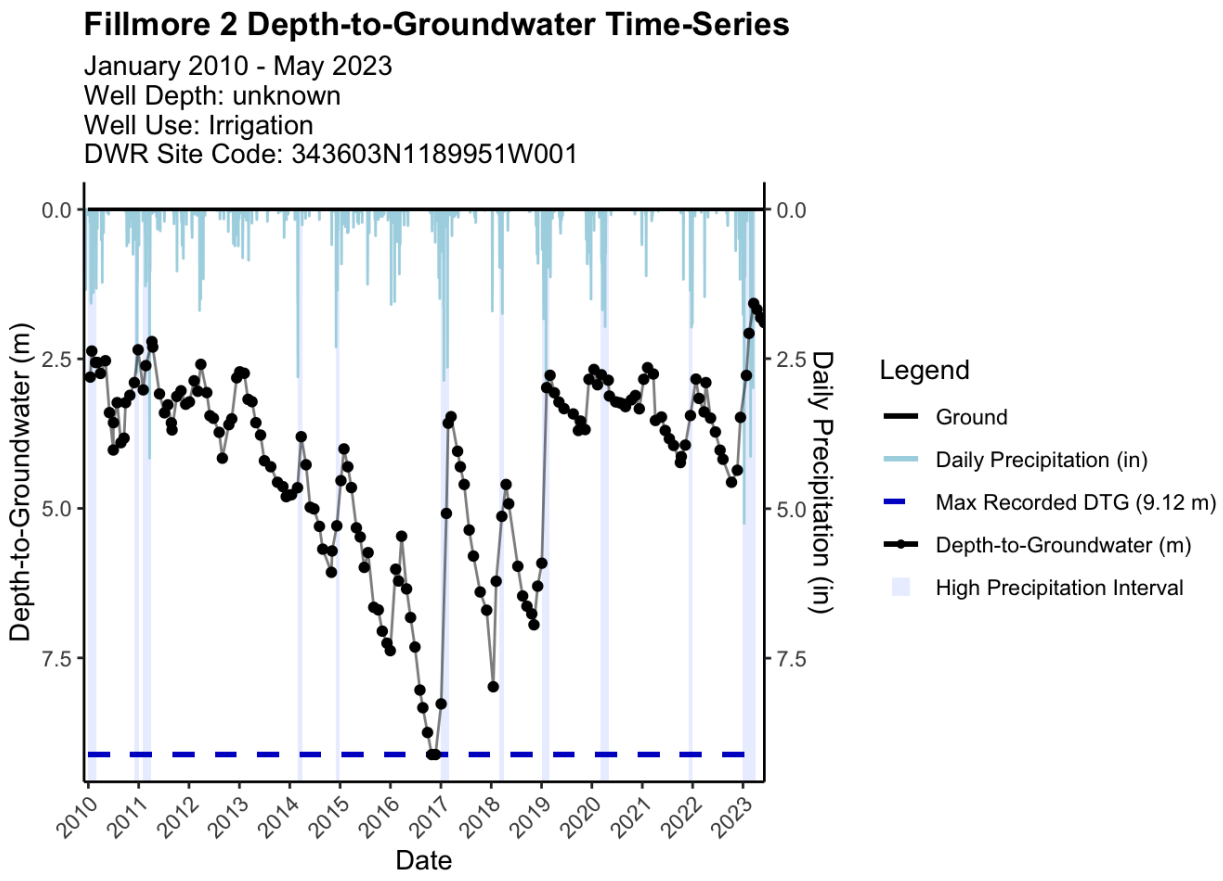

Figure 4.3.1h. Depth-to-groundwater time-series plot for Fillmore Well 2 located on the south border of East Grove, including an unknown total well depth, daily precipitation, and high precipitation intervals—months with total precipitation greater than one standard deviation above the mean. Daily precipitation values in inches are shown as light blue lines coming from the top of the graph, corresponding to dates on the x-axis and estimates of precipitation in inches on the right y-axis. The total well depth of this irrigation well is unknown, therefore the maximum depth-to-groundwater measurement at 9.12 meters below ground surface was used and represented by the blue dashed line at the bottom of the graph. This maximum depth-to-groundwater value was recorded in 2017, during the 2012–2019 California drought.

4.3.2 Water-Level Rise

East Grove Shallow Groundwater Monitoring Wells

Water-level rise events for all wells during the study period are displayed in a histogram (Figure 4.3.2a). Water-level rise was most commonly between 0.1 and 15 centimeters during a single event. Larger jumps in water level are less frequent, showing that smaller amounts of water-level rise are far more common.

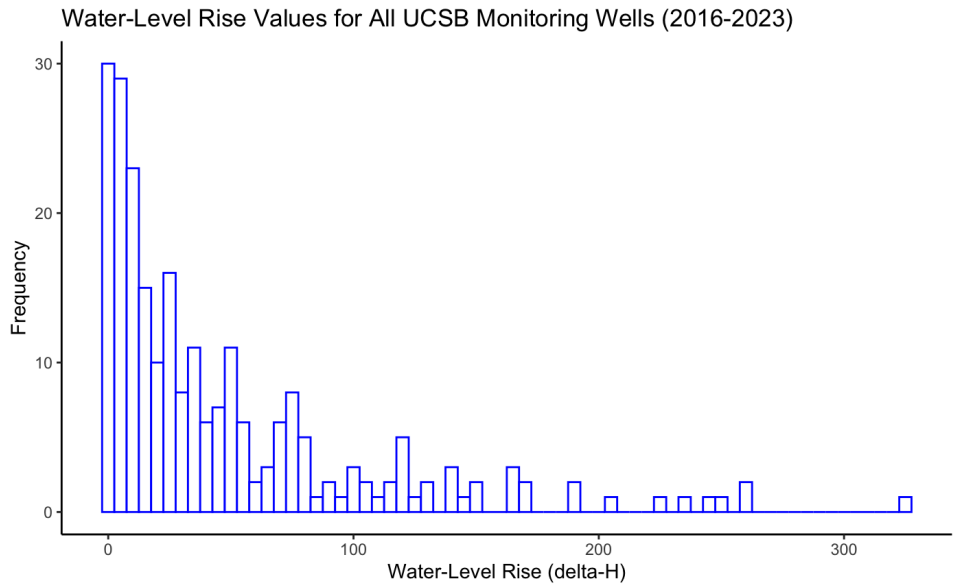

Figure 4.3.2a. Histogram of water-level rise (delta-H) values for all wells for all recharge events 2016 to 2023 (bin-width=5). Water-level rise values for individual water-level rise events for the East Grove UCSB shallow groundwater monitoring wells range from 0.2 centimeters to 323 centimeters, with a median of 27 centimeters. Water-level rise in all recharge events has a right-skewed distribution. Furthermore, the recharge events happened over varying lengths of time, ranging from 8 to 644 days (median = 51 days).

To analyze how water-level rise was associated with precipitation, we completed a Theil-Sen regression for all East Grove shallow groundwater monitoring wells (Figure 4.3.2b). The regression resulted in a linear regression with a slope of 2.09 and a p-value less than 0.0001. The slope represents the median ratio between water-level rise and precipitation, i.e., each centimeter of precipitation leads to 2 centimeters of water-level rise. The y-intercept was not statistically significant.

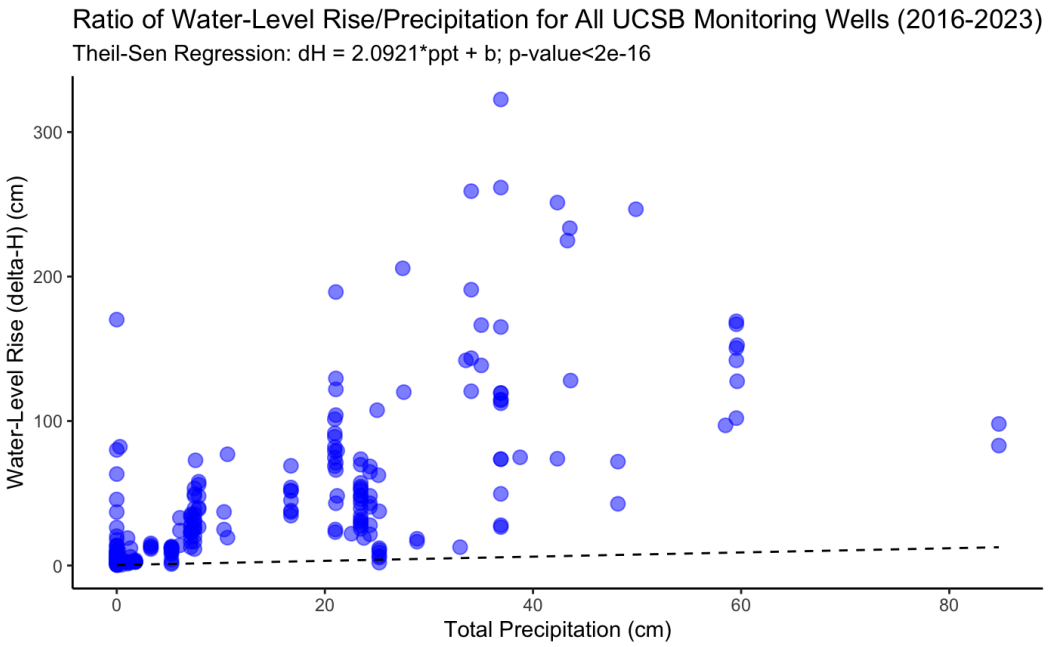

Figure 4.3.2b. Theil-Sen regression plot of the ratio between water-level rise (delta-H) and precipitation in all water-level rise events calculated for East Grove UCSB shallow groundwater monitoring wells during the study period. Theil-Sen regression is robust and resists influence from outliers. Thus, the association between the two variables is not as strong as it would be if a least-squares linear regression was used. There are some outliers in extremely high water-level rise and precipitation, due to some cases of very long time intervals between valleys and peaks. On average, 1 centimeter of precipitation leads to approximately 2 centimeters of water-level rise (slope=2.09, $p<0.0001$).

Separate Theil-Sen regression analyses were completed for each of the East Grove UCSB shallow groundwater monitoring wells (see Supplemental Materials, Section 3.2.2 for all regression plots). Results of the Theil-Sen regression (ratios of delta-H/precipitation) for the 20 UCSB shallow groundwater monitoring wells throughout East Grove were mapped in ArcGIS (Figure 4.3.2c).

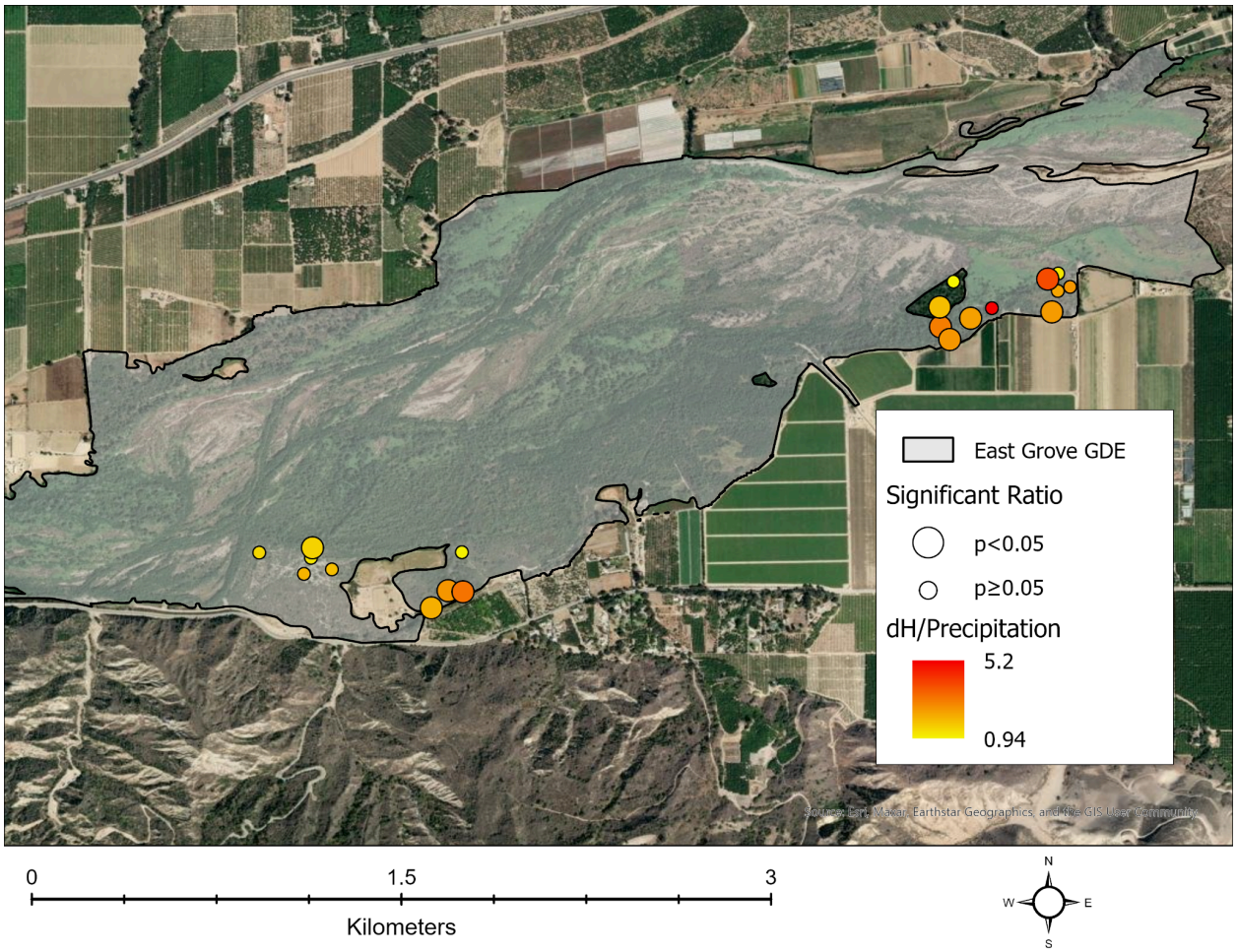

Figure 4.3.2c. Map of East Grove UCSB shallow groundwater monitoring wells, differing by their median Theil-Sen regression slopes of water-level rise (delta-H) to precipitation for individual recharge events, shown with a yellow to red gradient. Wells with significant Theil-Sen regressions are indicated with larger circles than wells without significant regressions. Higher slopes are clustered in the east, while lower slopes are more common in the west. This may result from differing soil types leading to variations in water-level rise, or differences in surface processes such as runoff or river flow.

Fillmore Subbasin Wells

Water-level rise values for individual recharge events of the 22 Fillmore Subbasin wells range from 0.3 centimeters (0.003 meters) to 1,669 centimeters (16.69 meters), with a median of 163 centimeters (1.63 meters). Water-level rise in all recharge events has a right-skewed distribution (Figure 4.3.2d).

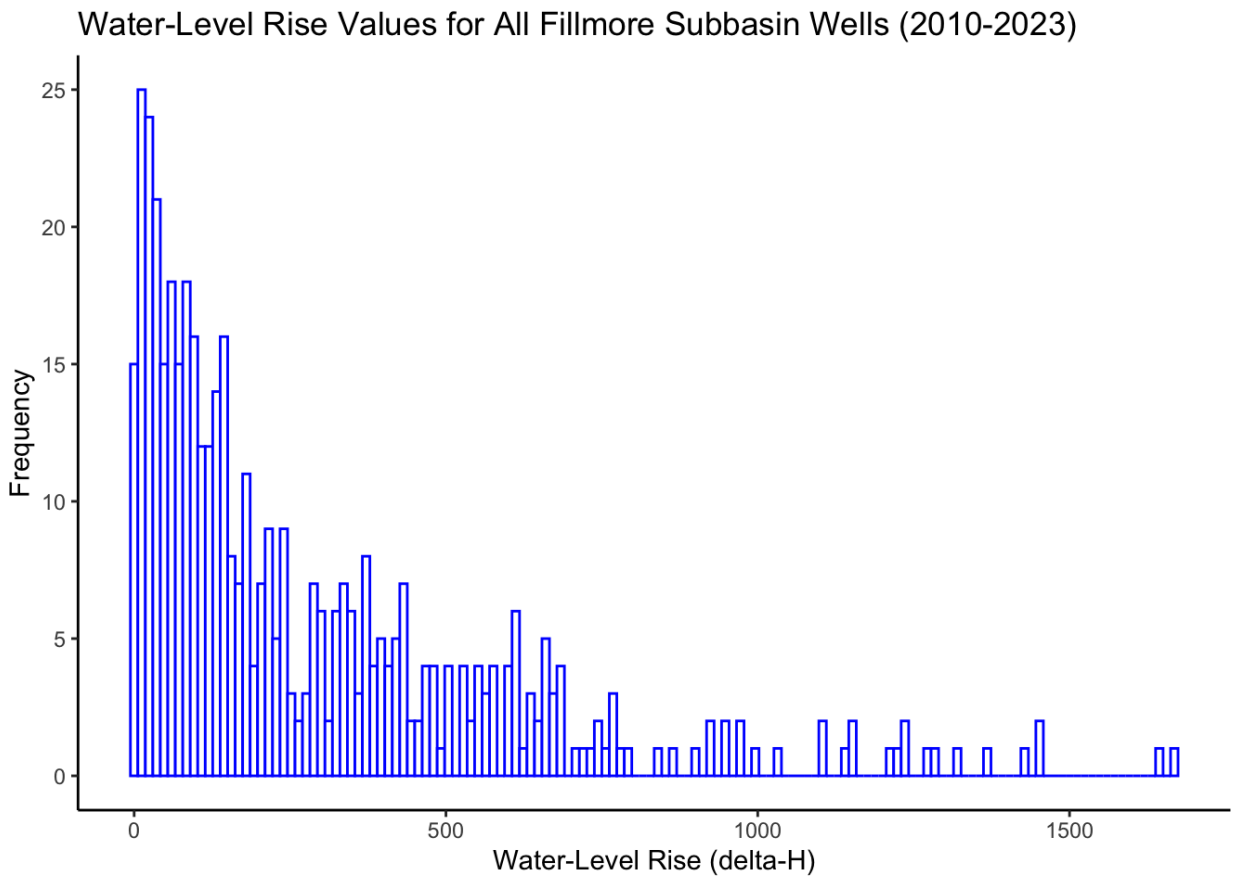

Figure 4.3.2d. Histogram of water-level rise (delta-H) values for all 22 Fillmore Subbasin wells for all recharge events 2010 to 2023 (bin-width=12). Water-level rise values for individual recharge events of the 22 Fillmore Subbasin wells range from 0.3 centimeters (0.003 meters) to 1,669 centimeters (16.69 meters), with a median of 163 centimeters (1.63 meters). The distribution of water-level rise in all recharge events is right-skewed.

Theil-Sen regressions were performed between water-level rise and total daily precipitation for all 22 wells in the Fillmore Subbasin during the 2010 to 2023 time series. The regression for the water-level rise (delta-H) and precipitation in all recharge events was plotted (Figure 4.3.2e). Theil-Sen plots for all wells can be found in Supplemental Materials, Section 3.2.2.

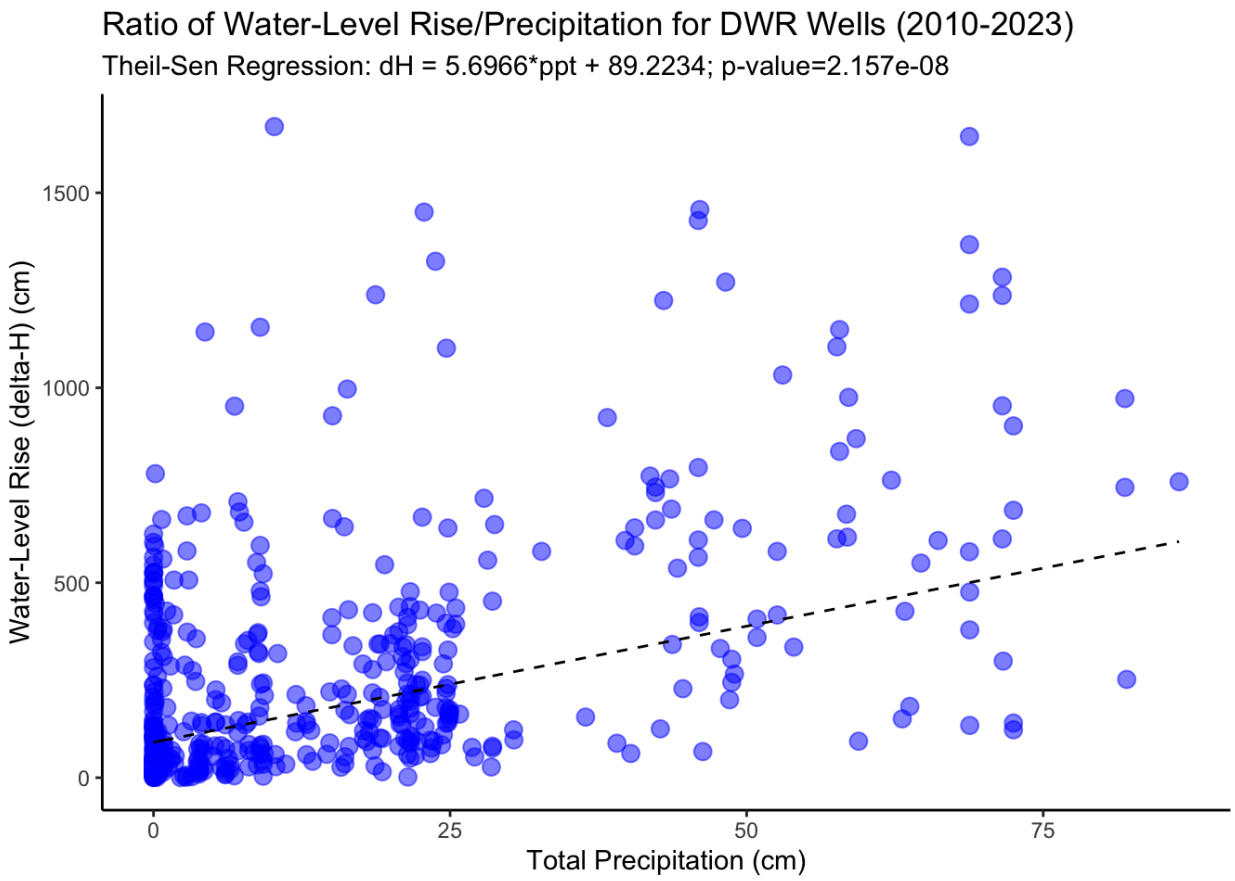

Figure 4.3.2e. Theil-Sen regression plot of the ratio between water-level rise (delta-H) and precipitation in all recharge events for all 22 wells in the Fillmore Subbasin. Theil-Sen regression is robust and resists influence from outliers. Thus, the association between the two variables is not as strong as it would be if a least-squares linear regression was used. The slope of 5.7 represents the median ratio between water-level rise and precipitation, i.e. each centimeter of precipitation leads to 5.7 centimeters (0.057 meters) of water-level rise (y-intercept=89.223, $p<0.0001$). The association is statistically significant. Theil-Sen plots for all wells can be found in Supplemental Materials, Section 3.2.2.

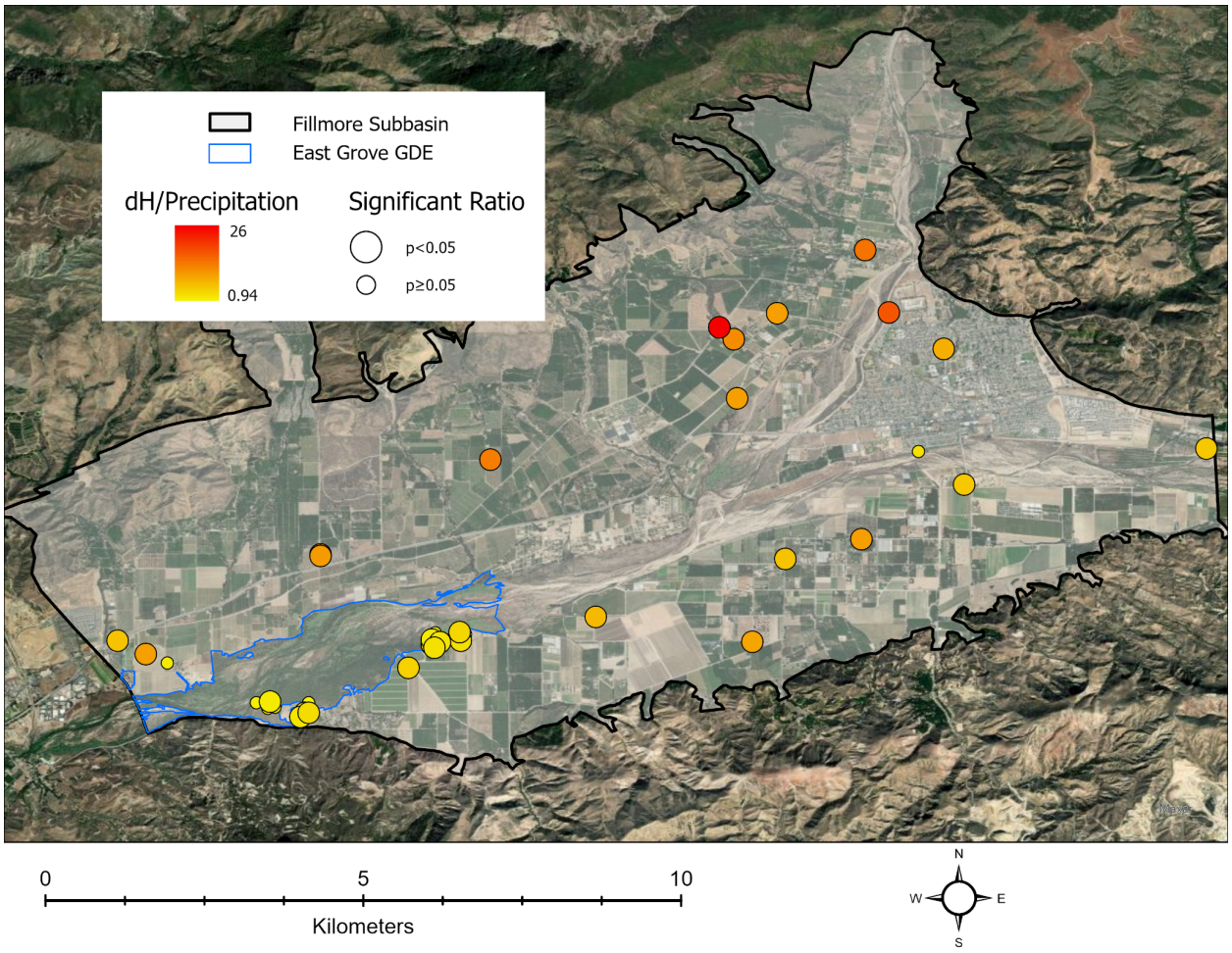

Figure 4.3.2f. Map of East Grove (blue outline) UCSB shallow groundwater monitoring wells and all Fillmore Subbasin (black outline) wells, differing by their median Theil-Sen regression slopes of water-level rise (delta-H) to precipitation for individual recharge events, shown with a yellow to red gradient. Wells with significant Theil-Sen regressions are indicated with larger circles than wells without significant regressions. Deeper wells had significantly higher regression slopes than shallow groundwater monitoring wells, as shown by the clustering of smaller slopes within East Grove. Wells to the north had higher ratios between water-level rise and precipitation, ranging to 26 centimeters of water-level rise per 1 centimeter of precipitation. These high numbers could result from many confounding factors, including well depth, surface processes, pumping effects, or specific yields of different soil types.

Trend Comparison

The ratio slopes for water-level rise to precipitation events generated in the Thiel-Sen regressions varied significantly between the East Grove shallow monitoring wells and the 22 wells in the Fillmore Subbasin (Figure 4.3.2f). The regression output generated a mean ratio slope of 2.26 and 8.86 for the East Grove monitoring wells and the Fillmore Subbasin wells respectively. This

indicates that the Fillmore wells are more responsive to increases in precipitation, where one centimeter of precipitation leads to an average of 8.86 centimeters of water-level rise at the Fillmore wells, and leads to an average of 2.26 centimeters of water-level rise at the East Grove wells. This variation in slopes is likely caused by hydrologic modifications from groundwater pumping, as much of the Fillmore wells are production wells. Additionally, the 22 Fillmore wells are located at varied depths (see Section 3.2 in Supplemental Materials for total well depths) and location around the subbasin, and are not fixed around East Grove (Figure 3.3.1b). The difference in geology among the Fillmore Wells may also be an influencing factor (see Section 4.1 above for the subbasin's common lithology characteristics).

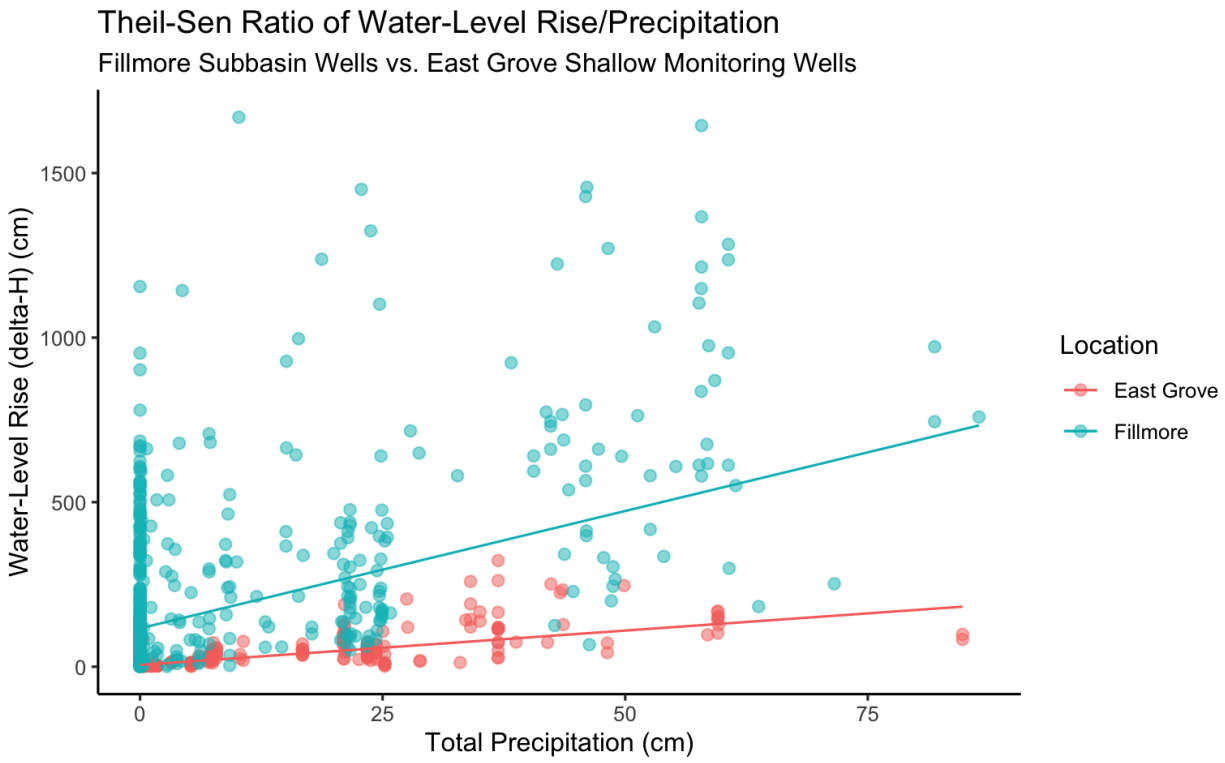

Figure 4.3.2f. Theil-Sen regression calculations for East Grove monitoring wells and Fillmore Subbasin production and monitoring wells. There was a significant Theil-Sen regression for both groups. The regression indicates that one centimeter of precipitation corresponds with roughly 2 centimeters of water-level rise in the East Grove shallow wells. However, one centimeter of precipitation corresponds to roughly 8 centimeters of water-level rise at the Fillmore wells.

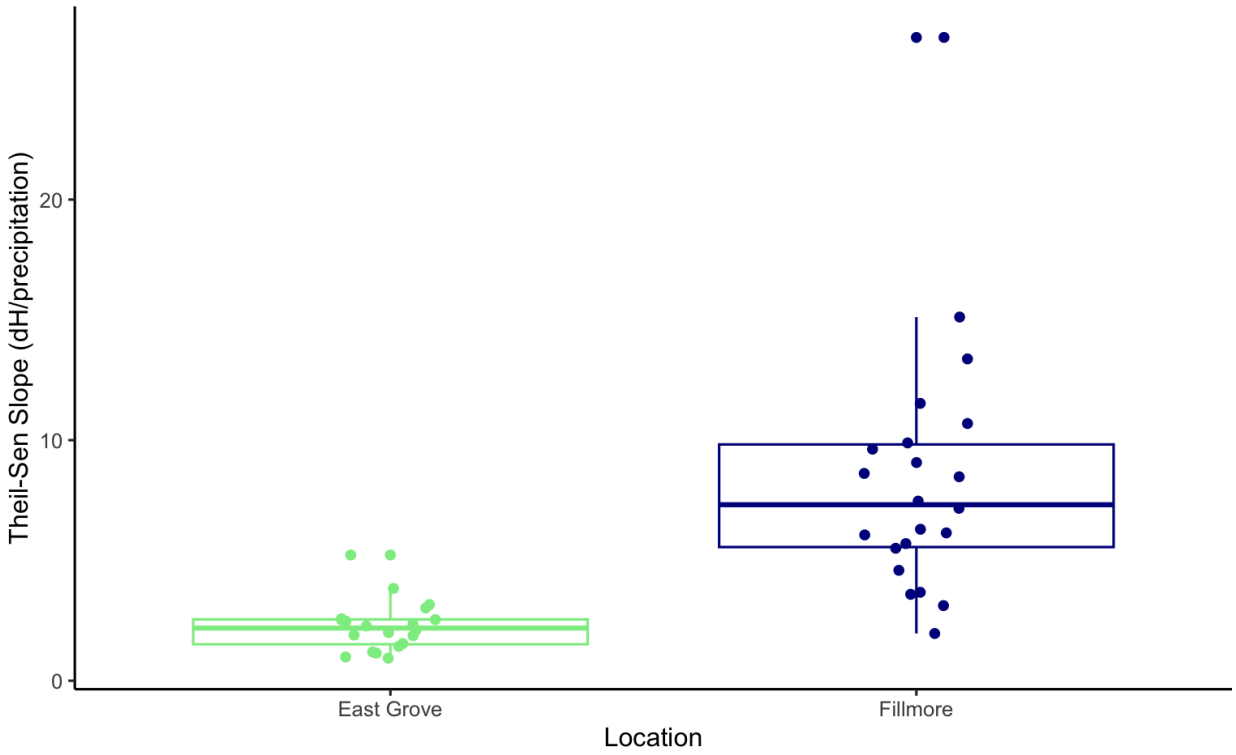

Figure 4.3.2f. Boxplot comparing Theil-Sen regression values of water-level rise to precipitation between the East Grove shallow groundwater monitoring wells and the deeper wells in the Fillmore Subbasin (outside of East Grove). There is a statistically significant difference in Theil-Sen ratios between the two groups (t-test: $t=-5.32$, $df=22.8$, $p<0.0001$). The mean ratios were 2.26 and 8.87 for East Grove and Fillmore wells, respectively. Various confounding factors could lead to this difference, including well depth, lack of specific yield, elevation, and relative distance from the Santa Clara River.

4.4 Remote Sensing

4.4.1 NDVI

Table 4.4.1. East Grove seasonal median NDVI values for the years 2016 to 2023. Winter values were the lowest of all the seasons from 2016 to 2023, due to plant senescence. Summer yielded the highest values, indicating peak productivity due to high vegetative greenness.

	2016	2017	2018	2019	2020	2021	2022	2023
Winter	0.25	0.20	0.24	0.21	0.34	0.35	0.37	0.22
Spring	0.46	0.40	0.36	0.45	0.54	0.49	0.47	0.32
Summer	0.37	0.45	0.42	0.57	0.61	0.54	0.56	0.55
Fall	0.25	0.39	0.37	0.53	0.54	0.51	0.50	0.47

Seasonal NDVI values for the years 2016 to 2023 were calculated from the composite images created in Google Earth Engine (Table 4.4.1). In the summer months of 2017, 2019, 2020, and 2022, NDVI increases from the previous year correlated with increased rainfall during the winter months (Figure 4.3.1d). Vegetation greenness in the summer increased during the wet years and decreased during the dry years.

Trends of changes in seasonal NDVI over time were calculated using Theil-Sen regression. This was plotted with trend lines showing NDVI changes for the fall, winter, spring, and summer seasons within a 100 m radius buffer for each shallow groundwater monitoring well (Figure 4.4.1a). NDVI values for each season in 2023 were lower than the previous year, which may be due to reduced vegetation as a result of increased surface flows (Figure 2.4.3a). However, further analysis of land cover type will be required to determine changes in vegetative cover over time. Fall trends showed a significant increase in NDVI over the study period (Theil-Sen regression: slope=2.898e-05, p-value=0.0003). Winter trends also had a significant increase in NDVI (Theil-Sen regression: slope=1.548e-05, p-value=0.03). Both spring and summer NDVI trends had a p-value of less than 0.0001, indicating a significant increase (spring Theil-Sen regression: slope=5.014e-05, p-value<0.0001; summer Theil-Sen regression: slope =7.169e-05, p-value<0.0001). Across all seasons, vegetative greenness has increased substantially since the year 2016, indicating potential for improved vegetation health within East Grove.

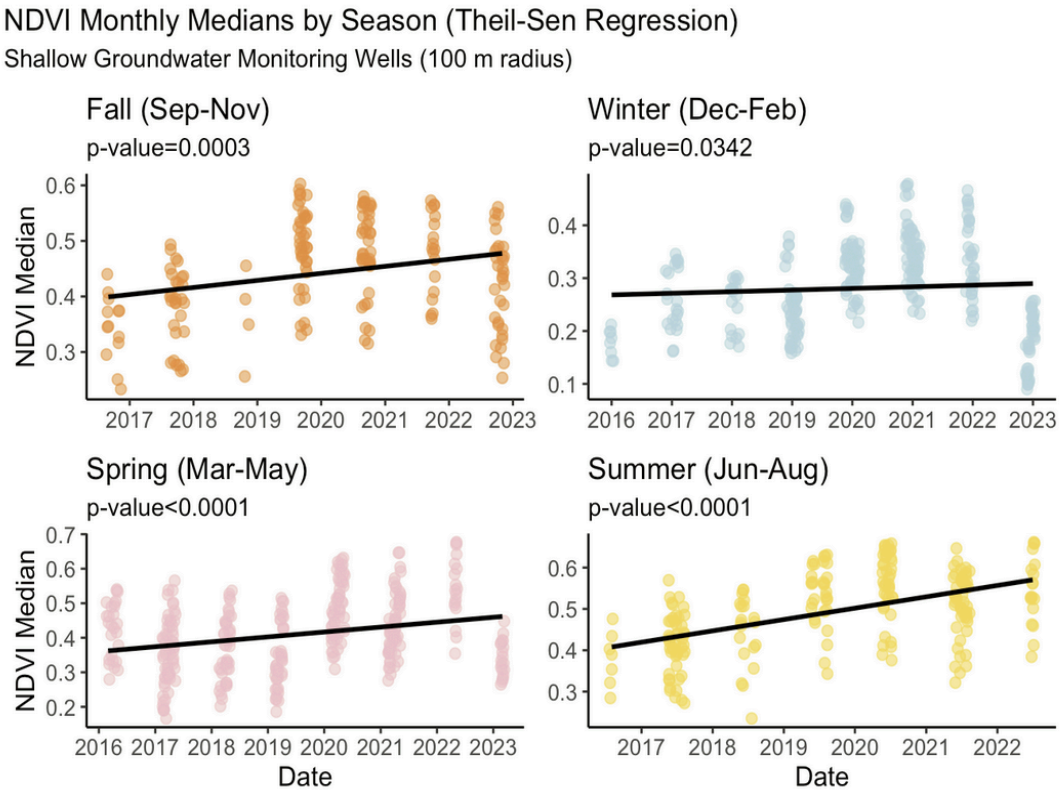

Figure 4.4.1a. Theil-Sen seasonal trends for each shallow groundwater monitoring demonstrate a significant increase in median NDVI from 2016 to 2023 for the winter (p-value=0.0342), summer (p-value<0.0001), spring (p-value<0.0001), and fall (p-value=0.0003) seasons. Summer showed a strong relationship between increases in shallow groundwater and vegetation greenness.

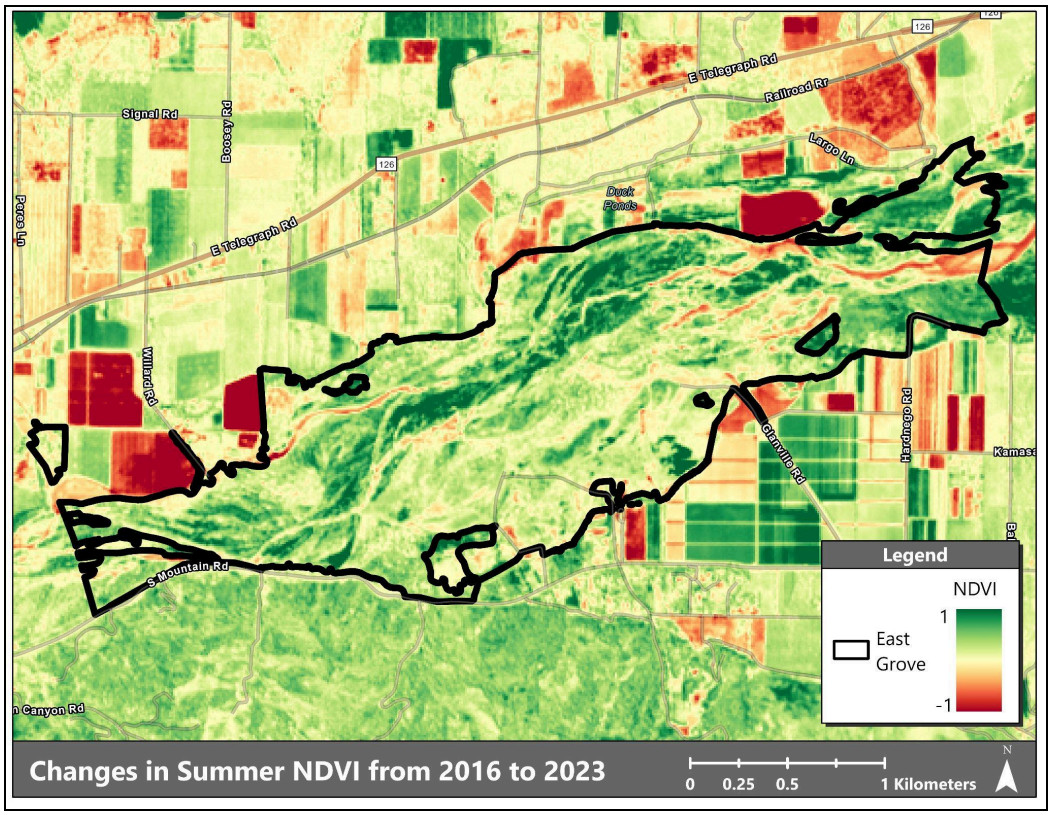

Figure 4.4.1b Changes in NDVI within the East Grove study area from summer 2016 and 2023. Values range from -1 to 1, with negative values indicating a decrease in NDVI and positive values indicating an increase in NDVI. NDVI values do not impart cover type discrepancies.

NDVI values were highest during summer, indicating that vegetation in East Grove experienced peak productivity. The median NDVI values in East Grove in the summers of 2016 and 2023 was 0.37 and 0.55, respectively. The difference in median NDVI between summer 2016 and 2023 was 0.18, representing an increase in NDVI during this time period and vegetation greenness. 84% of the area within East Grove demonstrated an improvement in NDVI values (Figure 4.4.1b). 16% of the area within East Grove had a decrease in NDVI, which may be an indicator of vegetative change due to high precipitation and increased surface water (Figure 4.4.1b). However, further examination of land cover is required to classify cover type NDVI changes.

4.4.2 NDMI

Table 4.4.2. East Grove seasonal median NDMI values for the years 2016 to 2023. The winter season had the lowest NDMI values amongst all seasons, except for the year 2016. Summer had the highest NDMI values across all seasons, with the exception of the year 2016. The winter NDMI values correspond with plant senescence periods and summer NDMI values, plant productivity periods.

	2016	2017	2018	2019	2020	2021	2022	2023
Winter	-0.01	-0.09	-0.04	-0.04	0.07	0.11	0.11	0.14
Spring	0.15	0.07	0.04	0.13	0.22	0.19	0.24	0.21
Summer	0.05	0.15	0.12	0.27	0.31	0.26	0.27	0.27
Fall	-0.05	0.09	0.06	0.24	0.27	0.22	0.21	0.23

Seasonal median NDMI values for the years 2016 to 2023 were calculated from the composite images created in Google Earth Engine (Table 4.4.2). The years 2017, 2019, 2020, 2022, and 2023 showed an increase in NDMI values, corresponding with wet years (Figure 4.3.1d). Decreases in NDMI during the summer months corresponded to dry years.

Trends of changes in seasonal NDMI over time were calculated using Theil-Sen regression. These values were plotted with a trend line showing NDMI increasing for the winter, summer, spring, and fall seasons (Figure 4.4.2a). The overall increase in median NDMI values between the years 2016 to 2023 indicates improvement in plant water content within the East Grove study area. All seasons demonstrated a significant increase in NDMI over the study period, with p-values of less than 0.0001 for each season (fall Theil-Sen regression: slope=4.407e-05, p-value<0.0001; winter Theil-Sen regression: slope=7.040e-05, p-value<0.0001; spring Theil-Sen regression: slope=7.384e-05, p-value<0.0001; summer Theil-Sen regression: slope=8.302e-05, p-value<0.0001) (Figure 4.4.2a).These trends indicate that vegetation within East Grove became less water-stressed over time.

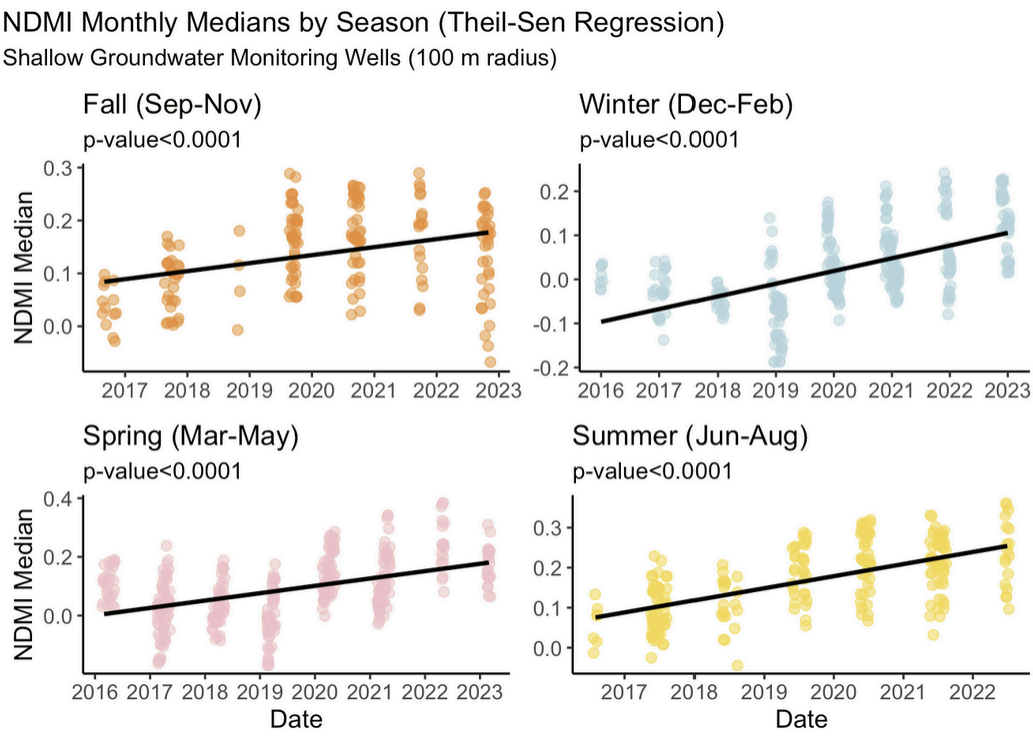

Figure 4.4.2a Seasonal trends demonstrate a general increase in median NDMI from 2016 to 2023 for the winter (p-value<0.0001), spring (p-value<0.0001), summer (p-value<0.0001), and fall seasons (p-value<0.0001). All seasons demonstrated a strong relationship between shallow groundwater levels and NDMI.

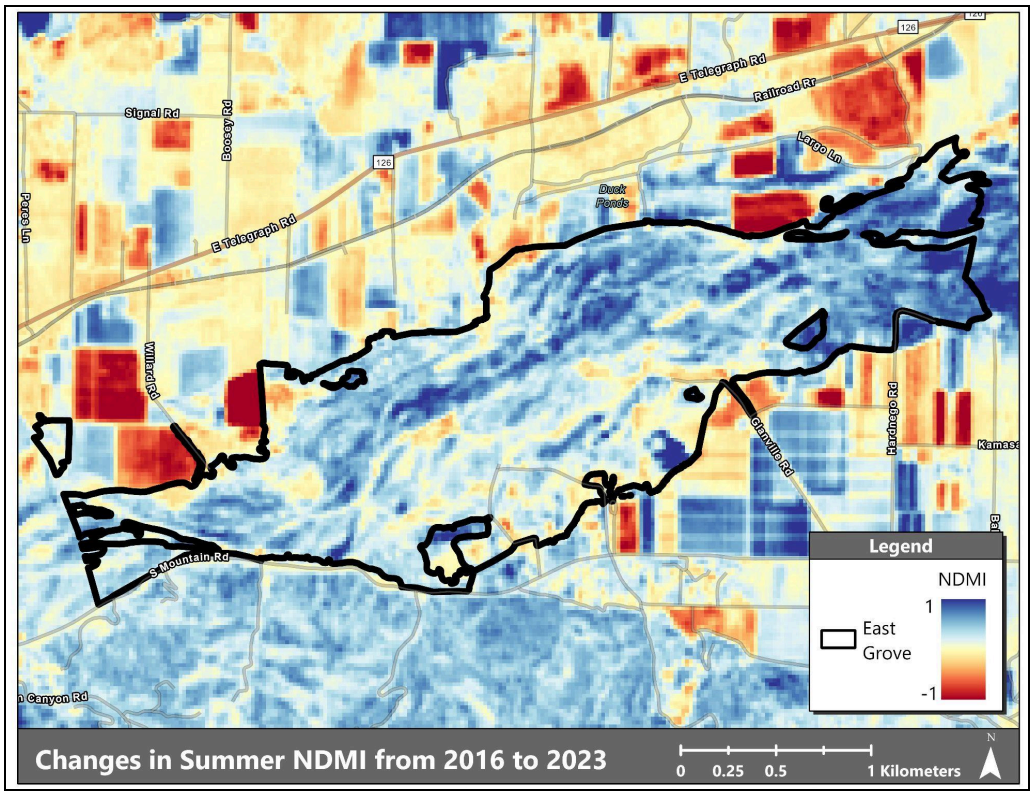

Figure 4.4.2b Changes in NDMI within the East Grove study area between summer 2016 and summer 2023.Values range from -1 to 1, with negative values indicating a decrease in NDMI and positive value indicating an increase in NDMI. NDMI values do not indicate cover type discrepancies.

NDMI values were highest during the summer, indicating that plants in East Grove experienced peak productivity (Table 4.4.2). The median NDMI values in East Grove in the summers of 2016 and 2023 were 0.05 and 0.27, respectively. The difference in median NDMI between summer 2016 and 2023 was 0.22, indicating a substantial increase in plant water content. 96% of the area within the East Grove study area demonstrated an improvement in NDMI values (Figure 4.4.2b), while 4% of the area had a decrease in NDMI. The areas that demonstrated a decrease in NDMI within East Grove could be attributed to changes in vegetation cover, but further analysis of cover types is required.

4.4.3 Ecohydrology

Time-Series Trends

During the study period, NDVI, NDMI, and depth-to-groundwater experienced upward trends of differing magnitudes. Depths to groundwater levels shallowed between January 2016 and March 2023 (Theil-Sen regression, $y=-0.05x+920.19$, $p<0.0001$). NDVI medians increased during the same time period (Theil-Sen regression, $y=(3.4e-5)x-0.22$, $p<0.0001$), as did NDMI median

values (Theil-Sen regression, y=(6.5e-5)x-1.076, p<0.0001). Figure 3.4.3a displays all monthly data from all wells for all three variables. Time-series by individual well can be found in 3.3.2A of Supplemental Materials.

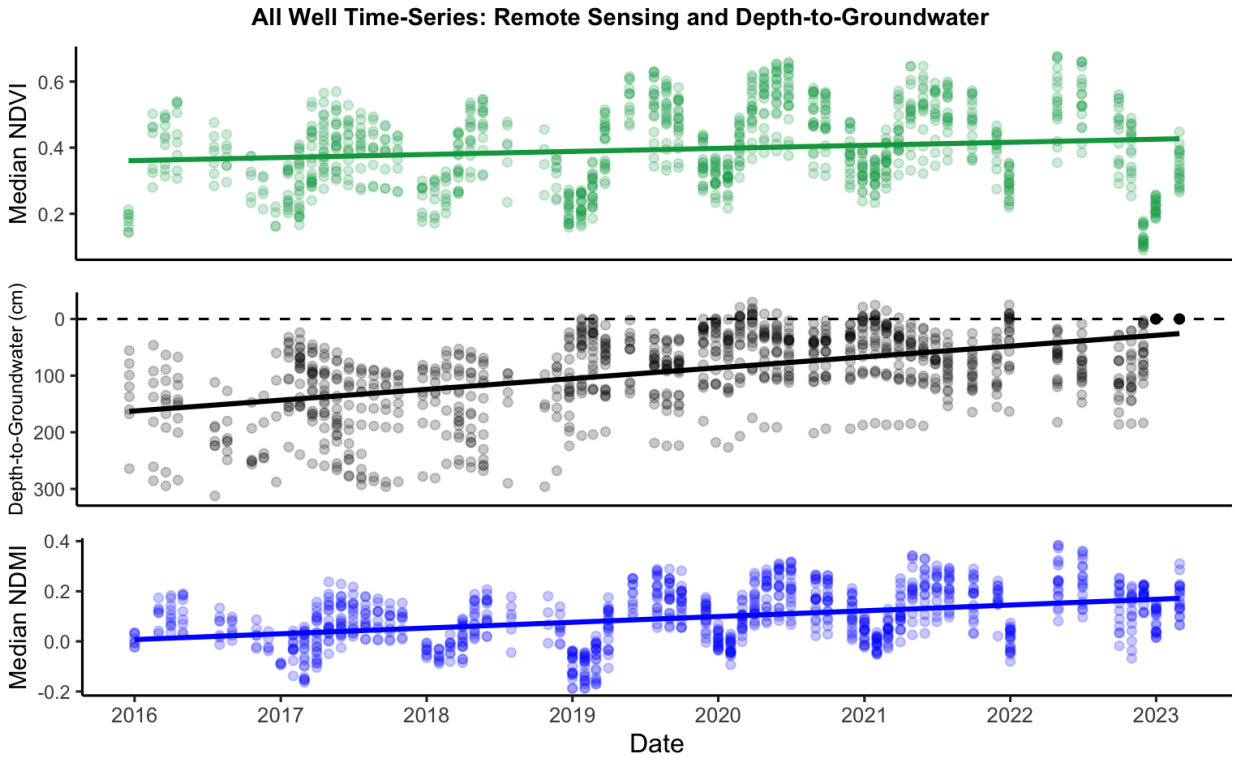

Figure 4.4.3a. Time-series plots of all wells' monthly data for depth-to-groundwater and two remote sensing variables: NDVI and NDMI. Theil-Sen regression lines are displayed for each variable. All variables experienced an upward trend during the study period, with lower values clustered towards 2016 and 2017 and higher values between 2020 and 2021. Some seasonal variation can be observed in all data sets, but this variation is most pronounced in the NDVI and NDMI data. This may be due to variations in plant phenology, which lead to reductions in plant productivity during winter months. Seasonal variations in groundwater depths may result from various factors, including surface flow, precipitation, or hydrologic conditions.

Rank Regression Analysis

The Ventura County Watershed Protection District Well #2 was excluded from any individual analysis because it was rendered unusable by storms in 2019 and has not been monitored since then.

All Months

Rank regression analyses on monthly data between depth-to-groundwater and both remote sensing indicators for all wells (NDVI and NDMI) resulted in significant linear relationships (p-value<0.0001) (Figure 4.4.3b, Figure 4.4.3c). These negative linear relationships indicate that

shallow depths to groundwater are associated with higher values of NDVI and NDMI. Regression graphs for individual wells can be found in Section 3.3.2B of Supplemental Materials.

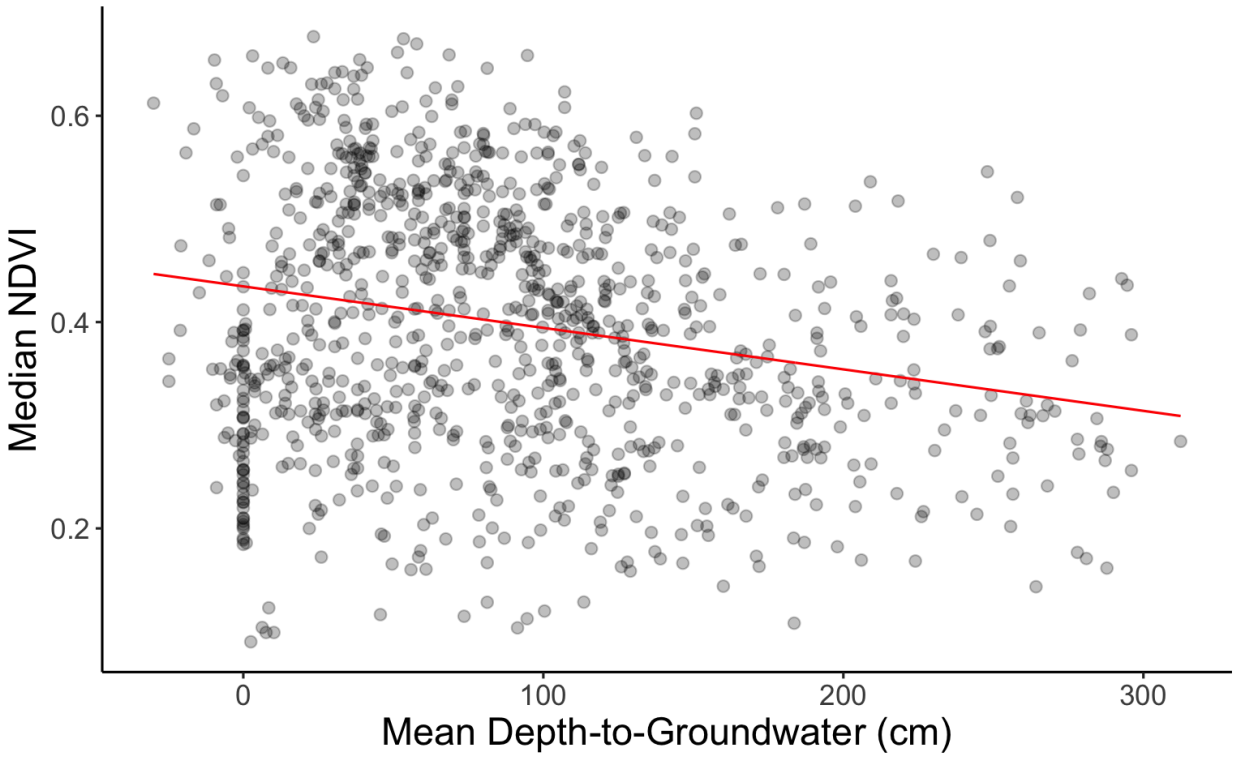

Figure 4.4.3b. Scatter plot of NDVI monthly data points for all shallow groundwater monitoring wells: one point represents one well's monthly mean depth-to-groundwater and monthly median NDVI value for a 50-meter radius around the well. The rank regression line is shown in red (rank-based estimation: NDVI = -0.000402*depth+0.435, p-value<0.0001). The significant negative relationship calculated by the rank regression indicates that shallower depths to groundwater are associated with higher NDVI values, while deeper groundwater depths are associated with lower NDVI values. Thus, plants may be greener when shallow groundwater is closer to the surface.

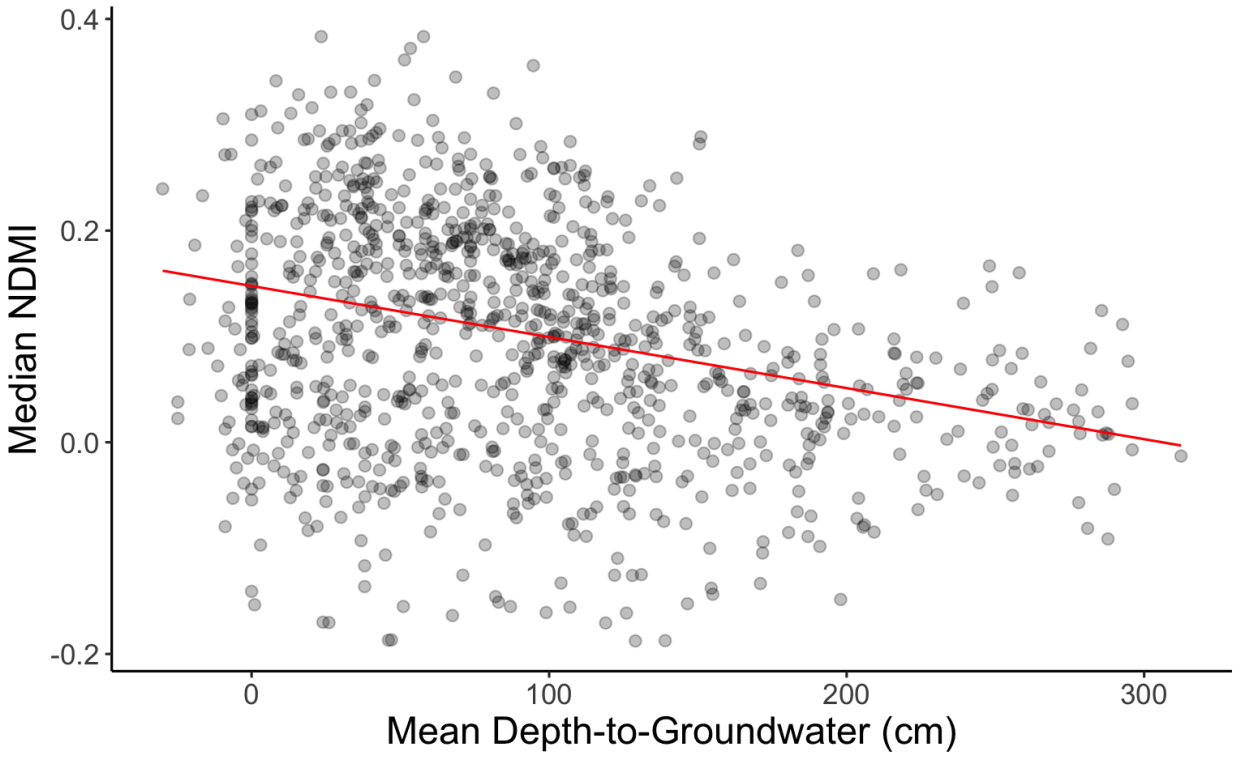

Figure 4.4.3c. Scatter plot of NDMI monthly data points for all shallow groundwater monitoring wells: one point represents 1 well's monthly mean depth-to-groundwater and monthly median NDMI value for a 100-meter radius around the well. The rank regression line is shown in red (rank-based estimation: NDMI = -0.000482*depth+0.148, p-value<0.0001). The significant negative relationship calculated by the rank regression indicates that shallower depths to groundwater are associated with higher NDMI values, while deeper groundwater depths are associated with lower NDMI values. Thus, plants may have higher water content when shallow groundwater is closer to the surface.

When rank regression analyses between depth-to-groundwater and the remote sensing indicators were performed for each individual well, most of them failed to reject the null hypothesis. None of the individual wells maintained a significant rank-regression relationship between median monthly NDVI and mean depth-to-groundwater (Table 4.4.3a). Of the 20 individual wells, 7 had significant rank-regression coefficients between median monthly NDMI and mean depth-to-groundwater (Table 4.4.3b).

Table 4.4.3a. Slopes and p-values for all individual wells' rank regression analyses between depth-to-groundwater and NDVI. No regressions were found to be statistically significant. On an individual well level, we cannot be confident of the negative relationship observed between depth-to-groundwater and NDVI values.

Well ID	Rank Regression Coefficient	p-value

Taylor 1	4.55E-04	0.45
Taylor 2	-3.02E-04	0.41
HRP 1	-1.19E-04	0.55
HRP 2	-6.73E-04	0.12
HRP 3	-1.34E-04	0.57
HRP 4	-1.51E-04	0.27
HRP 5	-6.02E-05	0.88
HRP 6	4.60E-06	0.98
HRP 7	7.78E-05	0.75
HRP 8	-8.90E-06	0.97
HRP 9	-3.39E-05	0.89
VCWPD 1	-3.46E-05	0.91
VCWPD 2	3.73E-04	0.62
VCWPD 3	-1.47E-04	0.67
VCWPD 4	-7.81E-05	0.81
VCWPD 5	6.34E-04	0.29
VCWPD 6	-1.15E-04	0.69
VCWPD 7	1.41E-05	0.97
VCWPD 8	-4.23E-04	0.06
VCWPD 9	9.56E-05	0.74
VCWPD 10	1.07E-04	0.68

Table 4.4.3b. Slopes and p-values for all individual wells' rank regression analyses between depth-to-groundwater and NDMI. For most individual wells, we cannot be confident of the negative relationship observed between depth-to-groundwater and NDMI values for most wells. However, 7 out of 20 regressions were found to be statistically significant (Hedrick Ranch Preserve Wells #1-6, Ventura County Watershed Protection District Well #8). Shallower depths to groundwater were associated with higher NDMI values for these 7 wells.

Well ID	**Rank Regression Coefficient**	**p-value**
Taylor 1	-5.39E-04	0.36
Taylor 2	-5.39E-04	0.13

HRP 1	-5.06E-04	<0.01
HRP 2	-1.11E-03	<0.01
HRP 3	-6.26E-04	<0.01
HRP 4	-2.76E-04	0.01
HRP 5	-5.41E-04	0.04
HRP 6	-4.36E-04	<0.01
HRP 7	-3.09E-04	0.08
HRP 8	-2.83E-04	0.16
HRP 9	-2.93E-04	0.13
VCWPD 1	-2.48E-04	0.45
VCWPD 2	4.17E-04	0.41
VCWPD 3	-2.66E-04	0.44
VCWPD 4	-3.31E-04	0.32
VCWPD 5	1.24E-04	0.86
VCWPD 6	-2.54E-04	0.42
VCWPD 7	-1.45E-04	0.76
VCWPD 8	-5.09E-04	0.01
VCWPD 9	-2.06E-04	0.45
VCWPD 10	-1.52E-04	0.49

The small number of significant relationships and the spread seen in the above scatterplots indicate that there may not be a strong correlation between depth-to-groundwater and NDVI variables. In fact, median NDVI and mean depth-to-groundwater have a weak negative correlation of -0.18 (Spearman's rho). NDMI and mean depth-to-groundwater have a weak negative correlation of -0.27 (Spearman's rho). Table 4.4.3c displays the Spearman's rank-order correlation values for each well. All absolute values are less than 0.5, indicating weak associations between the variables.

Table 4.4.3c. All individual wells' Spearman's rank order correlations between depth-to-groundwater and remote sensing indicators, reported as "rho." All wells had weak or

very weak negative associations between depth-to-groundwater and NDVI/NDMI. Thus, we cannot be confident of the rank regressions calculated between these variables.

Well ID	**NDVI rho**	**NDMI rho**
Taylor 1	0.03	-0.14
Taylor 2	-0.03	-0.14
HRP 1	-0.14	-0.37
HRP 2	-0.07	-0.28
HRP 3	-0.06	-0.33
HRP 4	-0.22	-0.44
HRP 5	0.06	-0.14
HRP 6	0.08	-0.23
HRP 7	0.16	-0.09
HRP 8	0.20	-0.04
HRP 9	0.15	-0.04
VCWPD 1	0.05	-0.03
VCWPD 2	0.15	0.19
VCWPD 3	0.01	0.01
VCWPD 4	-0.01	-0.12
VCWPD 5	0.13	0.03
VCWPD 6	0.02	-0.06
VCWPD 7	0.11	0.07
VCWPD 8	-0.12	-0.17
VCWPD 9	0.13	-0.01
VCWPD 10	0.14	0.02

Summer Months

After isolating values from summer months (June, July, August), rank regression analyses on monthly data between depth-to-groundwater and both remote sensing indicators for all wells (NDVI and NDMI) resulted in significant negative relationships (p-value<0.0001) (Figure 4.4.3d, Figure 4.4.3e). These results indicate that shallow depths to groundwater are associated

with higher values of NDVI and NDMI in summer. Individual well's regression graphs can be found in Section 3.3.2C of Supplemental Materials.

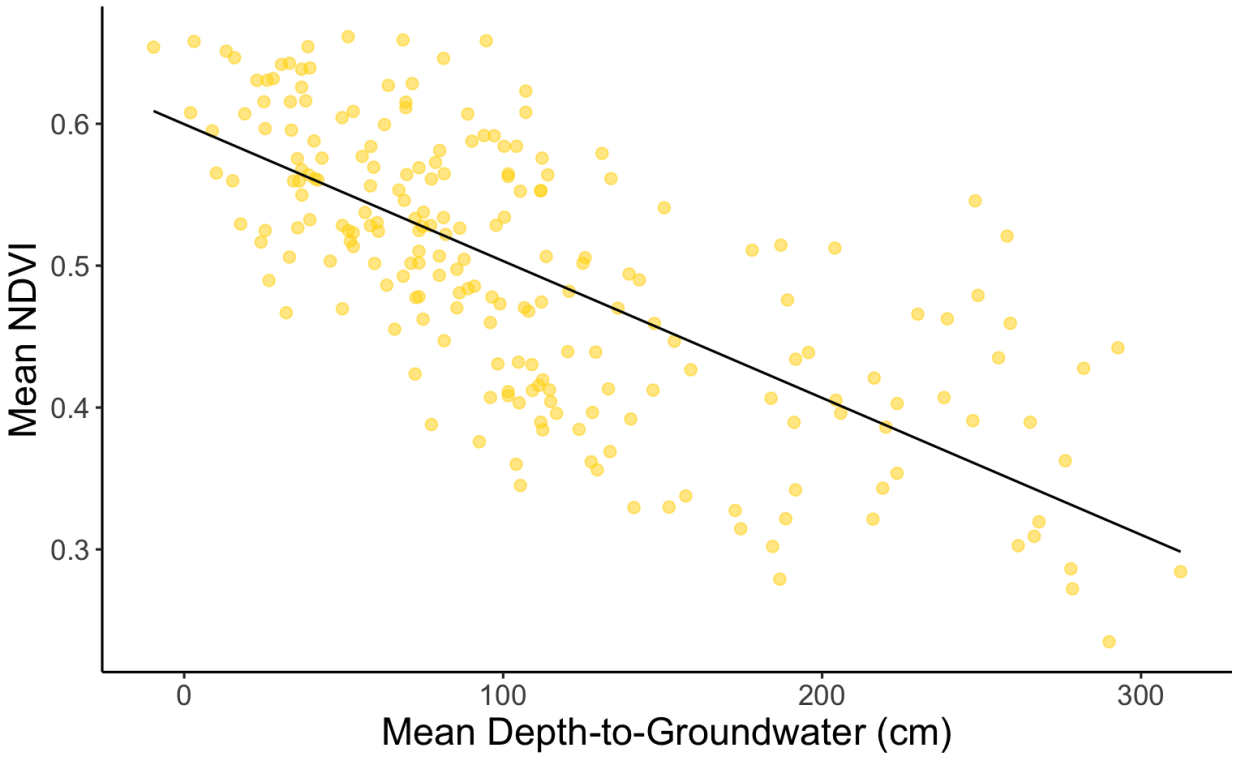

Figure 4.4.3d. Scatter plot of NDVI summer monthly data points for all shallow groundwater monitoring wells. Rank regression line is shown in red (rank-based estimation: NDVI = -0.000956*depth+0.59, p-value<0.0001). The significant negative relationship calculated by the rank regression indicates that shallower depths-to-groundwater are associated with higher NDVI values, while deeper groundwater depths are associated with lower NDVI values. The slope of the summer rank regression is more than twice as strong as the slope of the total year rank regression ($9.6*10^{-4} > 4*10^{-4}$). Thus, plants appear to be greener when shallow groundwater is closer to the surface, especially in summer.

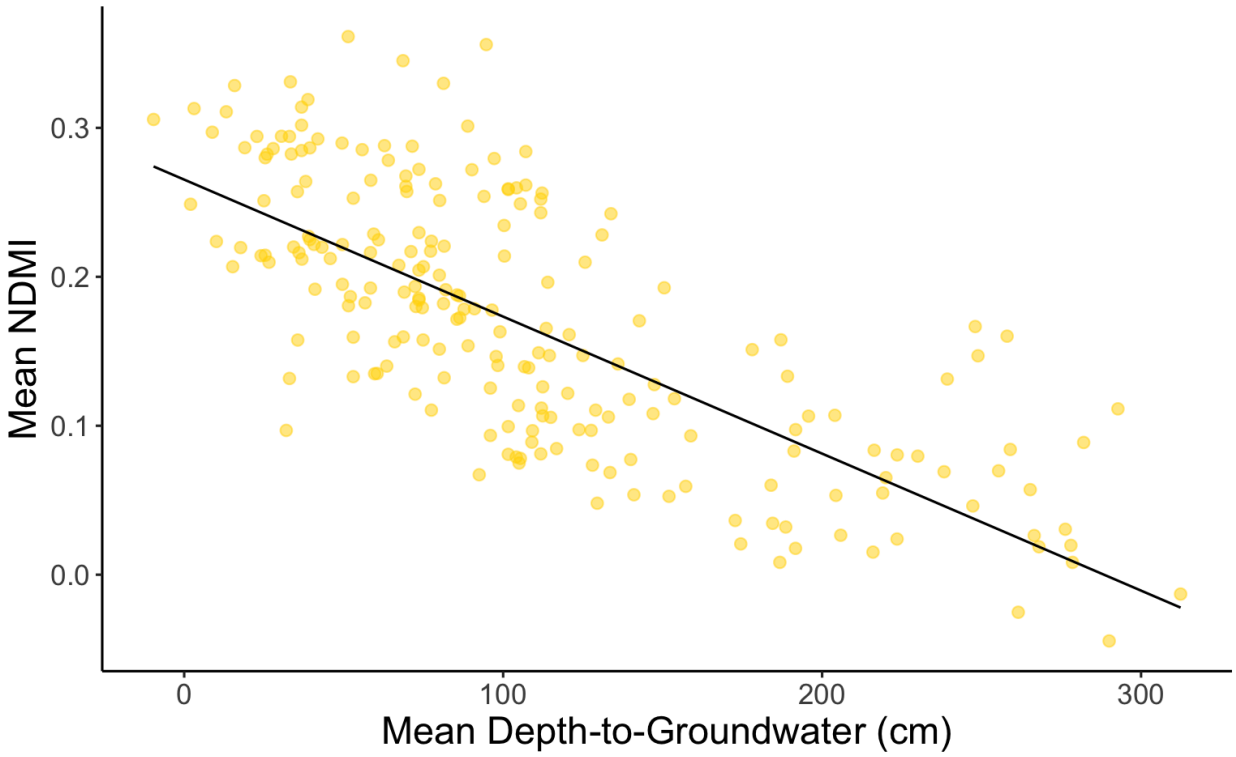

Figure 4.4.3e. Scatter plot of NDMI summer monthly data points for all shallow groundwater monitoring wells. The rank regression line is shown in red (rank-based estimation: NDMI = -0.00092*depth+0.265, p-value<0.0001). The significant negative relationship calculated by the rank regression indicates that shallower depths to groundwater are associated with higher NDMI values, while deeper groundwater depths are associated with lower NDMI values. The slope of the summer rank regression is nearly twice as strong as the slope of the total year rank regression ($9.2*10^{-4} > 4.8*10^{-4}$). Thus, plants appear to have higher water content when shallow groundwater is closer to the surface, especially in summer.

When isolating summer months, many more of the individual wells experienced significant rank regression relationships between the remote sensing indicators and depth-to-groundwater. All but 2 of the individual wells maintained a significant rank-regression relationship between median monthly NDVI and mean depth-to-groundwater (Table 4.4.3d), and all but 3 had significant rank-regression coefficients between median monthly NDMI and mean depth-to-groundwater (Table 4.4.3e).

Table 4.4.3d. Slopes and p-values for all individual wells' rank regression analyses between depth-to-groundwater and NDVI in summer months. 18 out of 20 relationships were found to be statistically significant. Thus, for all wells except VCWPD 3 and 5, shallower depths to groundwater were associated with higher NDVI values in summer months.

Well ID	Rank Regression Coefficient	p-value

Taylor 1	-1.84E-03	<0.01
Taylor 2	-1.20E-03	<0.01
HRP 1	-1.28E-03	<0.01
HRP 2	-1.99E-03	<0.01
HRP 3	-9.95E-04	0.01
HRP 4	-5.50E-04	0.02
HRP 5	-2.56E-03	<0.01
HRP 6	-7.31E-04	0.02
HRP 7	-8.32E-04	0.00
HRP 8	-7.47E-04	0.01
HRP 9	-4.69E-04	0.03
VCWPD 1	-1.05E-03	0.01
VCWPD 3	-1.03E-03	0.09
VCWPD 4	-1.28E-03	<0.01
VCWPD 5	-9.01E-04	0.36
VCWPD 6	-1.07E-03	<0.01
VCWPD 7	-7.69E-04	0.03
VCWPD 8	-9.97E-04	<0.01
VCWPD 9	-8.32E-04	<0.01
VCWPD 10	-6.28E-04	<0.01

Table 4.4.3e. Slopes and p-values for all individual wells' rank regression analyses between depth-to-groundwater and NDMI in summer months. 17 out of 20 relationships were found to be statistically significant. Thus, for all wells except VCWPD 3, 5, and 7, shallower depths to groundwater were associated with higher NDMI values in summer months.

Well ID	**Rank Regression Coefficient**	**p-value**
Taylor 1	-1.63E-03	0.01
Taylor 2	-1.12E-03	<0.01
HRP 1	-8.31E-04	<0.01
HRP 2	-2.08E-03	<0.01

HRP 3	-8.86E-04	<0.01
HRP 4	-3.64E-04	0.02
HRP 5	-1.41E-03	<0.01
HRP 6	-7.02E-04	<0.01
HRP 7	-7.82E-04	<0.01
HRP 8	-7.47E-04	<0.01
HRP 9	-5.44E-04	<0.01
VCWPD 1	-9.66E-04	<0.01
VCWPD 3	-7.19E-04	0.08
VCWPD 4	-1.13E-03	0.01
VCWPD 5	-1.00E-03	0.13
VCWPD 6	-9.80E-04	<0.01
VCWPD 7	-6.97E-04	0.18
VCWPD 8	-9.55E-04	<0.01
VCWPD 9	-7.42E-04	<0.01
VCWPD 10	-6.55E-04	<0.01

The increased number of significant relationships and the spread seen in the above scatterplots indicate a stronger correlation between these variables when isolated to summer months. In fact, median NDVI and mean depth-to-groundwater have a strong negative correlation of -0.71 (Spearman's rho). NDMI and mean depth-to-groundwater have a strong negative correlation of -0.78 (Spearman's rho). Table 4.4.3f displays Spearman's rank-order correlation values for each well.

Table 4.4.3f. All individual wells' Spearman's rank order correlations between depth-to-groundwater and remote sensing indicator for summer months only, reported as "rho." Mean correlations for NDVI and NDMI are -0.68 and -0.65, respectively. Most wells have correlations with absolute values greater than or equal to 0.5, indicating a strong correlation between depth-to-groundwater and NDVI/NDMI for the East Grove shallow groundwater monitoring wells.

Well ID	**NDVI rho**	**NDMI rho**
Taylor 1	-0.73	-0.47

Taylor 2	-0.80	-0.75
HRP 1	-0.79	-0.86
HRP 2	-0.84	-0.84
HRP 3	-0.77	-0.87
HRP 4	-0.88	-0.90
HRP 5	-0.86	-0.82
HRP 6	-0.61	-0.72
HRP 7	-0.87	-0.88
HRP 8	-0.78	-0.88
HRP 9	-0.56	-0.64
VCWPD 1	-0.60	-0.60
VCWPD 3	0.08	0.03
VCWPD 4	-0.72	-0.70
VCWPD 5	-0.71	-0.50
VCWPD 6	-0.66	-0.53
VCWPD 7	-0.36	-0.01
VCWPD 8	-0.75	-0.66
VCWPD 9	-0.73	-0.66
VCWPD 10	-0.71	-0.72

The negative relationship between depth-to-groundwater and both remote sensing indicators is much stronger when summer values are isolated. This implies that shallower groundwater is more strongly correlated with higher values of NDVI and NDMI in summer months when precipitation is lower.

5. Discussion

5.1 Implications for Surface Water‑Groundwater Interactions

The findings of dominant coarse-grained unconsolidated material throughout this portion of the Santa Clara River Watershed are consistent with previous understanding of the Fillmore Subbasin lithology, where few permeable clay layers are found (Stillwater Sciences 2021). With few connecting clay layers, the groundwater can flow more easily and infiltrate through the subsurface, as low permeability layers have been known to restrict flow and can disconnect flows from surface water and groundwater (Rhodes et al. 2017; Brunner et al. 2011). A permeable subsurface may also allow for the shallow groundwater to be more responsive to precipitation events, as seen by the water-level rise analyses. Additionally, the dominant coarse-grained subsurface would have contributed to the system's upward-oriented vertical hydraulic gradient, as coarser grain sizes have been found to influence vertical flow direction and rates (Veras et al. 2016). The upward orientation of the vertical hydraulic gradient indicates the system's hydraulic potential for groundwater to flow upward, consistent with previous findings of upward groundwater flow in the Fillmore Subbasin (Stillwater Sciences 2021). The system's potential for upwelling is crucial, as it gives more confidence in previous assessments of East Grove being a potential groundwater dependent ecosystem. Through the water-level rise analyses and calculating the vertical hydraulic gradient, we better understand the interconnected relationship between groundwater and surface water. Surface water and groundwater are closely linked, therefore, managing groundwater resources is crucial to avoid potential adverse impacts to beneficial users and uses of interconnected surface waters such as special-status fish species and native riparian vegetation. Specifically, management and limits on groundwater extractions and pumping will be necessary as these activities have been found to impact the connectivity of surface waters and groundwater and can contribute to a loss of streamflow to aquifers (Jasechko et al. 2021).

5.2 Implications for Ecosystem Health

We observed peak NDVI and NDMI values during the summer months, which is indicative of the peak growing season of vegetation in East Grove. Lower values were recorded during the winter months, which is indicative of reduced vegetative activity. These seasonal fluctuations are essential for understanding the phenological cycles of plant communities and their response to changes in shallow groundwater availability. Median vegetative greenness and plant water content increased in East Grove across all seasons over the period of 2016-2023, as estimated by remote sensing indicators (NDVI and NDMI, respectively).

At the same time, groundwater levels shallowed in East Grove's subsurface. In exploring this data, we found that shallower depths to groundwater over this period are associated with higher NDVI and NDMI values, indicating that phreatophytes in East Grove may benefit from increased accessibility to shallow subsurface water. However, the observed improvement in vegetation health indicators could be attributed to climatic shifts, such as the end of California's most severe drought and the appearance of atmospheric rivers in 2019, 2021, and 2023 (CIRA 2024). In our analysis of the relationship between water-level rise and precipitation, we also found an association between groundwater levels in East Grove's shallow subsurface and these climate events. Therefore, with these results alone, we cannot confirm if the shallowing of groundwater below East Grove directly benefits the riparian ecosystem. Precipitation may be a confounding variable between the availability of shallow subsurface flows and plant greenness and water content. However, this region is known for having wet winters and dry summers (Kibler et al. 2021). To parse out the effect of precipitation on our results, we incorporated season as a variable in our analysis.

We found that there was substantial seasonality in the relationship between depth-to-groundwater and our proxies for ecosystem health. Specifically, data points in the summer months (June, July, and August) had a much stronger negative correlation between depth-to-groundwater and plant greenness and between depth-to-groundwater and plant water content. Therefore, ecosystem health in the summer may depend more on shallow groundwater availability than at other times of the year. The Fillmore Subbasin is in Ventura County, a region that receives less than 0.1 inches of rainfall during summer months (Western Regional Climate Center 2013). Additionally, surface flows in the Santa Clara River are not constant, and the river is often dry in the summer months (GSI 2008). Due to the lack of other water sources, East Grove's phreatophytes (cottonwood and willow trees) likely rely on subsurface water during the region's dry summers (Kibler et al. 2021). Therefore, we are confident that increases in shallow groundwater storage have a larger impact on plant health in summer months when there are few other water sources.

5.3 Implications for Water Management

Groundwater Sustainability Agencies are mandated under SGMA to address potential "significant and unreasonable impacts on surface water beneficial uses" that result from groundwater use in the basin (Sustainable Groundwater Management Act 2014). Groundwater uses that may cause depletion of interconnected surface waters include excessive groundwater pumping (California Department of Water Resources February 2024) and the water-intensive invasive *Arundo donax* (Stephens and Associates 2021), whose taproot system can outcompete the shallower rooting depths of surrounding native vegetation (Bywater-Reyes et al. 2022; Kibler et al. 2021). Subsequently, East Grove has been designated as a "beneficial user" of the Fillmore basin (Stephens and Associates 2021) due to its high ecological value. Moreover, iparian zones such as East Grove are recognized as critical habitat for federally listed bird species, such as the southwestern willow flycatcher (50 CFR § 17 (1995); Stillwater Sciences 2021). The gaining

river reach in East Grove is also known to support critical spawning and rearing habitats for the federally listed southern steelhead trout (*Oncorhynchus mykiss*) and the threatened Santa Ana sucker (*Catostomus sant*aanae) (50 CFR § 223 (2006); 50 CFR § 17 (2000); National Marine Fisheries Service 2016; Stillwater Sciences 2021; Stoecker and Kelley 2005). These aquatic species are recognized under both the federal and California Endangered Species Acts in which managing entities are mandated to maintain the hydrologic integrity of areas that support threatened and endangered species (16 U.S.C. § 1531-1544, Cal. Fish & G. Code § 2050-2118). The presence of interconnected surface waters, as regulated under SGMA, and the legal obligations to protect threatened and endangered species under federal and state laws, underscores the need for local water agencies to actively assess and mitigate impacts to East Grove through management interventions.

The Fillmore Piru Groundwater Sustainability Agency is responsible for implementing the requirements of SGMA for the Fillmore and Piru groundwater subbasins within the Santa Clara River Valley. As part of their regulatory obligations, the agency submitted a Groundwater Sustainability Plan to the Department of Water Resources in 2021 (Stephens and Associates 2021). This plan identified the presence of interconnected surface waters in East Grove and addressed historical documentation of streamflow depletion resulting from surface water diversions and groundwater pumping in the surrounding basin (Stephens and Associates 2021). However, the agency did not establish a management plan for depletion of interconnected surface waters as required by the state's Groundwater Sustainability Plan regulations (Cal. Code Regs. Tit. 23, § 355.2). It is recommended that the agency conduct further assessments to understand the impacts of groundwater extraction on interconnected surface waters in identified gaining reaches of the river, including East Grove. Additionally, the agency should develop a management plan to mitigate adverse impacts of streamflow depletion on the beneficial users and uses in the basin.

The regulatory commitments of the Groundwater Sustainability Agency also extend to making considerations to the impacts of groundwater pumping on groundwater dependent ecosystems (Cal. Code Regs. Tit. 23, § 354.16). As such, the agency developed a management plan for an identified groundwater dependent ecosystem located between the Fillmore and Piru subbasin borders, known as the Cienega Riparian Ecosystem (Stephens and Associates 2021). This decision was prompted by a large-scale die-off of riparian vegetation following the 2012 to 2019 California drought (Stephens and Associates 2021; Kibler et al. 2021). While a management plan exists for the Cienega Riparian Ecosystem, East Grove lacks such a designation (Stephens and Associates 2021).

To comprehensively assess impacts of groundwater extractions on East Grove and other likely groundwater-dependent ecosystems, it is recommended that the Fillmore Piru Groundwater Sustainability Agency monitor depth-to-groundwater level data from a representative shallow

groundwater monitoring network and incorporate this data into their groundwater elevation sustainable management criteria (Stephens and Associates 2021). According to The Nature Conservancy's Groundwater Dependent Ecosystem guidance document (Rohde et al. 2018), die-back of groundwater dependent vegetation is likely if groundwater levels consistently exceed 30 feet below ground surface. Therefore, new monitoring networks should focus on the 30-foot subsurface zone and be monitored seasonally to effectively sustain riparian woodlands over time. Groundwater pumping data is collected semiannually in the subbasin (Stephens and Associates 2021). It is recommended that data collection be conducted on a seasonal basis to better assess how groundwater pumping at deeper depths may influence shallow aquifer conditions within the Fillmore Subbasin and consequently impact the health of groundwater-dependent ecosystems (Stephens and Associates 2021).

5.4 Limitations

5.4.1 Lithology

63 wells were obtained for analysis on lithology; however, only two wells (including the nested wells) were located within East Grove, due to limited availability or quality. It is important to note that well-driller descriptions may also vary in detail and accuracy, which could impact categorization in the simplified lithologic categories and cross-sections. Lithological cross-sections are constructed from a limited number of observations and at varying depths; we are limited by the availability of high-quality drilling logs in our area of interest. Direct observation is often impractical, hence what is occurring between logs must be inferred using stratigraphical principles. A combination of correlation strategies would be ideal. However, using time-stratigraphic or biostratigraphic correlation would not be feasible at such shallow depths. In general, the smaller the distance between any two logs, the stronger the inferred correlation. Sometimes the distance between logs in cross-sections is hundreds of meters. Just how widespread layers are in these regions is less clear.

5.4.2 Vertical Hydraulic Gradient

The nested monitoring well utilized for our vertical hydraulic gradient analysis had only nine water level measurements, recorded during the exceptionally wet year of 2023. Ongoing evaluations of depth-to-groundwater levels should be considered at this site to obtain a more comprehensive understanding of the magnitude and direction of groundwater flow at East Grove.

Another constraint is the absence of additional depth-to-groundwater data from wells screened at various depths. To address this limitation, it is advisable to install colocated wells with different shallow and deep total well depths within East Grove and other recognized groundwater-dependent ecosystems along the Santa Clara River, such as the Fillmore Ciénega

riparian zone (Kibler et al. 2021). This implementation will help validate the findings regarding the upward-oriented vertical hydraulic gradient presented in this study, as well as provide additional insight into the magnitude and consistency of groundwater upwelling conditions.

5.4.3 Groundwater Fluctuations

This study lacked consistent depth-to-groundwater measurements—whether in the East Grove shallow groundwater monitoring wells or the Fillmore Subbasin wells accessed via the SGMA Data Viewer. Thus, the analyses lacked continuous data, meaning there is the possibility of error in the groundwater fluctuations observed. Even so, the length of the study period and number of measurements provide confidence in the conclusions made by our analyses.

During the most recent drought, many East Grove shallow groundwater monitoring wells were observed to have "no water" on some measurement dates. This meant that the depth-to-groundwater was below the total well depth and could not be recorded. Thus, our analyses necessarily ignored those data points, which may have led to minor survivor bias in our results.

The wells accessed on the SGMA Data Viewer—outside of East Grove—were primarily production wells for irrigation or domestic use. Thus, pumping in these wells may have influenced the measured groundwater levels. There were no records on well production or draw-down caused by pumping. Furthermore, errors may have resulted from the tools different parties used for groundwater level measurements: manual e-tape, electric sounders, or pressure transducers. Despite possible sources of error, observed fluctuations in depth-to-groundwater were consistent across the deeper wells, supporting our assumptions.

The precipitation estimates utilized in this study were derived from PRISM, meaning they are modeled approximations rather than direct measurements of rainfall in or around East Grove (Daly et al. 2008). Additionally, the ratios of water-level rise to precipitation overlook the impact of various surface processes on groundwater levels and storage, such as river flows or irrigation runoff. This limitation arises from the water-table fluctuation method, which we used because we lacked reliable data on surface flow. Notably, the shallow groundwater monitoring wells are situated outside of the riverbed, suggesting that the river's perennial surface flows are unlikely to directly influence observed groundwater fluctuations. The water-table fluctuation method relies on several key assumptions:

1. The changes in depth-to-groundwater observed in the shallow groundwater time-series graphs are "natural water-table fluctuations caused by groundwater recharge and discharge (USGS 2017)."
2. The specific yield of each shallow groundwater monitoring well is "known and constant (USGS 2017)." (We lacked consistent information on soil types and specific yield, and

thus omitted specific yield from our calculations, necessarily resulting in ratios of water-level rise to precipitation rather than recharge ratios.)

3. Water-level rise (delta-H) can only be estimated when recharge in t_j is greater than water-level decline (USGS 2017).

These critical assumptions mean that water-table fluctuation analyses are highly approximated. However, there is a significant association between precipitation and water-level rise in this system. Therefore, precipitation has an influence on water-level changes in East Grove and the Fillmore Subbasin.

5.4.4 Remote Sensing

NDVI and NDMI are often used as indicators of vegetation health, but they are not direct measures of plant productivity or plant water content. They are calculated using reflectance bands observed by a satellite, and do not account for confounding factors that would be noted in empirical measurements of plant transpiration or photosynthesis. Thus, any conclusions made using these values are highly approximated and are not substitutes for empirical data on ecosystem and plant health (Redowan & Kanan 2012). The NDVI and NDMI estimates used in all analyses were monthly median values, whether calculated for all of East Grove or within radii around the East Grove shallow groundwater monitoring wells. Monthly medians do not capture all variation in the data, and are not continuous measurements of either remote sensing indicator. Some variation is lost in using these estimates.

Additionally, relationships between groundwater depth and remote sensing indicators are approximated using monthly median NDVI and NDMI values of a certain radius, and mean depth-to-groundwater measurements of a given month. Thus, the variables are not matched by exact date, so the analyses by month are approximated and have room for error. Furthermore, NDVI values may not accurately reflect the health of the vegetation in East Grove, since it measures the amount of chlorophyll in vegetation and the overall density of green leaves. NDVI also does not differentiate between vegetation cover types, which may have varying seasonal phenological responses. Different vegetation types also have varying responses to moisture stress, and NDMI does not accurately capture these differences. Thus, land classification is required for a more accurate analysis of vegetation health.

6. Conclusion

This study aims to assess how changes in groundwater flow and storage within the Santa Clara River's Fillmore Subbasin may impact ecosystem health in East Grove—a "likely groundwater-dependent ecosystem" (Stillwater Sciences 2021). To answer this question, we undertook four distinct analyses and many technical methods to acquire insight into the complex relationship between the ecosystem on the surface and the layers of soil, rock, and water beneath. We found that the region's geohydrology may encourage the upward movement of groundwater

into the shallow subsurface. Results validated the hypothesis that East Grove is a groundwater dependent ecosystem, where rising groundwater is present in riparian zones (Eamus et al. 2016). Assuming that the riparian vegetation in East Grove is dependent on shallow subsurface flows, we then needed to assess how changing groundwater levels in the aquifer may impact ecosystem health. Using monitoring well measurements and remote sensing, we found a positive association between shallow groundwater levels and NDVI/NDMI. This relationship was especially strong in the region's dry summers, when phreatophytes may rely more on subsurface water for transpiration.

The Sustainable Groundwater Management Act requires Groundwater Sustainability Plans to "consider impacts to groundwater dependent ecosystems," but does not provide guidelines for this requirement (Sustainable Groundwater Management Act 2014). Stakeholders and agencies within the Santa Clara River Watershed are concerned with protecting East Grove as a system with "high ecological value" (Rohde et al. 2018; Stillwater Sciences 2021). Our results may provide a potential baseline evaluation of East Grove's condition that can be used to assess the impacts of future drought or groundwater extraction. Furthermore, stakeholders in the area can implement our methodological framework to identify and evaluate other groundwater dependent ecosystems in the watershed. To strengthen these methods, future efforts should prioritize integrating data on surface water flows—from conservation releases, natural streamflow, and irrigation runoff—and verify our findings with on-the-ground assessments of ecosystem health. Furthermore, managers should incorporate assessments on the direct impact of groundwater pumping on East Grove. The addition of these data and analyses would help the Fillmore and Piru Groundwater Sustainability Agency to determine minimum groundwater-level thresholds for the basin—a requirement for completing the Fillmore Subbasin Groundwater Sustainability Plan—while also considering the success and survival of the valuable East Grove ecosystem.

References

Batelaan, O., De Smedt, F., & Triest, L. (2003). Regional groundwater discharge: phreatophyte mapping, groundwater modelling and impact analysis of land-use change. *Journal of Hydrology*, *275*(1-2), 86–108. https://doi.org/10.1016/s0022-1694(03)00018-0

Bell, I., Berry, E., Booth, D., McKelvey, Z., Prentice-Dekker, B., & Steele, M. (2016). Economic Analysis of Invasive Giant Reed (Arundo donax) Control for the Lower Santa Clara River. (Master's thesis, University of California, Santa Barbara).

Beller, E. E., B. K. Orr, M. N. Salomon, R. M. Grossinger, S. J. Dark, E. D. Stein, T. R. Longcore, G. C. Coffman, A. A. Whipple, R. A. Askevold, B. Stanford, J. R. Beagle, & Downs, P. W. (2011). Historical ecology of the lower Santa Clara River, Ventura River, and Oxnard Plain: an analysis of terrestrial, riverine, and coastal habitats. *Prepared for the State Coastal Conservancy. A report of SFEI's Historical Ecology Program,* SFEI Publication #641, San Francisco Estuary Institute, Oakland, CA.

Beller, E. E., P. W. Downs, R. M. Grossinger, B. K. Orr, & Salomon, M. N. (2016). From past patterns to future potential: using historical ecology to inform river restoration on an intermittent California river. *Landscape Ecology, 31*, 581-600. https://link.springer.com/article/10.1007/s10980-015-0264-7

Brunner, P., Cook, P.G. & Simmons, C.T. (2011). Disconnected Surface Water and Groundwater: From Theory to Practice. *Groundwater*, *49,* 460-467. https://doi.org/10.1111/j.1745-6584.2010.00752.x

Bywater-Reyes, S., Diehl, R.M., Wilcox, A., Stella, J., & Kui, L. (2022). A Green New Balance: Interactions among riparian vegetation plant traits and morphodynamics in alluvial rivers. *Earth Surface Processes and Landforms*, *47*. doi: 10.1002/esp.5385.

California Department of Water Resources. (2018). Summary of the "Natural Communities Commonly Associated with Groundwater" Dataset and Online Web Viewer. https://water.ca.gov/-/media/DWR-Website/Web-Pages/Programs/Groundwater-Management/Data-and-Tools/Files/Statewide-Reports/Natural-Communities-Dataset-Summary-Document_ay_19.pdf

California Department of Water Resources. (2023). California Irrigation Management Information System. *CA Department of Water Resources CIMIS*. https://cimis.water.ca.gov/WSNReportCriteria.aspx

California Department of Water Resources. (2024). Depletions of Interconnected Surface Water: An Introduction. https://og-production-open-data-cnra-892364687672.s3.amazonaws.com/resources/218e3

361-c142-400f-a97f-5dfa79cd4997/depletionsofisw_paper1_intro_draft.pdf?Content-Type=application%2Fpdf&X-Amz-Algorithm=AWS4-HMAC-SHA256&X-Amz-Credential=AKIAJJIENTAPKHZMIPXQ%2F20240321%2Fus-east-1%2Fs3%2Faws4_request&X-Amz-Date=20240321T163735Z&X-Amz-Expires=3600&X-Amz-SignedHeaders=host&X-Amz-Signature=2d2b9d9b844a3c99e52b4ec7523c7ca7a93f6e99d17383896197f8831eae5866

California Department of Water Resources. (2023). SGMA Data Viewer. https://sgma.water.ca.gov/webgis/config/custom/html/SGMADataViewer/doc/

California Department of Water Resources. (2023). Statement of Findings Regarding the Determination of Incomplete Status of the Santa Clara River Valley – Fillmore Subbasin Groundwater Sustainability Plan. *Groundwater Sustainability Plan Assessments. SGMA Portal*. https://sgma.water.ca.gov/portal/gsp/assessments/73

California Department of Water Resources. (n.d.). Groundwater. *Water.ca.gov.* Retrieved March 10, 2024, from https://water.ca.gov/water-basics/groundwater#:~:text=Layers%20of%20alluvial%20aquifers%20make

California State Water Resources Control Board. (2014). The Sustainable Groundwater Management Act. *California State Water Boards*. https://www.waterboards.ca.gov/water_issues/programs/sgma/about_sgma.html

California Code of Regulations, Title 23, Section 351-355. (2014).

California Endangered Species Act, California Fish & Game Code § 2050-2118. (1997).

CIRA. (2024). West Coast Atmospheric Rivers. RAMMB-CIRA Satellite Library. *CIRA Colorado State University*. https://satlib.cira.colostate.edu/event/west-coast-atmospheric-rivers/

Congressional Research Service. (2015). California Agricultural Production and Irrigated Water Use. *www.crs.gov*. https://sgp.fas.org/crs/misc/R44093.pdf

Cordero, J. F. (2015). Native Persistence: Marriage, Social Structure, Political Leadership, and Intertribal Relations at Mission Dolores, 1777–1800. *Journal of California and Great Basin Anthropology*. UC Merced. https://escholarship.org/uc/item/1s8646hp

Cooper, D., D'Amico, D. & Scott, M. (2003). Physiological and Morphological Response Patterns of Populus deltoides to Alluvial Groundwater Pumping. *Environmental Management*, *31*, 0215–0226. https://doi.org/10.1007/s00267-002-2808-2

Court, D., F. Ogushi, J. Glatzer, J. McDonald, K. Keith, & S. Hard. (2000). Prioritizing Sites along the Santa Clara River for Conservation of Threatened and Endangered Species. (Master's thesis, University of California, Santa Barbara). https://santaclarariver.org/wp-content/uploads/2022/05/SantaClara_final.pdf

Daly, C., Halbleib, M., Smith, J. I., Gibson, W. P., Doggett, M. K., Taylor, G. H., & Pasteris, P. A. (2008). Physiographically based mapping of climatological temperature and precipitation across the conterminous United States. *International Journal of Climatology*. https://prism.oregonstate.edu/documents/pubs/2008intjclim_physiographicMapping_daly.pdf

Daniel B. Stephens and Associates. (2021). Fillmore Basin: Groundwater Sustainability Plan. Sustainable Groundwater Management Act Portal. *California Department of Water Resources.* https://sgma.water.ca.gov/portal/gsp/preview/73

Department of Water Resources. (2014). SGMA Groundwater Management. *Ca.gov*. https://water.ca.gov/Programs/Groundwater-Management/SGMA-Groundwater-Management

Diffenbaugh N., Swaina D., & Touma, D. (2015). Anthropogenic warming has increased drought risk in California. *Proceedings of the National Academy of Sciences*. https://doi.org/10.1073/pnas.1422385112

Dong, C., MacDonald, G. M., Willis, K., Gillespie, T. W., Okin, G. S., & Williams, A. P. (2019). Vegetation Responses to 2012–2016 Drought in Northern and Southern California. *Geophysical Research Letters*, *46*(7), 3810–3821. https://doi.org/10.1029/2019gl082137

Downs, P. W., Dusterhoff, S. R., & Sears, W. A. (2013). Reach-scale channel sensitivity to multiple human activities and natural events: Lower Santa Clara River, California, USA. *Geomorphology, 189*, 121-134. DOI:10.1016/j.geomorph.2013.01.023

Eamus, D., Fu, B., Springer, A.E., & Stevens, L. (2016). Groundwater Dependent Ecosystems: Classification, Identification Techniques and Threats. I*ntegrated Groundwater Management: Concepts, Approaches, Challenges.* https://link.springer.com/book/10.1007/978-3-319-23576-9

Environmental Science Associates. (2021). Considerations For Evaluating Effects To Groundwater Dependent Ecosystems In The Upper Santa Clara River Basin—Memorandum. https://scvgsa.org/wp-content/uploads/2021/02/GDE-Consideratons_DRAFT_Feb-2021.pdf

Fan, Y., Miguez-Macho, G., Jobbágy, E. G., Jackson, R. B., & Otero-Casal, C. (2017). Hydrologic regulation of plant rooting depth. *Proceedings of the National Academy of Sciences of the United States of America, 114*(40), 10572–10577. https://doi.org/10.1073/pnas.1712381114

Fillmore & Piru Basins Groundwater Sustainability Agency. (n.d.) Sustainable Groundwater Management Act Overview. https://www.fpbgsa.org/gsa-formations/sustainable-groundwater-management-act-overview/

Final Rule Determining Endangered Status for the Southern Steelhead Trout. Endangered and Threatened Wildlife and Plants, 50 CFR § 17 (2006).

Final Rule Determining Endangered Status for the Southwestern Willow Flycatcher. Endangered and Threatened Wildlife and Plants, 50 CFR § 17 (1995).

Final Rule Determining Threatened Status for the Santa Ana Sucker.Endangered and Threatened Wildlife and Plants, 50 CFR § 17 (2000).

Garssen, A. G., Verhoeven, J. T. A., & Soons, M. B. (2014). Effects of climate-induced increases in summer drought on riparian plant species: A meta-analysis. *Freshwater Biology, 59*(5), 1052–1063. https://doi.org/10.1111/fwb.12328

Gao, B.C. (1996). NDWI - A normalized difference water index for remote sensing of vegetation liquid water from space. *Remote Sensing of Environment, 58*(3), 257–266.

Gleick, P., Cooley, H., & Poole, K. (2014). The Untapped Potential of California's Water Supply: Efficiency, Reuse, and Stormwater – Issue Brief. (Pacific Institute IB:14-05-C). *Pacific Institute.* https://pacinst.org/wp-content/uploads/2014/06/ca-water-capstone-1.pdf

Goldstein-Greenwood, J. (2023). Theil-Sen Regression: Programming and Understanding an Outlier-Resistant Alternative to Least Squares. *University of Virginia Library. University of Virginia.* https://library.virginia.edu/data/articles/theil-sen-regression-programming-and-understanding-an-outlier-resistant-alternative-to-least-squares

Groundwater Exchange. (2018). Undesirable result. *Groundwater Exchange*. https://groundwaterexchange.org/glossary/undesirable-result/

GSI Water Solutions, Inc. (2008). Assessment of Future Surface Water Conditions in the Dry Gap of the Santa Clara River: Prepared for Newhall Land and Farming Company. https://nrm.dfg.ca.gov/FileHandler.ashx?DocumentID=11066

Higgins, P. (1996). The Tataviam: Early Newhall Residents. *Old Town Newhall Gazette*. https://scvhistory.com/scvhistory/higgins-tataviam.htm

Howard, J.K., Dooley, K., Brauman, K.A., Klausmeyer, K.R., & Rohde, M.M. (2023) Ecosystem services produced by groundwater dependent ecosystems: a framework and case study in California. *Front. Water 5*, 1115416. doi: 10.3389/frwa.2023.1115416

Jaeckel, L. A. (1972). Estimating Regression Coefficients by Minimizing the Dispersion of the Residuals. *Annals of Mathematical Statistics, 43*(5*)*, 1449-1458. https://doi.org/10.1214/aoms/1177692377

Jasechko, S., Seybold, H., Perrone, D., Fan, Y., & Kirchner, J. W. (2021). Widespread potential loss of streamflow into underlying aquifers across the USA. *Nature, 591*(7850), 391-395. https://doi.org/10.1038/s41586-021-03311-x

Jasechko, S., & Perrone, D. (2020). California's Central Valley groundwater wells run dry during recent drought. *Earth's Future*, *8*, e2019EF001339. https://doi.org/10.1029/2019EF001339

Johnson, A. I. (1967). Specific yield: compilation of specific yields for various materials. Report. Water Supply Paper 1662. *US Geological Survey.* doi: 10.3133/wsp1662D

Laerd Statistics. (2018). Spearman's Rank-Order Correlation. *Laerd Statistics*. Retrieved 18 February 2024, from https://statistics.laerd.com/statistical-guides/spearmans-rank-order-correlation-statistical-guide.php

Kibler, C. L., Schmidt, E. C., Roberts, D. A., Stella, J. C., Kui, L., Lambert, A. M., & Singer, M. B. (2021). A brown wave of riparian woodland mortality following groundwater declines during the 2012–2019 California drought. *Environmental Research Letters*, *16*(8), 084030. https://doi.org/10.1088/1748-9326/ac1377

Kim, D., Zhang, H., Zhou, H. et al. (2015). Highly sensitive image-derived indices of water-stressed plants using hyperspectral imaging in SWIR and histogram analysis. *Sci. Rep., 5*, 15919. https://doi.org/10.1038/srep15919

Kløve, B., Ala-Aho, P., Bertrand, G., Gurdak, J. J., Kupfersberger, H., Kværner, J., Muotka, T., Mykrä, H. Preda, E., Rossi, P., Uvo, C. B., Velasco, E., & Pulido-Velazquez, M. (2014). Climate change impacts on groundwater and dependent ecosystems. *Journal of Hydrology, 518*, 250–266. https://doi.org/10.1016/j.jhydrol.2013.06.037

Levi, S., & Yeats, R. S. (1993). Paleomagnetic constraints on the initiation of uplift on the Santa Susana Fault, Western Transverse Ranges, California. *Tectonics, 12*(3), 688–702. https://doi.org/10.1029/93TC00133

Mattia Saccò, Mammola, S., Altermatt, F., Alther, R., Rossano Bolpagni, Brancelj, A., Dávid Brankovits, Cene Fišer, Vasilis Gerovasileiou, Griebler, C., Guareschi, S., Hose, G. C., Korbel, K., Lictevout, E., Florian Malard, Martínez, A., Niemiller, M. L., Robertson, A. L., Krizler Cejuela Tanalgo, & Bichuette, M. E. (2023). Groundwater is a hidden global keystone ecosystem. *Global Change Biology*, *30*(1). https://doi.org/10.1111/gcb.17066

Maven. (2019). SGMA IMPLEMENTATION: Developing Sustainable Management Criteria. *MAVEN'S NOTEBOOK*. *California Water News Central*. https://mavensnotebook.com/2019/07/31/sgma-implementation-developing-sustainable-management-criteria/

McEwan, D. & Jackson, T. (1996). Steelhead Restoration and Management Plan for California. *State of California Resources Agency: Department of Fish and Wildlife (formerly Department of Fish and Game)*. https://nrm.dfg.ca.gov/FileHandler.ashx?DocumentID=3490

Minor, A. Scott, Kellog, S. Karl, Stanley, G. Richard, Gurrola, D. Larry, Keller, A. Edward, Brandt, & Theodore, R. (2009). Geologic Map of the Santa Barbara Coastal Plain Area, Santa Barbara County, California. *USGS, Scientific Investigations Map.* https://pubs.usgs.gov/sim/3001/downloads/pdf/SIM3001pamphlet.pdf

Miro, M.E. & Famiglietti, J.S. (2019). A framework for quantifying sustainable yield under California's Sustainable Groundwater Management Act (SGMA). *Sustain. Water Resour. Manag., 5*, 1165–1177. https://doi.org/10.1007/s40899-018-0283-z

Moore, T. (2018). DRAFT 2018 SGMA BASIN PRIORITIZATION: FILLMORE & PIRU SUBBASINS COMMENTS. *Fillmore and Piru Basins GSA*. https://fpbgsa.org/wp-content/uploads/2018/07/DRAFT-2018-SGMA-Basin-Prioritization_Fillmore-Piru-Basins-Comments.pdf

Mound Basin GSA. (n.d.) Home. *Mound Basin GSA*. https://www.moundbasingsa.org/

National Marine Fisheries Service. (2012). Southern California Steelhead Recovery Plan. *Southwest Region, Protected Resources Division, Long Beach, California*.

National Marine Fisheries Service. (2016). 5-Year Review: Summary and Evaluation of Southern California Coast Steelhead Distinct Population Segment. *National Marine Fisheries Service. West Coast Region. California Coastal Office. Long Beach, California.*

Natural Resource Agency State of California. (2010). STATE OF THE STATE'S WETLANDS. https://resources.ca.gov/CNRALegacyFiles/docs/SOSW_report_with_cover_memo_10182010.pdf

Nelson, R. & Szeptycki, L. (2014). Groundwater, Rivers, Ecosystems and Conflicts. *Stanford Woods Institute for the Environment.* https://waterinthewest.stanford.edu/groundwater/conflicts/index.html

Oakley, N. S., Hatchett, B. J., McEvoy, D., & Rodriguez, L. (2019). Projected Changes in Ventura County Climate. *Western Regional Climate Center, Desert Research Institute, Reno, Nevada.*

Pennsylvania State University. (2023). T1.1 - Robust Regression Methods. Stat 501: Regression Methods. *The Pennsylvania State University.* https://online.stat.psu.edu/stat501/lesson/t/t.1/t.1.1-robust-regression-methods

Pettorelli, N., Vik, J.O., Mysterud, A., Gaillard, J., Tucker, C.J., & Stenseth, N.C. (2005). Using the satellite-derived NDVI to assess ecological responses to environmental change. T*RENDS in Ecology and Evolution, 20*(9), 503–10. doi:10.1016/j.tree.2005.05.011

Practitioners of Nature, Wishtoyo Chumash Village. (2011). Excerpt from the Declaration of the Gathering of Indigenous Spiritual Leaders. https://www.wishtoyo.org/spiritual-physical-and-community-wellness

PRISM Climate Group. (2023). Time-Series Values for Individual Locations. *Oregon State University.* https://prism.oregonstate.edu/explorer/

Redowan, M. & Kanan, A.H. (2012). Potentials and Limitations of NDVI and other Vegetation Indices (VIS) for Monitoring Vegetation Parameters from Remotely Sensed Data. *Bangladesh Res. Pub. J*., *7*(3), 291-299. http://www.bdresearchpublications.com/admin/journal/upload/09334/09334.pdf

Rhew, I.C., Vander Stoep, A., Kearney, A., Smith, N.L., & Dunbar, M.D. (2011). Validation of the normalized difference vegetation index as a measure of neighborhood greenness. *Ann Epidemiol., 21*(12), 946-52. doi: 10.1016/j.annepidem.2011.09.001

Rhodes, K. A. et al. (2017).The importance of bank storage in supplying baseflow to rivers flowing through compartmentalized, alluvial aquifers. *Wat. Resour. Res. 53*, 10539–10557. https://doi.org/10.1002/2017WR021619

Rohde, M. M., Biswas, T., Housman, I.W., Campbell, L.S., Klausmeyer, K.R., & Howard, J.K. (2021). A Machine Learning Approach to Predict Groundwater Levels in California Reveals Ecosystems at Risk. *Front. Earth Sci., 9*, 784499. doi: 10.3389/feart.2021.784499 (a)

Rohde, M. M., Roberts, D. A., Singer, M. B., & Stella, J. C. (2021). Groundwater dependence of riparian woodlands and the disrupting effect of anthropogenically altered streamflow. *Proc National Academy of Sciences, 118*, e2026453118. (b)

Rohde, M. M., Matsumoto, S., Howard, J., Liu, S., Riege, L., & Remson, E. J. (2018). Groundwater Dependent Ecosystems under the Sustainable Groundwater Management Act: Guidance for Preparing Groundwater Sustainability Plans. *The Nature Conservancy, San Francisco, California.* https://www.scienceforconservation.org/assets/downloads/GDEsUnderSGMA.pdf

Rohde, M. M., Saito, L., & Smith, R. (2020). Groundwater Thresholds for Ecosystems: A Guide for Practitioners. *Global Groundwater Group, The Nature Conservancy.* https://www.groundwaterresourcehub.org/content/dam/tnc/nature/en/documents/groundwater-resource-hub/GroundwaterThresholdFramework_Final_updated_Dec2020.pdf

Rohde, M.M., Sweet, S.B., Ulrich, C., & Howard, J. (2019) A Transdisciplinary Approach to Characterize Hydrological Controls on Groundwater-Dependent Ecosystem Health. *Front. Environ. Sci., 7*, 175. doi: 10.3389/fenvs.2019.00175

Rotzien, J., Lowe, D., & Schwalbach, J. (2014). Processes of Sedimentation and Stratigraphic Architecture of Deep-Water Braided Lobe Complexes: The Pliocene Repetto and Pico Formations, Ventura Basin, U.S.A. *Journal of Sedimentary Research*, *84*, 910–934. https://doi.org/10.2110/jsr.2014.71

Scott, M. L., Shafroth, P. B., & Auble, G. T. (1999). Responses of Riparian Cottonwoods to Alluvial Water Table Declines. *Environmental Management*, *23*(3), 347–358. https://doi.org/10.1007/s002679900191

Soil Survey Staff. (2023). Gridded Soil Survey Geographic (gSSURGO) Database for California. United States Department of Agriculture. *Natural Resources Conservation Service*. Available online at https://gdg.sc.egov.usda.gov/

Stillwater Sciences. (2011). Geomorphic assessment of the Santa Clara River watershed: synthesis of the lower and upper watershed studies, Ventura and Los Angeles counties, California. *Prepared by Stillwater Sciences, Berkeley, California for Ventura County Watershed Protection District, Los Angeles County Department of Public Works, and the U.S. Army Corps of Engineers–L.A. District.*

Stillwater Sciences. (2021). Assessment of Groundwater Dependent Ecosystems for the Fillmore and Piru Basins Groundwater Stability Plan. *Technical Memo for Fillmore and Piru Basins Groundwater Sustainability Agency, Fillmore.* https://s29420.pcdn.co/wp-content/uploads/2022/02/Appendix-D_GDE-Tech-Memo-1.pdf

Stillwater Sciences. (n.d.) Southern steelhead — Santa Clara River Parkway. https://parkway.scrwatershed.org/theriver/species/southern-steelhead.html

Strashok, O., Ziemiańska, M., & Strashok, V. (2022). Evaluation and Correlation of Normalized Vegetation Index and Moisture Index in Kyiv (2017–2021). *Journal of Ecological Engineering*, *23*(9), 212-218. https://doi.org/10.12911/22998993/151884

Stromberg, J.C. (2013). Root patterns and hydrogeomorphic niches of riparian plants in the American Southwest J. *Arid Environment*. *94,* 1–9.

Stoecker, M. & Kelley, E. (2005). Santa Clara River Steelhead Trout: Assessment and Recovery Opportunities. *Prepared for The Nature Conservancy and The Santa Clara River Trustee Council.* pp. 294.

Sustainable Groundwater Management Act, California Water Code § 10720-10733 (2014).

The Nature Conservancy. (2023). What are Groundwater Dependent Ecosystems and why are they important? *The Nature Conservancy.* https://groundwaterresourcehub.org/

Tomlinson, M. (2011). Ecological water requirements of groundwater systems: a knowledge and policy review. *Waterlines Report 68. National Water Commission*.

Torgo, L. (2012). "Regression Models for Forecasting: Using Regression Models to Predict Time Series with Applications in Epidemiology." *The R Journal, 4*(2), 51-64. https://journal.r-project.org/archive/2012/RJ-2012-014/RJ-2012-014.pdf

Endangered Species Act of 1973, United States Congress. 16 U.S.C. § 1531-1544. (1973).

United States Fish and Wildlife Service. (2019). One river remains: Untouched by development, the Santa Clara River remains the only wild river in Southern California. *United States Fish and Wildlife Service.* https://www.fws.gov/story/2019-04/one-river-remains-untouched-development-santa-clara-river-remains-only-wild-river#:~:text=But%20one%20wild%20river%20remains%3A%20the%20Santa%20Clara%20River.&text=Beginning%20with%20headwaters%20in%20both,estuary%20on%20McGrath%20State%20Beach.

United States Geological Survey. (2017). Water-Table Fluctuation (WTF) Method. Groundwater Resources Program. *US Geological Survey*. https://water.usgs.gov/ogw/gwrp/methods/wtf/

United States Geological Survey. (2017). Water-Table Fluctuation (WTF) Method: Key Assumptions and Critical Issues. *Groundwater Resources Program. US Geological Survey*. https://water.usgs.gov/ogw/gwrp/methods/wtf/issues_limititations.html

United Water Conservation District. (2023). Unpublished Depth to Water Data.

Vaghti, M. G., and S. E. Greco. (2007). Riparian vegetation of the Great Valley. Pages 425–455 in M. G. Barbour, T. KeelerWolf, and A. A. Shoenherr, editors. Terrestrial Vegetation of California, Third Edition. University of California Press, Berkeley.

Ventura County Watershed Protection District. (2023). Unpublished Well Completion Report for Well IDs: 03N20W08B04S, 03N20W08B05S, 03N20W08B06S, 03N20W08B07S.

Veras, T. B., et al. (2016). Vertical hydraulic gradient research in hyporheic zone of Beberibe River in Pernambuco State (Brazil). *RBRH*, *21*(4), 674–684. https://doi.org/10.1590/2318-0331.011615153

Wang T.Y., Ping, W., W. Ze-Lin, N. Guo-Yue, Y. Jing-Jie, Ning, M., W. Ze-Ning, P.P. Sergey, & Deng-Hua,Y. (2021). Drought adaptability of phreatophytes: insight from vertical root distribution in drylands of China. *Journal of Plant Ecology, 14*(6), 1128–1142. https://doi.org/10.1093/jpe/rtab059

Western Regional Climate Center. (n.d.) Climate of California. W*estern Regional Climate Center*. Retrieved 19 February 2024, from https://wrcc.dri.edu/Climate/narrative_ca.php

Western Regional Climate Center. (2013). VENTURA, CALIFORNIA-NCDC 1981-2010 Monthly Normals. *Western Regional Climate Center*. https://wrcc.dri.edu/cgi-bin/cliMAIN.pl?ca9285